

## **Distribution Agreement**

In presenting this thesis or dissertation as a partial fulfillment of the requirements for an advanced degree from Emory University, I hereby grant to Emory University and its agents the non-exclusive license to archive, make accessible, and display my thesis or dissertation in whole or in part in all forms of media, now or hereafter known, including display on the world wide web. I understand that I may select some access restrictions as part of the online submission of this thesis or dissertation. I retain all ownership rights to the copyright of the thesis or dissertation. I also retain the right to use in future works (such as articles or books) all or part of this thesis or dissertation.

Signature:

---

Kellie Vinal

Date

Mechanisms of pathogen-associated 16S rRNA methyltransferase NpmA target  
recognition and enzymatic activity

By

Kellie Vinal  
Doctor of Philosophy

Graduate Division of Biological and Biomedical Sciences  
Microbiology and Molecular Genetics

---

Graeme L. Conn, Ph.D.  
Advisor

---

Ichiro Matsumura, Ph.D.  
Committee Member

---

Philip N. Rather, Ph.D.  
Committee Member

---

Nicholas T. Seyfried, Ph.D.  
Committee Member

---

William M. Shafer, Ph.D.  
Committee Member

Accepted:

---

Dean of the James T. Laney School of Graduate Studies

---

Date

Mechanisms of pathogen-associated 16S rRNA methyltransferase NpmA target  
recognition and enzymatic activity

By

Kellie Vinal  
B.S., North Carolina State University, 2009

Advisor: Graeme L. Conn, Ph.D.

An Abstract of

A dissertation submitted to the Faculty of the James T. Laney School of Graduate Studies  
of Emory University in partial fulfillment of the requirements for the degree of Doctor of  
Philosophy

Graduate Division of Biological and Biomedical Sciences  
Microbiology and Molecular Genetics

2016

## ABSTRACT

Mechanisms of pathogen-associated 16S rRNA methyltransferase NpmA target recognition and enzymatic activity

By

Kellie Vinal

Antibiotic resistance remains a pervasive problem in the treatment of bacterial infections. The continual evolution of resistance mechanisms in bacteria treated with antibiotics, together with horizontal gene transfer between bacterial species, contribute significantly to this growing health concern. Ribosomal RNA (rRNA) methyltransferase enzymes of both drug-producer and pathogen origin are being reported with increased incidence and now threaten the clinical efficacy of many ribosome-targeting antibiotics. The 16S rRNA methyltransferase NpmA specifically methylates adenosine 1408 (A1408) in the aminoglycoside binding site of the bacterial ribosome small subunit (30S), conferring exceptionally high levels of resistance to structurally diverse aminoglycoside antibiotics. NpmA was the first m<sup>1</sup>A1408 methyltransferase enzyme isolated from a human pathogen and is capable of conferring an unprecedented level of resistance in diverse bacterial species. As such, there is an urgent need to understand NpmA's mechanisms of action as a platform for developing novel inhibitors of this emerging resistance determinant.

The work presented here reveals the precise molecular mechanism employed by NpmA to recognize and modify its substrate, the 30S subunit. Through structural, functional, and biochemical analyses we define the molecular features necessary for NpmA to catalyze m<sup>1</sup>A1408 modification and ultimately confer resistance. Our crystal structure of NpmA bound to the 30S subunit, the first reported complex structure of its kind, captures NpmA in a "pre-catalytic" state in which the enzyme is poised for methyl transfer. We show that initial enzyme-substrate docking is driven by electrostatic interactions between the NpmA  $\beta$ 2/3 linker and a conserved tertiary surface of the 30S subunit comprising three disparate 16S rRNA helices brought into proximity only upon 30S assembly. Docking of NpmA on the 30S subunit triggers precisely controlled structural reorganization of two other NpmA regions, the  $\beta$ 5/6 and  $\beta$ 6/7 linkers, which orient functionally critical residues to flip A1408 from helix 44 and stabilize this flipped conformation for methyl transfer. A newly developed fluorescence polarization binding assay, together with structural and biochemical assays, allowed us to specifically probe the NpmA-30S interaction and identify critical residues involved in substrate recognition and catalytic activity. These analyses revealed that catalysis by NpmA is mediated primarily by precise tertiary structure, particularly of the  $\beta$ 6/7 linker, which plays crucial roles in base flipping of A1408 and catalysis. Taken together, our data provide a molecular framework for aminoglycoside-resistance rRNA methyltransferases that might serve as a functional paradigm for related enzymes and provide a starting point for inhibitor development to ultimately extend the efficacy of aminoglycosides in the clinic.

Mechanisms of pathogen-associated 16S rRNA methyltransferase NpmA target  
recognition and enzymatic activity

By

Kellie Vinal  
B.S., North Carolina State University, 2009

Advisor: Graeme L. Conn, Ph.D.

A dissertation submitted to the Faculty of the James T. Laney School of Graduate Studies  
of Emory University in partial fulfillment of the requirements for the degree of Doctor of  
Philosophy

Graduate Division of Biological and Biomedical Sciences  
Microbiology and Molecular Genetics

2016

## ACKNOWLEDGEMENTS

I would like to sincerely thank my advisor, Dr. Graeme L. Conn, for taking a chance on me and for challenging me to grow as both a scientist and a human. I have enjoyed our meetings immensely, from the strategy sessions working through baffling results, to crunch time pep talks, to the giggle-infused graph color adjustment sessions. Thank you for giving me the flexibility to figure things out my own way (even when it makes your head explode) and most of all, for having confidence in me.

I would also like to thank Dr. William Shafer and Dr. David Steinhauer for continually encouraging me throughout my graduate school journey. I'm incredibly grateful that you both have remained my advocate and I know that I wouldn't be defending my PhD without your support. Thank you to Dr. Timothy Read, Dr. Philip Rather, Dr. Karla Passalacqua, Dr. Anice Lowen, and Dr. Charles Moran for helpful advice, especially in my early days at Emory. Thank you Dr. Tatsuya Sueyoshi for introducing me to the world of science, for always laughing with me, and for sending me off well prepared on my scientific journey.

Thank you so much to my thesis committee—Dr. William Shafer, Dr. Philip Rather, Dr. Ichiro Matsumura, and Dr. Nicholas Seyfried. Your input, guidance, and advice have been invaluable throughout this process.

Thank you to all the members of the Conn laboratory both past and present. Thank you Dr. Natalia Zelinskaya for always being supportive and for teaching me everything I know about protein purification, 30S ribosomal subunit purification, and giant radioactive gels. Thank you to Sam Schwartz and Brenda Calderon—I'm grateful for your scientific advice, our life chats, and all the support and giggles. Thank you Dr. Pooja Desai, Dr. Sunita Subramanian, Dr. Marta Witek, Dr. Ginny Vachon, and Dr. Emily Kuiper for fostering a supportive, collaborative working space and generally making The Fun Lab live up to its name. Thank you to Dr. Christine Dunham and the rest of the Dunham lab for scientific guidance, feedback, and laughs along the way.

Thank you to my family for supporting me through this crazy journey. Thank you, Dad, for inspiring scientific curiosity and wonder in me from the very beginning and for your unrelenting support. Thank you, Mom, for believing in me and always supporting me through the rough times.

Thank you to my science communication gurus, mentors, allies, and friends I've made along the way. Your support has been incredibly meaningful to me and I'm forever grateful to know you.

Most of all, thank you to my friends and loved ones, near and far. Thank you especially to my girl gang—you goddesses, you powerhouses. Thank you for inspiring me, creating with me, teaching me to find my strength, and laughing endlessly with me. Thank you to Mason Brown for joining me on this ride and always encouraging my wild ideas, scientific or otherwise. Thank you To my Tough Love Yoga family: thank you for seeing me, thank you for teaching me, thank you for changing me. Thank you to my Burning Man family, for inspiring me to infuse wonder and intention and love in every thing I do.

## TABLE OF CONTENTS

<b>CHAPTER 1: Introduction</b> .....	<b>1</b>
<b>Part I: The bacterial ribosome as an antibiotic target</b> .....	<b>2</b>
Ribosome structure and assembly.....	2
Ribosome function .....	4
Antibiotics that interfere with ribosome function.....	8
<b>Part II: Aminoglycosides</b> .....	<b>10</b>
Aminoglycoside properties, action, and origin.....	10
<b>Part III: Aminoglycoside resistance</b> .....	<b>14</b>
Antibiotic resistance is ancient .....	14
Mechanisms and origins of aminoglycoside resistance .....	15
<b>Part IV: Aminoglycoside-resistance 16S rRNA methyltransferases</b> .....	<b>15</b>
Mechanism of resistance.....	15
Features of the A1408 vs. G1405 aminoglycoside-resistance 16S rRNA methyltransferase families .....	17
<b>Part V: 16S rRNA methyltransferases identification and the rise of the 16S rRNA     methyltransferase threat</b> .....	<b>18</b>
<b>Part VI: NpmA</b> .....	<b>19</b>
<b>Part VII: Clinical significance and epidemiology</b> .....	<b>23</b>
<b>Chapter 1 References</b> .....	<b>27</b>
<b>CHAPTER 2: Molecular recognition and modification of the 30S ribosome by the aminoglycoside-resistance methyltransferase NpmA</b> .....	<b>35</b>
<b>Chapter 2 Introduction</b> .....	<b>37</b>
<b>Chapter 2 Results and Discussion</b> .....	<b>40</b>
Directed RNA structure probing orients NpmA on h44 .....	40
Overview of the 30S-NpmA-sinefungin complex .....	40
Identification of residues critical for NpmA activity .....	41
Sequence independent, tertiary contacts distant from the methylation site direct 30S- NpmA recognition .....	43
Pre-catalytic state shows A1408 flipped from h44 and poised for methylation .....	45
Mechanisms of molecular recognition, conformational adaptation and A1408 modification .....	46

Mechanistic conservation and variation among aminoglycoside-resistance 16S rRNA methyltransferases.....	48
Modification enzymes may target nucleotides in the decoding center by a common mechanism .....	49
Feasibility of horizontal gene transfer to other pathogens.....	51
<b>Chapter 2 Materials and Methods.....</b>	<b>52</b>
<b>Chapter 2 Figures .....</b>	<b>54</b>
<b>Chapter 2 References.....</b>	<b>59</b>
<b>Chapter 2 Supplementary Information .....</b>	<b>64</b>
<b>CHAPTER 3: Substrate recognition and modification by a pathogen-associated aminoglycoside-resistance 16S rRNA methyltransferase.....</b>	<b>82</b>
<b>Chapter 3 Introduction.....</b>	<b>85</b>
<b>Chapter 3 Materials and Methods.....</b>	<b>87</b>
<b>Chapter 3 Results.....</b>	<b>91</b>
A fluorescence assay to probe 30S-NpmA interaction .....	91
The NpmA $\beta$ 2/3 linker drives interaction with the 30S subunit .....	93
Contributions of the NpmA $\beta$ 5/6 and $\beta$ 6/7 linkers to 30S-NpmA binding affinity ..	96
Role of the $\beta$ 5/6 linker in 30S substrate recognition.....	97
Role of the $\beta$ 6/7 linker in SAM binding and 30S substrate recognition.....	98
<b>Chapter 3 Discussion .....</b>	<b>100</b>
<b>Chapter 3 Tables and Figures.....</b>	<b>108</b>
<b>Chapter 3 References.....</b>	<b>116</b>
<b>Chapter 3 Supplementary Information .....</b>	<b>122</b>
<b>CHAPTER 4: Conclusion.....</b>	<b>128</b>
<b>Chapter 4 References.....</b>	<b>138</b>

**CHAPTER 1:**

**Introduction**

## **PART I: THE BACTERIAL RIBOSOME AS AN ANTIBIOTIC TARGET**

### **Ribosome structure and assembly**

The ribosome is a complex macromolecular machine comprising more than fifty RNA and protein components and is the largest known enzyme in nature (1). In all living cells, the ribosome synthesizes new proteins through the process of translation and is thus essential to the survival of all living organisms. The ribosomal structure is highly conserved among diverse bacterial species and striking similarities are observed in comparisons of ribosomes from prokaryotes, archaea, and eukaryotes. Although evolution has driven sequence changes that affect the ribosomal proteins (r-proteins) and ribosomal RNAs (rRNAs) of vastly different organisms, the overall architecture of the ribosome remains generally conserved (1). Each ribosome consists of a small and a large ribonucleoprotein subunit, each defined by their sedimentation coefficients (reflecting relative mass and denoted by Svedberg units (S) that are precisely assembled and positioned (2, 3).

In prokaryotes, the large (50S) subunit is comprised of ~34 unique proteins (r-proteins, denoted L1-L36 in *E. coli*) and ~3,000 nucleotides of rRNA, while the small (30S) subunit contains 22 proteins (denoted S1-S22) and ~1,500 nucleotides of rRNA (3). Additionally, the large subunit consists of two rRNAs, 23S and 5S, while the small subunit has one rRNA, 16S. Individual subunits of the ribosome are first assembled, typically existing separately in the cell, and only when they are translating an mRNA do these subunits associate to form the complete prokaryotic (70S) ribosome (4). The rRNAs (16S, 23S, and 5S RNA) are initially synthesized as a single transcript that is

subsequently processed and cleaved by endonucleases at precise locations during assembly to form the three mature rRNA species (2, 5). rRNA secondary structures are formed as the nascent transcript exits the RNA polymerase, which prompts interaction with r-proteins as their binding sites are revealed and also incorporation of posttranscriptional chemical modifications of rRNA (2, 6).

During assembly of the 30S subunit, assembly proteins first bind naked rRNA and a hierarchy of secondary and tertiary assembly proteins subsequently guide cooperative complex formation (7-11). Specifically, primary binding proteins S4, S7, S8, S15, S17, and S20 bind directly to 16S rRNA first, which prompts binding of secondary (S6, S9, S13, S16, S18, S19) and tertiary (S2, S3, S5, S10, S11, S12, S14, S21) binding proteins (11, 12). As these proteins are progressively added, structural changes in the 16S rRNA induce cooperative assembly (8). Assembly of the 50S subunit occurs similarly, though with significantly more complexity, as 23S rRNA binds nearly twice as many proteins as 16S rRNA and proper 23S-5S interactions must be mediated (6).

In *E. coli*, ribose and base entities of both rRNA and transfer RNA (tRNA) molecules undergo over 80 posttranscriptional modifications as they mature (e.g. addition of carbonyl, methyl, amino, or thio groups, or isomerization of uridine to pseudouridine). These processes are mediated predominantly by methyltransferase, pseudouridine synthase, and acetyltransferase enzymes (6, 13). Most of these modifications are conserved and essential, though studies have shown that for ribosomal assembly and function, a handful of these modifications are non-essential (6, 14). Ribosomal proteins also undergo posttranslational modification, including methylation of S11, L3, L11, L7/L12, L16, and L33, methylthiolation of S12, and acetylation of S5, S18 and L7 (15).

Proper folding and stabilization of rRNA during ribosomal assembly is controlled by intramolecular interactions and assistance by metal ions and at least three classes of proteins: RNA chaperones, ribosome-dependent GTPases, and RNA helicases (6). Once assembled, the quality of the ribosome is assessed by methylase RsmA (formerly KsgA). During assembly RsmA binds to h45 of 16S rRNA to prevent immature 30S subunits from entering translation and subsequently dimethylates A1518 and A1519 to indicate or “mark” the 30S subunit as functionally competent when assembly is complete (8, 16). Other factors such as the number of active ribosomes and efficiency of energy output by the cell are also tightly regulated (6).

### **Ribosome function**

Ultimately, the role of the ribosome is to translate genetic material encoded in the mRNA nucleotide sequences into proteins, a process aided by tRNA molecules, aminoacyl-tRNA synthetase enzymes, and a host of ribosome-associated GTPase factors (4). Before translation begins, aminoacyl-tRNA synthetases attach a specific, cognate amino acid to each tRNA. Each aminoacyl-tRNA is then delivered to the ribosome as a ternary complex with guanosine nucleotide triphosphate (GTP) and the protein translation elongation factor Thermo-unstable (EF-Tu). During translation, each tRNA base-pairs with a complementary codon in the mRNA as it travels through the ribosome, inserting the amino acid it carries into the growing protein (3).

The process of translation consists of three main stages: initiation, elongation, and termination/recycling. Each ribosomal subunit plays a distinct critical role during translation. The small ribosomal subunit, the site of decoding, mediates and monitors

proper interaction between the tRNA anticodon and mRNA codon to control the sequence of amino acids as a protein is synthesized. The large ribosomal subunit, the site of the peptidyl-transferase center (PTC), catalyzes peptide bond formation between amino acids of the growing polypeptide chain (3, 6). In both subunits of the ribosome, three binding sites for tRNA molecules exist that correspond to three distinct functional tRNA states: the A (aminoacyl) site, P (peptidyl) site, and E (exit) site. While the A site binds aminoacyl-tRNAs carrying the next amino acid to be appended into the polypeptide chain, the P site assists in positioning of the peptidyl-tRNA, and the E site temporarily holds deacylated tRNA before its dissociation from the ribosome (3). Sequentially, the 30S subunit binds first to mRNA to initiate translation, then to the 50S subunit to form the full 70S ribosome. As a unit, the 70S ribosome travels down the mRNA sequence three nucleotides at a time with each component working in concert to pair proper tRNA:mRNA matches and extend the polypeptide chain to produce new proteins. Once a protein is complete, the ribosome dissociates into 50S and 30S counterparts and the process begins again (4).

Translation initiation occurs when the Shine-Dalgarno (SD) sequence, located approximately 6 to 9 nucleotides upstream of the translation start codon in the mRNA, interacts with the complementary anti-SD sequence at the 3' end of 16S rRNA (6). After this initial interaction, initiation factors IF1, IF2, and IF3 mediate incorporation of the formylmethionine tRNA ( $\text{tRNA}^{\text{fmet}}$ ), a unique tRNA that recognizes the start codon, directly into the P site of the ribosome (4, 6). IF2 binds to  $\text{fmet-tRNA}^{\text{fmet}}$ , while IF1 binds in the A site of the 30S subunit to prevent A-site tRNA binding, and IF3 fills the E site to prevent association with the 50S until the end of initiation. Together, the initiation

complex (IF1, IF2, IF3, and tRNA<sup>fmet</sup>) occupies each of the tRNA sites in a conformation which has been hypothesized to properly orient the 30S for protein synthesis (17). Once the 30S subunit is properly oriented at the end of the initiation step, the initiation factors are ejected, allowing the 30S and 50S subunits to associate.

To begin elongation, an aminoacylated tRNA corresponding to the second encoded amino acid, or codon currently occupying the A site, is brought into the A site as a complex with EF-Tu and GTP (3, 6). The decoding center of the A site, located at the top of 16S rRNA helix 44, serves to monitor codon-anticodon pairing once an aminoacylated tRNA has entered the A site. Two universally conserved nucleotides, A1492 and A1493, monitor codon-anticodon base pairing, particularly in the first two nucleotide positions of the codon. mRNA codon-tRNA anticodon pairing induces a conformational change in 16S rRNA such that A1492 and A1493 flip out of the RNA helix to interact with the codon-anticodon pair in the A site. Additionally, tRNA binding in the A site induces rotation of nucleotide G530, which helps stabilize the flipped-out conformational of A1492 and A1493 (1). Ultimately, cognate codon-anticodon pairing triggers a cascade of protein-mediated signals and conformational rearrangements that stabilize binding of the tRNA and activate the GTPase center of the ribosome (1, 3, 17). In the case of a codon-anticodon mismatch in the A site, there is insufficient interaction potential for A1492 and A1493 to initiate the signal for peptide bond formation (1). Upon GTP hydrolysis by EF-Tu, EF-Tu releases the aminoacyl end of the A-site tRNA and accommodation (for a cognate interaction) or release (for non-cognate) occurs. Accommodation involves repositioning of the A-site tRNA acceptor stem to promote peptide bond formation in which the tRNA acceptor stem swings into the 50S subunit

peptidyl-transferase site (6). The amino acid attached to the 3' end of the A-site tRNA is then positioned within the peptidyl-transferase center on the 50S subunit, properly positioned adjacent to the peptide chain attached to the P-site tRNA. Peptide bond formation occurs essentially spontaneously, and involves transfer of the peptide chain to the A-site tRNA after deacylation of the P-site tRNA (17). Once the peptide chain is transferred onto the A-site tRNA, the deacylated tRNA is moved from the P site to the E site to be expelled from the ribosome, and the A-site tRNA moves to the P site (3, 4, 6). This translocation of the ribosome in the 3' mRNA direction, facilitated by the GTPase EF-G, indicates the ribosome is ready to decode the next mRNA codon for another round of elongation (6, 17).

The process of elongation continues, a single codon at a time, until a stop codon in the mRNA (UAA, UAG, or UGA) enters the ribosomal A site, which initiates a termination reaction that hydrolyzes and releases the completed polypeptide chain from the P site tRNA (4). In bacteria, the termination codon is recognized by release factor proteins RF1 and RF2. Specifically, RF1 terminates at codons UAG and UAA, while RF2 recognizes UGA and UAA. A third release factor, RF3, then binds to the ribosome-RF1/2 complex, assisting in the removal of RF1/2 from the A site (6, 17). The ribosome, still bound to the mRNA and deacylated tRNA in the P site, is then disassembled into its subunits with the assistance of ribosome recycling factor (RRF) and EF-G (4, 6). Initiation factor IF3 is then required to remove and replace the deacylated tRNA on the 30S subunit, subsequently allowing the mRNA to either form a new SD:anti-SD interaction with a downstream binding site or detach altogether (6, 17). The ribosome subunits are then ready to participate in another round of protein synthesis.

### **Antibiotics that interfere with ribosome function**

Soil microorganisms naturally produce a variety of antibiotics not only for inhibiting the growth of competing microbial species, but for survival advantage in their environment to combat challenges such as plant root pathogens and/or adaptation to nutrient deprivation (18-20). The complexity and strictly conserved nature of the ribosome, both in structure and function, paired with its necessity for survival, make the ribosome an attractive target for antimicrobial compounds. Both ribosomal assembly and function are intricately controlled, and loss of function can be induced by antibiotics via subtle binding-induced conformational shifts or perturbations (1). Crystallographic studies have revealed that ribosome-targeting antibiotics of diverse chemical composition tend to overlap in their binding sites and target mechanistically crucial regions of the ribosome such as the decoding center, peptidyl-transferase center, and nascent polypeptide exit tunnel. Though antibiotic binding sites on the ribosome are surprisingly few, these antibiotics exhibit diverse modes of action to interrupt protein synthesis (1, 21). Extensive biochemical and structural studies have elucidated the mechanisms by which these antibacterial agents interfere with protein synthesis. Most ribosome-targeting antibiotics, including chloramphenicols, lincosamides, aminoglycosides, macrolides, fusidic acids, oxazolidinones, tetracyclines, and streptogramins target the elongation phase of translation. Fewer antibiotics, most of which are less clinically relevant, target the initiation cycle and termination/recycling phase (22).

Specifically on the 30S subunit, antibiotic binding sites span the path of the mRNA and tRNAs during translation. Edeine and kasugamycin prevent a stable

interaction between the start codon and initiator tRNA in the P-site, thus inhibiting translation initiation (22). Streptomycins and tetracyclines interfere with tRNA delivery to the A site during elongation, while tuberactinomycins and some aminoglycosides impede mRNA-tRNA translocation through the ribosome (21, 22). Spectinomycin has been shown to inhibit tRNA translocation from the A site to the P site (21). However, antibiotics that target this region, including pactamycin, tetracycline, and the aminoglycosides, interfere primarily with the process of decoding (1). Within the decoding center, aminoglycosides such as geneticin and paromomycin coerce nucleotides A1492 and A1493 to flip from h44, erroneously signaling a cognate mRNA:tRNA match has been made and that peptide bond formation should occur, thus decreasing translation fidelity (1, 22).

Within the bacterial 50S subunit, antibiotics target sites that control peptide bond formation, GTP hydrolysis, and channeling of the peptide through the exit tunnel (1). Chloramphenicol, tiamulin, thiostrepton, clindamycin, and streptogramin A bind within or at regions surrounding the PTC and exert their actions in mechanistically different ways to interfere with peptide bond formation (21). Chloramphenicol not only blocks A site aa-tRNA binding, thus inhibiting formation of peptide bonds, but has also been shown to interfere with 50S subunit biogenesis. Streptogramins, which exist in two classes, exert synergistic effect by binding adjacent sites within the exit tunnel and promoting binding of the other classes to disrupt peptide bond formation (22). Each peptide leaving the ribosome after translation snakes through the protein- and rRNA-lined 50S subunit peptide exit tunnel. Macrolides bind adjacent to the PTC within this ribosomal exit tunnel, thus disrupting nascent peptide chain elongation and resulting in

premature release of peptidyl-tRNAs (22). Ketolides and macrolides, both used widely in the clinic, ultimately block the progression of nascent peptides through the exit tunnel, disrupting elongation (21).

The ribosome is a complex macromolecular machine, assembly and function of which are intricately controlled and essential for survival. Thus, the ribosome is an ideal target for antibiotic molecules. A variety of classes of antibiotics exert their effects on their ribosomal target in various ways. The focus of this work and the subject of Part II below will be on aminoglycoside antibiotics and their mechanisms of action.

## **PART II: AMINOGLYCOSIDES**

### **Aminoglycoside properties, action, and origin**

Aminoglycoside antibiotics are naturally produced by the secondary metabolism of bacteria belonging to Genera *Streptomyces* and *Micromonospora*, both of the Phylum Actinobacteria. These drugs exhibit potent, wide-spectrum activity in clinical and veterinary treatment settings against primarily aerobic gram-negative bacilli (23).

Aminoglycosides can also act in synergy with other antibiotics to eliminate some gram-positive organisms (23-25). In addition to their use as first line drugs in the case of a serious infection, they are used in livestock settings for growth promotion (26).

Aminoglycosides are effective against some staphylococci, some mycobacteria, and a variety of Gram-negative bacilli clinical settings. Gentamicin is most often used to reliably treat infections of Gram-negative bacilli because of its low cost. Gentamicin,

tobramycin, and amikacin are effective in treating meningitis, bacterial sepsis, and pneumonia and are often used interchangeably in the clinic. Tobramycin is used to fight *Pseudomonas aeruginosa* infection, spectinomycin is effective in treating gonorrhoea infections, and neomycin is used to treat ulcers, dermatitis, and general wounds. Notably, streptomycin is used to treat infection by *Mycobacterium tuberculosis* (the causative agent of tuberculosis), *Francisella tularensis* (tularemia), and *Yersinia pestis* (plague). Aminoglycosides are also used in combination with  $\beta$ -lactams to enhance bactericidal activity against *Staphylococcus aureus* (23).

Although these drugs are critical and clinically useful in a variety of settings, the potent antimicrobial activity of aminoglycosides is undermined and complicated by nephrotoxicity and ototoxicity if used in humans and animals in high doses. In fact, the retained potency of these drugs is likely in part due to their relatively limited use because of such severe side effects. Nephrotoxicity stems from the ability of aminoglycosides to be retained in epithelial cells lining the kidney, interfering with normal kidney function and ultimately causing renal failure (27). Additionally, aminoglycosides cannot be orally ingested and must be administered either intravenously, intramuscularly, or parenterally, further complicating practical clinical use (23). Despite these limitations, retained activity make aminoglycosides an important part of our antimicrobial army.

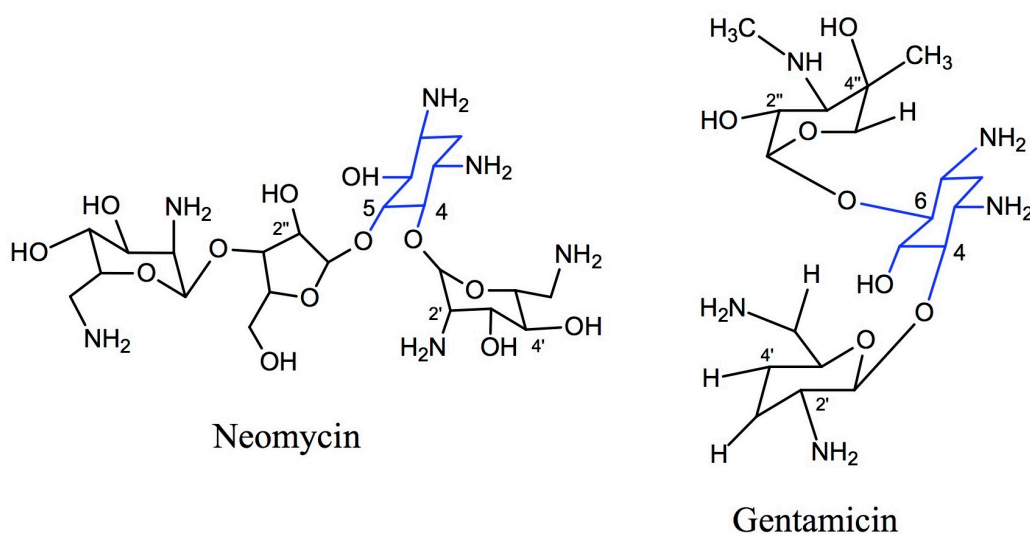


**Figure 1:** Aminoglycosides Neomycin (4,5-DOS) and Gentamicin (4,6-DOS) with 2-DOS core highlighted in blue.

The chemical basis for both the antimicrobial activity and potency of aminoglycoside action is typically an aminocyclitol core, either streptamine or 2-deoxystreptamine (2-DOS), connected by glycosidic linkages to one or more aminated sugars (28). Aminoglycosides can be broadly subdivided into three categories based on their structure. The most clinically relevant aminoglycosides, including gentamicin, netilmicin, amikacin, and tobramycin, possess a 2-DOS core with amino sugar substitutions at positions 4 and 6. Neomycin and paromomycin contain a 4,5-disubstituted 2-DOS core ring, while spectinomycin and streptomycin fall into a category of “other”, as spectinomycin for example contains no amino sugar (23). Aminoglycosides are basic and strongly polar, characteristics that promote passive, electrostatic binding to negatively charged lipopolysaccharide (LPS) on the outer membrane of gram-negative bacteria. Binding to LPS disrupts  $Mg^{2+}$  salt bridges between LPS molecules and initiates diffusion into a bacterial cell through outer membrane porin channels. Aminoglycosides

are then transported across the cytoplasmic membrane, a process that requires oxygen from the electron transport system, and once in the cytosol, these drugs bind the 30S subunit (23, 28).

Aminoglycoside antibiotics, as mentioned previously, exploit the extreme sequence and structural conservation of the ribosome, particularly in areas directly involved in decoding (1). The polar, cationic nature of aminoglycosides contributes to their high affinity for negatively charged rRNA. Crystallographic studies of rRNA oligonucleotides or 30S ribosomal subunits complexed with aminoglycosides have revealed the precise locations and mechanisms by which aminoglycosides exert their action. Regardless of 4,5- or 4,6-substitution, the 2-DOS ring of aminoglycosides binds in a similar fashion to the A site of the 30S subunit (29). Aminoglycosides bind in the major groove of helix 44 (h44) on the 30S subunit by inserting Ring I (attached to the 2-DOS ring at position 4) into the RNA helix, mimicking a nucleotide base (30-33). This sugar Ring I stacks against nucleotide G1491 and subsequently forms two hydrogen bonds to A1408, as well as a hydrogen bond with the phosphate of A1493 (30, 31, 33). These interactions induce a conformational change in the A site such that A1492 and A1493 bulge from h44, a state stabilized by these hydrogen bonds to functional groups of Rings I and II of the aminoglycoside (29-31, 33, 34). Bulging of A1492 and A1493 from h44 mimics the state typically stabilized by cognate mRNA:tRNA pairing, diminishing the ability of the ribosome to discern correct mRNA:tRNA matches. Impairment of the proofreading process controlling translational accuracy subsequently results in aberrant protein production and, eventually, cell death (24, 29, 30, 33).

### **PART III: AMINOGLYCOSIDE RESISTANCE**

#### **Antibiotic resistance is ancient**

The unearthing of antibiotics and their usefulness to treat bacterial infections over 70 years ago spurred an awakening of sorts, in which antibiotics were prescribed (in excess, some argue) to combat widespread bacterial infections and new drugs were sought and developed (35). However, beginning with resistance to sulfonamides in the 1930s, we have observed widespread antibiotic resistance to each clinically useful drug shortly after its introduction into the clinic (36). As natural products of microbes, it has been estimated that antibiotics have existed for over 40 million years. Despite the belief of many that antibiotic resistance is a modern occurrence, it is in fact likely that resistance to these antibiotics is correspondingly ancient (22). As our technology has advanced, so has our capacity to discover the multitude of resistance genes microbes encode and that these genes exist more commonly and in greater number than we expected. Genomic analyses of these genes across diverse microbial species reveal a surprisingly interconnected nature, suggesting the dissemination, horizontal transfer, and evolution of these resistance determinants has likely been occurring far longer than the age of human clinical and agricultural industrial antibiotic use. Furthermore, resistance genes to modern-day  $\beta$ -lactam, glycopeptide, and tetracycline antibiotics were extracted and identified from bacteria in permafrost sediments dating over 30,000 years old, definitively demonstrating that these resistance genes are not specific to the modern age of antibiotic use (35).

### **Mechanisms and origins of aminoglycoside resistance**

While some microbial species are innately resistant to antibiotics, others have evolved or acquired resistance mechanisms through horizontal gene transfer or via mobile genetic elements. Soil-derived actinomycetes in particular have been identified as a rich source of resistance determinants that have spread to other microbial species (22). Antibiotic-producing bacteria, out of necessity, have developed mechanisms to protect against their own drugs and this resistance to antibiotics is typically achieved by drug deactivation via enzyme modification (by acetyltransferases, nucleotidyltransferases, or phosphotransferases), prevention of drug permeability, efflux of intracellular drug molecules, sequestration or trapping of the drug, or direct modification of the target (22, 23, 26, 37-39). Additionally, biochemical studies have shown that mutation of specific nucleotides crucial for aminoglycoside binding is similarly effective for conferring resistance to aminoglycosides (29). By far, the resistance mechanism leading in prevalence in the clinics is inactivation of these drugs by aminoglycoside-modifying enzymes (26). However, of increasing prevalence and clinical importance are 16S rRNA-modifying enzymes which are most common among aminoglycoside-producing bacteria (26).

## **PART IV: AMINOGLYCOSIDE-RESISTANCE 16S rRNA**

### **METHYLTRANSFERASES**

#### **Mechanism of resistance**

Many microbial species that produce aminoglycosides also intrinsically harbor genes encoding methyltransferase enzymes that modify the 16S rRNA binding site of these drugs (23). High-level resistance against aminoglycosides can be achieved by specific methylation of 16S rRNA by these methyltransferases, as this modification disturbs the interaction between aminoglycosides and their 16S target (1, 23-25, 39-43). Base methylation can impart a new positive charge at neutral pH and can thus affect aminoglycoside binding via both steric hindrance and charge repulsion. Specifically, A1408- and G1405-modifying 16S rRNA methyltransferases transfer a methyl group from S-adenosyl-L-methionine (SAM) to one of these two specific 16S rRNA sites to confer aminoglycoside resistance, releasing S-adenosyl-homocysteine (SAH) as the by-product. These aminoglycoside-resistance 16S rRNA methyltransferases are categorized into two groups based on their methylation target: N7 of G1405 (to produce m<sup>7</sup>G1405) or N1 of A1408 (to produce m<sup>1</sup>A1408). They can be further subdivided by origin as either antibiotic producer or pathogenic bacterial enzymes, though these enzymes are functionally identical.

16S-RMTases that incorporate the m<sup>7</sup>G1405 16S rRNA modification, including Sgm from the sisomicin producer *Micromonospora zionensis* and the Arm/Rmt enzymes from various human pathogens, confer resistance to aminoglycosides with 4,6-disubstituted 2-DOS (e.g. amikacin and gentamicin), but not those that are 4,5-disubstituted (e.g. streptomycin and apramycin). In contrast, however, A1408-modifying enzymes confer resistance to structurally diverse aminoglycosides (26, 44). These differences in resistance profile arise because of the distinct impacts of the precise position to which the methyl group is transferred within in the A site. For example, ring

III of a 4,6-disubstituted 2-DOS aminoglycoside such as gentamicin forms a direct hydrogen bond with the N7 of G1405 upon rRNA binding which is blocked by the  $m^7G1405$  modification. In contrast, rings III and IV of aminoglycosides containing the 4,5-disubstituted 2-DOS core are spatially located out of range of G1405 and thus methylation at this site does not perturb their interaction. Generally, ring I of aminoglycosides interact with the N1 position of A1408 position within rRNA, such that methylation at this site confers resistance to apramycin as well as some examples of both the 4,5- and 4,6-disubstituted 2-DOS groups (26). Why binding of some drugs but not others is impacted by  $m^1A1408$  modification is unclear but likely arises from additional interactions made by some aminoglycosides that are sufficient to overcome loss of interaction with A1408.

### **Features of the A1408 vs. G1405 aminoglycoside-resistance 16S rRNA**

#### **methyltransferase families**

Both  $m^1A1408$  and  $m^7G1405$  16S rRNA methyltransferases, like most SAM-dependent methyltransferases, have a structurally conserved Rossmann-like core fold, consisting of a seven-stranded  $\beta$ -sheet, the first four strands of which interact with SAM (38, 45-47). However, adornments to this core fold vary drastically between the  $m^1A1408$  and  $m^7G1407$  methyltransferases, specifically at their N-termini and the connecting sequences of the final three strands of the core  $\beta$ -sheet.  $m^1A1408$  methyltransferases have a short N-terminal  $\beta$ -hairpin and extended sequences linking  $\beta$ -strands 5 and 6 ( $\beta5/\beta6$  linker) and  $\beta$ -strands 6 and 7 ( $\beta6/\beta7$  linker). In contrast,  $m^7G1405$  methyltransferases possess a large (~80-100 residues) helical N-terminal domain and

shorter regions linking the last three strands of the core  $\beta$ -sheet (45, 48). Both classes of enzymes, however, require the fully assembled 30S ribosomal subunit as their substrate (41).

## **PART V: 16S rRNA METHYLTRANSFERASES IDENTIFICATION AND THE RISE OF THE 16S rRNA METHYLTRANSFERASE THREAT**

It was first revealed in the 1980s that some aminoglycoside-producing *actinomycetes* harbor 16S rRNA methyltransferase genes in order to protect themselves from their own antibiotic products (39). By encoding these enzymes, aminoglycoside-producing bacteria could retain high levels of resistance to aminoglycosides and maintain competitive advantage in their environment. These 16S rRNA methyltransferase genes are located within clusters of aminoglycoside biosynthesis genes, further underscoring the likely ecological advantage of coexistence of these genes (26). Initially, 16S rRNA methyltransferase genes were thought to be derived solely from antibiotic producing microbes, but subsequent studies have reported the presence of these genes outside of aminoglycoside-producing microbial species (44).

The first identified 16S rRNA methyltransferase from a clinical isolate of *Pseudomonas aeruginosa* strain AR2 conferred an unprecedented level of resistance to a variety of aminoglycosides. Upon further investigation, the resistance was attributed to plasmid-encoded exogenous 16S rRNA methyltransferase RmtA (26, 49). Around the same time, the orthologous methyltransferase ArmA was identified from a *Klebsiella*

*pneumonia* strain and the *armA* gene sequence was found on a plasmid from a *Citrobacter freundii* clinical strain (44). Discovery of these plasmid-encoded resistance enzymes in clinically important pathogenic bacteria spurred new analyses that have ultimately revealed, to date, nine distinct 9 m<sup>7</sup>G1405 16S rRNA methyltransferases of acquired origin: ArmA, RmtA, RmtB1/2, RmtC, RmtD1/2, RmtE, RmtF, RmtG, and RmtH (44). These enzymes were found to share moderate to high similarity in amino acid sequence. In contrast, only one acquired m<sup>1</sup>A1408 16S rRNA methyltransferase (NpmA) has been identified to date, with an amino acid sequence quite distinct from that of enzymes derived from aminoglycoside producing bacteria. NpmA, which confers a wider range of aminoglycoside resistance (e.g. 4,6-disubstituted 2-DOS such as amikacin, kanamycin, tobramycin, gentamicin, and sisomicin, 4,5-disubstituted 2-DOS such as neomycin and ribostamycin, and other aminoglycosides such as apramycin and spectinomycin) was identified from an *E. coli* clinical strain in 2007 (26, 44). Furthermore, the *npmA* gene was found to be flanked by two insertion sequence elements, suggesting the mobile potential of this resistance determinant. Its unique target, amino acid sequence, broad range of resistance conferred and potential for mobile dissemination make investigation of the origin and mechanism of action of NpmA of particular importance (44).

## **PART VI: NpmA**

NpmA, originally isolated from pathogenic *E. coli* strain ARS3, confers pan-aminoglycoside resistance and is of particular importance as it is the first reported m<sup>1</sup>A1408 16S rRNA methyltransferase enzyme to be isolated from a pathogenic source, the *E. coli* strain ARS3 (41). Initial characterization of *npmA* revealed not only that the methyltransferase gene was located within a transposable element of a plasmid, but the sequences surrounding this transposable element share striking similarity with that of various multidrug resistant plasmids (41). Until the discovery of NpmA, genes encoding A1408-modifying 16S rRNA methyltransferases had exclusively been found in the chromosomes of aminoglycoside-producing actinomycetes. In contrast, G1405-modifying methyltransferases have been found on plasmids of gram-negative pathogens as well as the chromosomes of aminoglycoside-producing actinomycetes. In fact, *npmA* exhibits low-level identity (<31%) to that of chromosomally-encoded 16S rRNA methyltransferases KamA, KamB, KamB2, KamB3, KamC, and Amr. Compared with the G+C content of A1408 methyltransferase genes of aminoglycoside-producing origin (>70%), *npmA* exhibited a significantly lower percentage (34%), suggesting that NpmA might originate from a source distinct from that of soil microbes (41). The unique origin of NpmA, combined with its puzzling sequence dissimilarity to related enzymes, underpinned the necessity to understand where this enzyme comes from, its precise mechanism of action, and potential for transmissibility and aminoglycoside resistance in genetically distinct microbes.

Initial characterization of NpmA revealed that the enzyme could effectively methylate only properly assembled 30S ribosomal subunits, not naked 16S rRNA or 50S ribosomal subunits. Functional analyses revealed that NpmA methylates the N1 position

on A1408 of 16S rRNA (41), a position which plays a crucial role in binding of 4,6- and 4,5-disubstituted 2-deoxystreptamines. Accordingly, NpmA was confirmed to confer resistance to a broad range of aminoglycosides but not to non-A site binding antibiotics such as spectinomycin or streptomycin. Based on this data, it was hypothesized that incorporation of the m<sup>1</sup>A1408 modification by NpmA would disrupt A1408-A1493 base pairing, thus disrupting the aminoglycoside binding pocket, thus preventing aminoglycoside binding. However, details of the specific points of contact between NpmA, its 30S subunit substrate, crucial NpmA residues, and precise mechanism of action remained elusive (41).

The crystal structure of NpmA bound to its cosubstrate SAM allowed for more detailed analysis of enzyme-cosubstrate interaction. Structural analyses confirmed that A1408-modifying methyltransferase NpmA is a Class I methyltransferase possessing a characteristic Rossmann-like SAM binding fold (45). Of the A1408 methyltransferases, enzymes from drug producers, e.g. KamA and KamB, and NpmA share the amino acid sequence “DXGTGDG”, which is the hallmark SAM binding motif for this class of enzymes (41). Analysis of x-ray crystallographic structures of NpmA and KamB bound to SAM or SAH, in conjunction with functional assays using site-directed mutagenesis of these enzymes, have specifically identified NpmA residues Asp30 and Asp55 as crucial for forming the SAM binding pocket (45, 50). Interestingly, although mutation of conserved residues in other RNA methyltransferases (e.g. D55 in KamB or D156 in Sgm) rendered these enzymes unable to confer resistance, mutation of conserved D55 of NpmA to alanine did not hinder ability of the enzyme to catalyze methylation or confer resistance *in vivo*, suggesting that NpmA might have the capacity to overcome defects in

SAM binding via its interaction with the 30S subunit (50). A similar phenomenon has been reported in m<sup>1</sup>A1408 methyltransferase Kmr, which methylates A1408 despite a complete lack of SAM binding affinity (51).

Although SAM-binding regions of this class of enzymes are relatively conserved, the points of contact and specific molecular mechanisms mediating substrate recognition can vary drastically. KamB and NpmA have almost identical structures with the only substantial variability seen in the extended loop that links  $\beta$ -strands 5 and 6 ( $\beta$ 5/6 linker). As one of only three unique extensions to the core SAM-binding fold, it was proposed that the NpmA  $\beta$ 5/6 linker is involved in interaction with the 30S substrate, contributing to target binding and specificity (45). Additionally, structural insertions in the region connecting  $\beta$ -strands 6 and 7 ( $\beta$ 6/7 linker) have previously been identified to influence methyltransferase-substrate interaction (46). In KamB, Trp193, Arg196, and Arg 201 in the linkers of  $\beta$ -strands 6 and 7 have been identified as critical for target rRNA recognition and methyltransferase activity. In contrast, in NpmA, only Trp197 appears to be essential (50). In NpmA, Trp107 and Trp197 are predicted to play vital roles in stabilization and methylation (50, 52). Similarly in KamB, equivalent conserved residues Trp105 and Trp193 that line the SAM binding pocket have been predicted to bind and properly position ribosomal nucleotide A1408 for proper methyltransfer (45).

Structural analysis of the NpmA-SAM complex, mutagenesis of proposed critical residues and subsequent functional analyses, and comparison to related enzymes revealed valuable insight into NpmA's mode of action and substrate specificity. However, without a crystal structure of NpmA bound to its 30S substrate, the specific contacts to the 30S and precise mechanism of action remained unclear. Observed differences in NpmA

structure and origin, conserved residues, and properties of action in comparison to related enzymes necessitate further study. Most alarming is the potential for transmissibility and resistance in diverse microbial species with little to no adaptation. A deeper understanding of the mechanism NpmA employs to recognize and bind its substrate, as well as the mechanism of its enzymatic activation, are crucial to understand precisely how this enzyme works, as this may provide insight for development of specific inhibitors for A1408 methyltransferase enzymes.

## **PART VII: CLINICAL SIGNIFICANCE AND EPIDEMIOLOGY**

Emergence of exogenously acquired 16S rRNA methyltransferase genes is of increasing concern as a threat to aminoglycoside antibiotics in the clinic, especially considering the potential for their global dissemination. 16S rRNA methyltransferases were initially thought to be solely derived from drug-producers, however, pathogen-derived enzymes isolated from clinical strains are beginning to be reported with increased incidence, and are of concern due to the consistently high levels of resistance they confer (25, 37, 42, 53). The genes encoding these enzymes are transmissible by way of transposons or plasmids, often in conjunction with multi-drug resistance genes, and thus horizontal transmission is a serious threat to clinical efficacy of aminoglycosides as continued treatment for serious infections caused by gram-positive and gram-negative bacteria (25, 26, 37).

To date, 16S rRNA methyltransferase genes have been isolated from pathogenic microbes all over the world. RmtB and ArmA, both acquired G1405-modifying enzymes, have been reported in East Asia, North and South America, Europe, and Oceania from several *Enterobacteriaceae* family members, including *Shigella flexneri* and *Acinetobacter* species (26). RmtB-producing microbes have been isolated from both pets and livestock, suggesting that zoonotic transmission might be possible for these resistance determinants. Additionally, ArmA was detected in a *Salmonella enterica* strain isolated from chicken meat on a French island in the Indian Ocean, hinting at the potential for 16S rRNA methyltransferase gene transmission through the food chain (54). Although some 16S rRNA methyltransferases have been sporadically found, others have been identified with increasing incidence from relatively unexpected sources, which highlights the necessity to characterize molecular mechanisms of these enzymes and more directly examine the epidemiological impact of this resistance determinant (26).

Of primary concern is the potential for accumulation of multidrug resistance in pathogenic microbes. In an increasing number of members of the *Enterobacteriaceae* family, 16S rRNA methyltransferases are coproduced with NDM-1 metallo- $\beta$ -lactamase, sometimes existing on the same conjugative plasmid (55, 56). In a *Pseudomonas aeruginosa* clinical strain in Brazil, RmtD was reported to be coproduced with SPM-1, a clinically relevant NDM-1 metallo- $\beta$ -lactamase. Interestingly, this strain was isolated from an urban river, suggesting the potential for environmental-propagated dissemination of these genes (57). Additionally, reports have shown that ArmA has been coproduced with several carbapenemases in *Acinetobacter baumannii* and *Enterobacteriaceae* strains in the United States, China, India, Poland, Greece and South Korea (26). If microbes

producing 16S rRNA methyltransferases were to acquire and coproduce carbapenem hydrolyzing  $\beta$ -lactamases, treatment of Gram-negative pathogens would be severely hindered in the clinic (26).

Currently, there is no established screening protocol for detection of m<sup>1</sup>A1408 methyltransferase enzymes. To combat this resistance determinant, an intentional effort must be coordinated not only to examine current coproduction of 16S rRNA methyltransferase enzymes with other resistance genes in pathogenic strains, but also to anticipate and track future threats to clinical aminoglycoside use. 16S rRNA methyltransferase enzymes are documented as conferring a high level of aminoglycoside resistance exclusively in Gram-negative pathogens to date, but studies have shown that when expressed under native promoters in heterologous Gram-positive bacteria, these enzymes are functional and confer high levels of resistance in *Bacillus subtilis* and *Staphylococcus aureus* (58, 59). The unprecedented higher and broader level of resistance conferred by NpmA, together with its potential for quick evolution and transmission, underscore the urgency of understanding this threat to clinical use of aminoglycoside antibiotics. The development of potent inhibitors to block 16S rRNA methyltransferase activity is one potential solution for restoring the clinical efficacy of these drugs, but a more robust understanding of the mode of interaction between these enzymes and their 30S substrate is required to tackle this goal.

### **Goals of this work**

The work presented here seeks to obtain a robust understanding of the precise molecular mechanism of interaction between 16S rRNA methyltransferase NpmA and its 30S

substrate. Ultimately, in elucidating the molecular details of substrate recognition, base flipping, and nucleotide modification for this resistance mechanism, we hope to lay the groundwork for development of specific inhibitors of the 16S rRNA methyltransferase enzymes. Additionally, insight gleaned from this work might provide a framework by which to understand the action of similar enzymes to combat the threat to clinically useful aminoglycoside antibiotics

## References

1. Poehlsgaard J, Douthwaite, S. (2005) The bacterial ribosome as a target for antibiotics. *Nature Reviews Microbiology* 3(11):870-881.
2. Connolly K, Culver, G. (2009) Deconstructing ribosome construction. *Trends in Biochem Sci* 34(5):256-263.
3. Steitz TA (2008) A structural understanding of the dynamic ribosome machine. *Nature Reviews Molecular Cell Biology* 9:242-253.
4. Snyder L, Champness, W. (2007) *Molecular Genetics of Bacteria* (ASM Press, Washington, DC) 3rd Ed.
5. Strunk BS, Karbstein, K. (2009) Powering through ribosome assembly. *RNA* 15(12):2083-2104.
6. Kaczanowska M, Ryden-Aulin, M. (2007) Ribosome biogenesis and the translation process in *Escherichia coli*. *Microbiology and Molecular Biology Reviews* 71(3):477-494.
7. Traub P, Nomura, M. (1969) Structure and function of *Escherichia coli* ribosomes. VI. Mechanism of assembly of 30 s ribosomes studied in vitro. *J Mol Biol* 40(3):391-413.
8. Woodson SA (2008) RNA folding and ribosome assembly. *Curr Opin Chem Biol* 12(6):667-673.
9. Williamson JR (2003) After the ribosome structures: How are the subunits assembled? *RNA* 9(2):165-167.

10. Earnest TM, Lai, J., Chen, K., Hallock, M.J., Williamson, J.R., Luthey-Schulten, Z. (2015) Toward a whole-cell model of ribosome biogenesis: kinetic modeling of SSU assembly. *Biophysical Journal* 109:1117-1135.
11. Shajani Z, Sykes, M.T., Williamson, J.R. (2011) Assembly of Bacterial Ribosomes. *Annual Review of Biochemistry* 80:501-526.
12. Held WA, Nomura, M. (1973) Rate-determining step in the reconstitution of Escherichia coli 30S ribosomal subunits. *Biochemistry* 12(17):3273-3281.
13. Decatur WA, Fournier, M.J. (2002) rRNA modifications and ribosome function. *Trends in Biochem Sci* 27(7):344-351.
14. Green R, Noller, H.F. (1996) In vitro complementation analysis localizes 23S rRNA postranscriptional modifications that are required for Escherichia coli 50S ribosomal subunit assembly and function. *RNA* 2:1011-1021.
15. Nesterchuk MV, Sergiev, P.V., Dontsova, O.A. (2011) Posttranslational modifications of ribosomal proteins in Escherichia coli. *Acta Naturae* 3(2):22-33.
16. Xu Z, O'Farrell, H.C., Rife, J.P., Culver, G.M. (2008) A conserved rRNA methyltransferase regulates ribosome biogenesis. *Nat Struct Mol Biol* 15:534-536.
17. Ramakrishnan V (2002) Ribosome structure and the mechanism of translation. *Cell Cycle* 108:557-572.
18. Laskaris P, Tolba, S., Calvo-Bado, L., Wellington, L. (2010) Coevolution of antibiotic production and counter-resistance in soil bacteria. *Environmental Microbiology* 12(3):783-796.
19. Martinez JL (2008) Antibiotics and antibiotic resistance genes in natural environments. *Science* 321:365-367.

20. Williams ST, Vickers, J.C. (1986) The ecology of antibiotic production. *Microbial Ecology* 12(1):43-52.
21. Yonath A (2005) Antibiotics targeting ribosomes: resistance, selectivity, synergism, and cellular regulation. *Annual Review of Biochemistry* 74:649-679.
22. Wilson DN (2014) Ribosome-targeting antibiotics and mechanisms of bacterial resistance. *Nature Reviews* 12:35-48.
23. Jana S, and Deb, J.K. (2006) Molecular understanding of aminoglycoside action and resistance. *Applied Microbiology and Biotechnology* 70:140-150.
24. Kotra LP, Haddad, J. and Mobashery, S. (2000) Aminoglycosides: perspectives on mechanisms of action and resistance and strategies to counter resistance. *Antimicrobial Agents and Chemotherapy* 44:3249-3256.
25. Doi Y, and Arakawa, Y. (2007) 16S ribosomal RNA methylation: emerging resistance mechanisms against aminoglycosides. *Antimicrobial Resistance* 45:88-94.
26. Wachino JI, Arakawa, Y. (2012) Exogenously acquired 16S rRNA methyltransferases found in aminoglycoside-resistant pathogenic Gram-negative bacteria: an update. *Drug Resist Updat* 15(3):133-148.
27. Mingeot-Leclercq MP, Tulkens, P.M. (1999) Aminoglycosides: nephrotoxicity. *Antimicrobial Agents and Chemotherapy* 43(5):1003-1012.
28. Mingeot-Leclercq MP, Glupczynski, Y., Tulkens, P.M. (1999) Aminoglycosides: activity and resistance. *Antimicrobial Agents and Chemotherapy* 43(4):727-737.
29. Pfister P, Hobbie, S., Vicens, Q., Bottger, E.C., and Westhof, E. (2003) The molecular basis for A-site mutations conferring aminoglycoside resistance:

relationship between ribosomal susceptibility and x-ray crystal structures.

*ChemBioChem* 4.

30. Carter AP, Clemons, W.M., Brodersen, D.E., Morgan-Warren, R.J., Wimberly, B.T., and Ramakrishnan, V. (2000) Functional insights from the structure of the 30S ribosomal subunit and its interaction with antibiotics. *Nature* 407:340-348.
31. Vicens Q, and Westhof, E. (2001) Crystal structure of paromomycin docked into the eubacterial ribosomal decoding A site. *Structure* 9:647-658.
32. Vicens Q, and Westhof, E. (2002) Crystal structure of a complex between the aminoglycoside tobramycin and an oligonucleotide containing the ribosomal decoding A site. *Chemistry & Biology* 9:747-755.
33. Francois B, Russell, R.J.M., Murray, J.B., Aboul-ela, F., Masquida, B., Vicens, Q., and Westhof, E. (2005) Crystal structures of complexes between aminoglycosides and decoding A site oligonucleotides: role of the number of rings and positive charges in the specific binding leading to miscoding. *Nucleic Acids Research* 33:5677-5690.
34. Kaul M, Barbieri, C.M., Pilch, D.S. (2005) Defining the basis for the specificity of aminoglycoside-rRNA recognition: a comparative study of drug binding to the A sites of Escherichia coli and human rRNA. *Journal of Molecular Biology* 346(1):119-134.
35. D'Costa VM, King, C.E., Kalan, L., Morar, M., Sung, W.W.L., Schwarz, C., Froese, D., Zacula, G., Calmels, F., Debruyne, R., Golding, G.B., Poinar, H.N., Wright, G.D. (2011) Antibiotic resistance is ancient. *Nature* 477:457-461.

36. Davies J, Davies, D. (2010) Origins and evolution of antibiotic resistance. *Microbiology and Molecular Biology Reviews* 74(3):417-433.
37. Koscinski L, Feder, M., and Bujnicki, J.M. (2007) Identification of a missing sequence and functionally important residues of 16S rRNA m1A1408 methyltransferase KamB that causes bacterial resistance to aminoglycoside antibiotics. *Cell Cycle* 6:1268-1271.
38. Conn GL, Savic, M., and Macmaster, R. (2008) DNA and RNA modification enzymes: structure, mechanism, function, and evolution., (Landes Bioscience).
39. Cundliffe E (1989) How antibiotic-producing organisms avoid suicide. *Annual Review of Microbiology* 43:207-233.
40. Savic M, Lovric, J. Tomic, T.I., Vasiljevic, B., and Conn, G.L. (2009) Determination of the target nucleosides for members of two families of 16S rRNA methyltransferases that confer resistance to partially overlapping groups of aminoglycoside antibiotics. *Nucleic Acids Research* 37.
41. Wachino JI, Shibayama, K., Kurokawa, H., Himura, K., Yamane, K., Suzuki, S., Shibata, N., Ike, Y., and Arakawa, Y. (2007) Plasmid-mediated novel m1A1408 methyltransferase NpmA, for 16S rRNA found in clinically isolated Escherichia coli resistant to structurally diverse aminoglycosides. *Antimicrobial Agents and Chemotherapy* 51:4401-4409.
42. Galimand M, Courvalin, P., and Lambert, T. (2003) Plasmid-mediated high-level resistance to aminoglycosides in Enterobacteriaceae due to 16S rRNA methylation. *Antimicrobial Agents and Chemotherapy* 47:2565-2571.

43. Shaw KJ, Rather, P.N., Hare, R.S., and Miller, G.H. (1993) Molecular genetics of aminoglycoside resistance genes and familial relationships of the aminoglycoside-modifying enzymes. *Microbiological Reviews* 57:138-163.
44. Doi Y, Wachino, J.I., Arakawa, Y. (2016) Aminoglycoside resistance: the emergence of acquired 16S ribosomal RNA methyltransferases. *Infectious Disease Clinics of North America* 30(2):523-537.
45. Macmaster R, Zelinskaya, N., Savic, M., Rankin, C.R., and Conn, G.L. (2010) Structural insights into the function of aminoglycoside-resistance A1408 16S rRNA methyltransferases from antibiotic-producing and human pathogenic bacteria. *Nucleic Acids Research* 38:7791-7799.
46. Schubert HL, Blumenthal, R.M., and Cheng, X. (2003) Many paths to methyltransfer: a chronical of convergence. *Trends in Biochem Sci* 28:329-335.
47. Kozbial PZ, and Mushegian, A.R. (2005) Natural History of S-adenosylmethionine-binding proteins. *BMC Structural Biology* 5.
48. Husain N, Tkaczuk, K.L., Tulsidas, S.R., Kaminska, K.H., Cubrilo, S., Maravic-Vlahovicek, G., Bujnicki, J.M., Sivaraman, J. (2010) Structural basis for the methylation of G1405 in 16S rRNA by aminoglycoside resistance methyltransferase Sgm from an antibiotic producer: a diversity of active sites in m7G methyltransferases. *Nucleic Acids Research* 38(12):4120-4132.
49. Yokoyama K, Doi, Y., Yamane, K., Kurokawa, H., Shibata, N., Shibayama, K., Yagi, T., Kato, H., Arakawa, Y. (2003) Acquisition of 16S rRNA methylase gene in *Pseudomonas aeruginosa*. *The Lancet* 362(9399):1888-1893.

50. Husain N, Obranic, S., Koscinski, L., Seetharaman, J., Babic, F., Bujnicki, J.M., Maravic-Vlahovicek, G., Sivaraman, J. (2011) Structural basis for the methylation of A1408 in 16S rRNA by a panaminoglycoside resistance methyltransferase NpmA from a clinical isolate and analysis of the NpmA interactions with the 30S ribosomal subunit. *Nucleic Acids Research* 39(5):1903-1918.
51. Savic M, Sunita, S. Zelinskaya, N., Desai, P.M., Macmaster, R., Vinal, K., Conn, G.L. (2015) 30S Subunit-Dependent Activation of the *Sorangium cellulosum* So ce56 Aminoglycoside Resistance-Confering 16S rRNA Methyltransferase Kmr. *Antimicrobial Agents and Chemotherapy* 59(5):2807-2816.
52. Dunkle JA, Vinal, K., Desai, P.M., Zelinskaya, N., Savic, M., West, D.M., Conn, G.L., and Dunham, C.M. (2014) Molecular recognition and modification of the 30S ribosome by the aminoglycoside-resistance methyltransferase NpmA. *PNAS* 59(5):2807-2816.
53. Schmitt E, Galimand, M., Panvert, M., Courvalin, P., Mechulam, Y. (2009) Structural Bases for 16S rRNA Methylation Catalyzed by ArmA and RmtB Methyltransferases. *Journal of Molecular Biology* 388:570-582.
54. Granier SA, Hidalgo, L., Millan, A.S., Escudero, J.A., Gutierrez, B., Brisabois, A., and Gonzalez-Zorn, B. (2011) ArmA methyltransferase in a monophasic *Salmonella enterica* isolate from food. *Antimicrobial Agents and Chemotherapy* 55(11):5262-5266.
55. Livermore DM, Mushtaq, S., Warner, M., Zhang, J.C., Maharjan, S., Doumith, M., Woodford, N. (2011) Activity of aminoglycosides, including ACHN-490,

- against carbapenem-resistant Enterobacteriaceae isolates. *Journal of Antimicrobial Chemotherapy* 66:48-53.
56. Poirel L, Al Maskari, Z., Al Rashdi, F., Bernabeu, S., Nordmann, P. (2011) Analysis of the resistome of a multidrug-resistant NDM-1-producing *Escherichia coli* strain by high-throughput genome sequencing. *Antimicrobial Agents and Chemotherapy* 55:4224-4229.
57. Fontes LC, Neves, P.R., Oliveira, S., Silva, K.C., Hachich, E.M., Sato, M.I., Lincopan, N. (2011) Isolation of *Pseudomonas aeruginosa* coproducing metallo- $\beta$ -lactamase SPM-1 and 16S rRNA methylase RmtD1 in an urban river. *Antimicrobial Agents and Chemotherapy* 55:3063-3064.
58. Liou GF, Yoshizawa, S., Courvalin, P., Galimand, M. (2006) Aminoglycoside resistance by ArmA-mediated ribosomal 16S methylation in human bacterial pathogens. *J Mol Biol* 359(2):358-364.
59. Wachino J, Shibayama, K., Kimura, K., Yamane, K., Suzuki, S., Arakawa, Y. (2010) RmtC introduces G1405 methylation in 16S rRNA and confers high-level aminoglycoside resistance on Gram-positive microorganisms. *FEMS Microbiology Letters* 311:56-60.

**CHAPTER 2:**

**Molecular recognition and modification of the 30S ribosome by the aminoglycoside-resistance methyltransferase NpmA**

**Molecular recognition and modification of the 30S ribosome by the aminoglycoside-resistance methyltransferase NpmA**

by

Jack A. Dunkle, Kellie Vinal, Pooja M. Desai, Natalia Zelinskaya, Miloje Savic,

Dayne M. West, Graeme L. Conn\* and Christine M. Dunham\*

Department of Biochemistry, Emory University School of Medicine, Atlanta GA 30322,

USA.

\*Correspondence: [gconn@emory.edu](mailto:gconn@emory.edu) or [cmdunha@emory.edu](mailto:cmdunha@emory.edu)

Data deposition: Crystallography, atomic coordinates, and structure factors have been deposited in the Protein Data Bank, [www.pdb.org](http://www.pdb.org) (PDB ID code 4OX9)

**Author contributions:** C.M.D. and G.L.C. designed the research; K.V. performed mutagenesis and MIC assays; P.M.D. and M.S. performed the RNA structure probing; N.Z. performed the methylation assays and purified NpmA; J.A.D. and D.M.W. crystallized the 30S; J.A.D. collected and processed X-ray crystallography data and refined the structure; J.A.D., C.M.D. and G.L.C. analyzed the structure and wrote the manuscript.

**Key words:** antibiotic resistance, methyltransferase, ribosome, RNA modification, base flipping

Published in Proceedings of the National Academy of Sciences

2014 Apr 29; 111(17): 6275-6280

## **Abstract**

Aminoglycosides are potent, broad spectrum, ribosome-targeting antibacterials whose clinical efficacy is seriously threatened by multiple resistance mechanisms. Here we report the structural basis for 30S recognition by the pathogen-derived aminoglycoside-resistance rRNA methyltransferase NpmA. These studies are supported by biochemical and functional assays that define the molecular features necessary for NpmA to catalyze m<sup>1</sup>A1408 modification and confer resistance. The requirement for the mature 30S as substrate for NpmA is clearly explained by its recognition of four disparate 16S rRNA helices brought into proximity by 30S assembly. Our structure captures a “precatalytic state” in which multiple structural reorganizations orient functionally critical residues to flip A1408 from helix 44 and position it precisely in a remodeled active site for methylation. Our findings provide a new molecular framework for the activity of aminoglycoside-resistance rRNA methyltransferases that may serve as a functional paradigm for other modification enzymes acting late in 30S biogenesis.

## **Introduction**

The ribosome is a complex macromolecular machine responsible for protein synthesis in all cells. The high sequence and structural conservation of key functional centers such as those for decoding and peptidyl transferase activity, make the ribosome a major target for antibiotics (1, 2). Aminoglycosides predominantly bind the ribosome in the decoding center of the 30S subunit and reduce the fidelity of decoding (3, 4). Chemical probing

and structures of aminoglycoside-bound ribosomal A-site model RNA and 30S subunit, localize the binding site within helix 44 (h44) (3, 5-7). Aminoglycoside binding causes two functionally critical rRNA nucleotides, A1492 and A1493, to flip from h44 and adopt positions that typically only arise from cognate tRNA-mRNA pairing (8). This drug-bound state thus allows for selection of incorrect tRNAs by the ribosome and results in aberrant protein production.

Aminoglycosides have historically been powerful tools in the clinic and though they remain in use today, the breadth of their application has been limited by toxicity and their replacement by alternative antibiotics. However, the emergence of pathogenic bacteria resistant to these alternatives has led to a reevaluation of aminoglycoside use, particularly against Gram-negative pathogens (9, 10). While efforts to circumvent aminoglycoside toxicity issues may broaden their application, any reprieve may be limited by the continued spread of resistance to this class of antibiotics. Currently, the most widely disseminated aminoglycoside-resistance determinants are drug modification enzymes but 16S ribosomal RNA (rRNA) methyltransferases that modify the drug binding site have recently emerged as a new and significant threat (10, 11). Unlike the drug modifying enzymes that typically act on a limited number of aminoglycosides, the two nucleobase modifications introduced by 16S rRNA aminoglycoside-resistance methyltransferases confer class-wide resistance to these drugs.

Aminoglycoside-resistance 16S rRNA methyltransferases are divided into two subfamilies that modify either G1405 or A1408 within h44 to produce m7G1405 or m1A1408, respectively (12). Although originally identified in Gram-positive aminoglycoside-producing actinomycetes, enzymes catalyzing these modifications have

been acquired by human and animal pathogens where they confer high level, broad spectrum resistance to classical and next generation aminoglycosides (10, 13). Enzymes of producer and pathogen origin have low sequence identity (typically ~25-30%) but recent structural studies have revealed high structural conservation within each subfamily (14-17). G1405 and A1408 modifying enzymes possess a common Class I methyltransferase S-adenosyl-L-methionine (SAM)-binding fold containing a seven-stranded,  $\beta$ -sheet core (Fig. S1A). However, they differ markedly in their auxiliary domains and/ or regions linking the core  $\beta$  strands. The G1405 methyltransferases have a large N-terminal domain that forms two  $\alpha$ -helical subdomains, while the A1408 enzymes possess a short  $\beta$  hairpin at their N terminus and large internal extensions between  $\beta$  strands  $\beta$ 5/ $\beta$ 6 and  $\beta$ 6/ $\beta$ 7. Despite these differences, both the G1405 and A1408 enzymes have an absolute requirement for the mature 30S as their substrate (18, 19). However, the molecular details of recognition and specific target nucleotide modification remain elusive.

Here, we report the 3.8 Å resolution X-ray crystal structure of the *Thermus thermophilus* (Tth) 30S ribosome subunit complexed with the A1408 methyltransferase NpmA, a plasmid-borne aminoglycoside resistance determinant identified in the clinical *E. coli* strain ARS3 (19). Together with complementary biochemical and functional studies, our results provide a first molecular framework for recognition and modification by an aminoglycoside-resistance rRNA methyltransferase that may be broadly applicable to other 16S rRNA modification enzymes that act on the 30S subunit.

## Results and Discussion

**Directed RNA structure probing orients NpmA on h44.** To determine the position and orientation of NpmA on the E. coli 30S subunit in solution, we performed directed hydroxyl radical probing using NpmA site-specifically derivatized with Fe-BABE (see Materials and Methods). Five single-Cys proteins representing a broad distribution of the probe across the NpmA surface were selected for directed structure probing experiments (**Fig. S2**). Three Fe(II)-modified NpmA proteins (NpmA-S89C, -E149C and -K151C) produced unique but partially overlapping 16S rRNA strand scission patterns in h44 at nts 1409-1412, 1419-1423 and 1481-1484 (**Fig. S2D**). These results clearly position the NpmA surface containing S89, E149 and K151 adjacent to h44. This places the extended region linking strands  $\beta 5$  and  $\beta 6$  ( $\beta 5/6$  linker), which contains the latter two residues, into close proximity with the target site. These results are in extremely good agreement with our Tth 30S-NpmA crystal structure (described below), which additionally identifies an extensive interaction surface with regions of 16S more distant from h44 and A1408.

**Overview of the 30S-NpmA-sinefungin complex.** The X-ray crystal structure of the Tth 30S subunit complexed with NpmA and the SAM analog sinefungin was determined at 3.8 Å resolution (**Fig. 1, Figs. S1B, S1C and Table S1**). Remarkably, this structure was obtained by soaking pre-formed 30S crystals (20) with the 25.2 kDa NpmA complexed with sinefungin. NpmA docks on h44 and the adjacent rRNA structure of a single 30S subunit, distant from any crystal contacts. Prior to crystallization experiments, we showed that NpmA methylates Tth 30S ribosomes as efficiently as those from E. coli confirming

our structure would represent an active state of the enzyme (**Fig. S1D**). These data, together with the corroborating evidence from our directed RNA probing using *E. coli* 30S, clearly demonstrate the veracity of our structure which captures NpmA in a “precatalytic state”, poised for methyl transfer to A1408.

NpmA forms an extensive interaction surface (1557 Å<sup>2</sup>) with the 16S rRNA structure formed by the juxtaposition of helices h24, h27, h44 and h45 (**Figs. 1B and 1C**). These four 16S rRNA helices are far apart in primary sequence but, in the context of the mature 30S subunit fold, form a single complex surface recognized by NpmA. This provides a clear structural rationale for the requirement of the fully assembled 30S as the substrate for NpmA and other A1408 methyltransferases. Despite the proximity of protein S12 to A1408 in the ribosomal A site (**Fig. 1A**), the 30S-NpmA interaction is mediated exclusively by recognition of the sugar-phosphate backbone of the conserved rRNA surface. In addition to verifying the location and likely role of the NpmA β5/6 linker adjacent to h44 as determined from RNA probing, the structure additionally identifies the NpmA β2/3 and β6/7 linker regions as playing critical roles in 30S docking (**Figs. 1B-F**). NpmA captures A1408 flipped from h44 and precisely positioned in its active site for catalysis. Our structure and comparisons with free NpmA suggest that docking and concerted conformational changes within the two unique extended regions (β5/6 and β6/7 linkers) mediate specific recognition of A1408 and control of catalysis through active site remodeling.

**Identification of residues critical for NpmA activity.** A limited number of NpmA residues proposed to be critical for SAM binding, recognition of the mature 30S or

catalysis have been previously investigated by mutagenesis and kanamycin minimum inhibitory concentration (MIC) measurements in *E. coli* (17). Mutation of two absolutely conserved Trp residues (W107 and W197) resulted in complete loss of resistance, clearly pointing to their critical role in catalysis or substrate positioning. However, no single point mutations of residues proposed to be involved in rRNA recognition reduced resistance. In contrast, similar studies on KamB, the A1408 methyltransferase from the tobramicin-producer *Streptoalloteichus tenebrarius*, identified several functionally important Arg and Lys residues (15). We reasoned that the extensive 30S-methyltransferase interaction surface must, in the case of NpmA, have sufficient redundancy that at least one contact may be lost without an observable effect on the level of kanamycin resistance. Therefore, we adopted two parallel strategies. First, each individual target mutation was made in two contexts, wild-type enzyme and a functionally compromised mutant (NpmA-E146A; kanamycin MIC 256-512  $\mu\text{g}/\text{ml}$ ). Second, two clusters of adjacent target residues, K66/K67 and K70/K71, were mutated at the same time (**Table S2**).

In the context of the NpmA-E146A mutant, individual mutation of residues distributed across the small N-terminal extension as well as the  $\beta$ 2/3,  $\beta$ 5/6 and  $\beta$ 6/7 linkers reduced resistance to kanamycin to 8-16  $\mu\text{g}/\text{ml}$  (**Table S2**). With two notable exceptions discussed below (R153E and R207E), each of these mutations produced no measurable decrease in activity when made in the wild-type context. This indicates that each of these residues contributes to the total binding interaction but loss of any one contact is sufficiently compensated by the remaining extensive interactions. Notably, three mutations made in the NpmA-E146A background did not further reduce the

kanamycin MIC (K8, F92 and Y145), indicating that second mutations made in the E146A context do not always inactivate the enzyme. These analyses demonstrate the importance of the entire buried NpmA surface for recognition and binding of the 30S. The NpmA  $\beta$ 2/3 linker is rich in Lys residues that, as a group, are well conserved among the A1408 methyltransferases. While individual mutation of these residues in the wild-type enzyme had no observable phenotype, kanamycin resistance was modestly reduced by double mutations (K66E/K67E or K70E/K71E) and completely ablated by the quadruple mutant (**Table S2**). As described below, these residues bridge the four disparate 16S rRNA helices contacted by NpmA, and collectively appear to play the predominant role in initial docking of NpmA onto the 16S rRNA surface.

**Sequence independent, tertiary contacts distant from the methylation site direct 30S-NpmA recognition.** The regions connecting  $\beta$  strands 2 and 3 ( $\beta$ 2/3 linker) and  $\beta$  strands 6 and 7 ( $\beta$ 6/7 linker) of NpmA are primarily responsible for recognition of the complex rRNA surface of the 30S (**Figs. 1D-F**). The  $\beta$ 2/3 linker contains an  $\alpha$  helix ( $\alpha$ 3) followed by a loop structure, that together comprise a highly basic extended surface sandwiched between the core of NpmA and the 30S subunit (**Fig. 1E and Fig. S3A**). This surface directly contacts all four rRNA helices bound by NpmA (h24, h27, h44 and h45). Helix  $\alpha$ 3 abuts h44 and forms two electrostatic contacts via K66 and K67 to h27 and h45 respectively, while the lysine-rich loop forms interactions via K70, K71 and K74 that measure the juxtaposition of h24 and h45 (**Figs. 2A and 2B**). Mutation of these residues decreased kanamycin resistance (**Table S2**), confirming their important role in 30S binding.

The  $\beta$ 2/3 linker is conformationally identical in the 30S-bound and free states (**Fig. S4**), suggesting it is a rigid structural element pre-formed for recognition of the complex electronegative surface created by h24, h27 and the h44/h45 junction. In contrast, the  $\beta$ 6/7 linker, which sits in a deep cleft between h44 and h45, undergoes a substantial local conformational change upon 30S binding (**Fig. S4**). Electrostatic and van der Waals contacts are made with the apex of the h45 tetraloop while R205 and R207 of NpmA reach into the minor groove of h44 and form electrostatic contacts with the phosphate of A1408 (**Fig. 2C**). The most significant conformational change upon 30S binding occurs in the NpmA  $\beta$ 5/6 linker. This change results in an electrostatic contact between R153 of the  $\beta$ 5/6 linker and the non-bridging phosphate oxygen of C1484 in h44 (**Fig. 2A**). C1484 is located approximately a half turn of helix away from A1408 in the center of a stretch of non-Watson-Crick base pairs that imparts an unusual RNA backbone geometry for recognition by NpmA.

Despite its extensive interactions across four rRNA helices and around the target nucleotide, NpmA makes only a single rRNA sequence-specific interaction. The universally conserved P106 introduces a sharp kink in the NpmA backbone that orients the F105 carbonyl group to hydrogen bond with the N6 amine of A1408 (**Fig. 3**). This single interaction between A1408 and F105 appears to serve as the only mechanism by which NpmA probes the identity of the target base. Limited need for direct discrimination of the target base may reflect the near universal conservation of A1408 in bacteria. Consistent with this, mutation of P106 has no impact on NpmA activity (17) and F105 is not strictly conserved (**Fig. S5**). Together, these observations suggest that NpmA is an

intrinsically promiscuous enzyme whose specificity is controlled primarily by 30S substrate recognition and subsequent allosteric changes that organize the active site.

**Pre-catalytic state shows A1408 flipped from h44 and poised for methylation.** In the presence of the catalytically inert SAM analog sinefungin, the 30S-NpmA complex is trapped in a “pre-catalytic” state revealing the molecular mechanism of A1408 positioning in the NpmA active site (**Fig. 3 and Fig. S6**). Initial unbiased FO – FO difference electron density maps clearly show A1408 flipped out of h44 and rotated approximately 180° around its helical axis (**Fig. 3A**). Two arginine residues within the  $\beta$ 6/7 linker, R205 and R207, make electrostatic interactions at the A1408 phosphate that appear to promote or stabilize the necessary RNA backbone structural reorganization (**Fig. 2C**). Our NpmA functional data show that only R207 is critical for activity (**Table S2**) indicating that it must be the main driver of local conformational changes that flip A1408 from h44. Precise positioning of R207 also appears dependent upon a charged hydrogen bond made with E146 (**Fig. 4**), mutation of which also substantially reduces NpmA activity (**Table S2**). While the position of R207 is similar in the 30S-bound and free NpmA structures (PDB ID 3MTE) (15), the major structural rearrangement of the  $\beta$ 5/6 linker is required to bring E146 into position to fulfill this role. Therefore, in addition to positioning R153 for recognition of h44, the structural reorganization of  $\beta$ 5/6 (**Fig. 4 and Fig. S4**) also directly promotes A1408 base flipping.

Removal of A1408 from the base stacked environment of h44 is stabilized by  $\pi$ -stacking of the adenine base between two universally conserved and functionally critical tryptophan residues, W107 and W197, in the NpmA active site (**Fig. 3B**). These residues

position the adenine N1 directly adjacent to the NpmA-bound SAM analog. Comparison of the free (PDB ID 3MTE) and 30S-bound NpmA structures indicates that a re-orientation of W107 and W197 is required to accommodate the target nucleotide into the NpmA active site (**Video S1**). Mutation of either Trp to Ala or Phe completely abolishes NpmA activity (15, 17), confirming their critical role in precise positioning of the target nucleotide.

Our structure of the 30S-NpmA complex reveals an NpmA active site that is poised for catalysis with the A1408 N1 atom positioned 3.4 Å away from the sinefungin amino group that replaces the reactive methyl of the authentic cofactor SAM (**Fig. 3B**). The positioning of substrate and coenzyme is consistent with an SN2 reaction mechanism with N1 as the nucleophile (**Fig. S6**). Comparison of the positions of sinefungin and SAM in the 30S-NpmA and free NpmA-SAM complex (PDB IDs 3P2K, 3MTE) (15, 17) demonstrates that all interactions that delineate the cofactor binding pocket are maintained. However, the local structural reorganization of the  $\beta$ 6/7 linker causes it to more closely approach the methionyl moiety of the cofactor and reorientation of L196 positions its backbone carbonyl to make the only additional hydrogen binding interaction with the cofactor in the 30S-bound form of NpmA (**Fig. 3C**). This new interaction with the cofactor may influence NpmA activity by specifically enhancing its affinity for SAM and/ or promoting product release, exploiting the >30-fold higher affinity of free NpmA for the reaction by-product SAH (17).

**Mechanisms of molecular recognition, conformational adaptation and A1408 modification.** We propose that a sequence of events occurs during the 30S-NpmA

molecular recognition process to activate catalysis and ensure target site specificity. Initial docking of NpmA exploits two complementary rigid surfaces, the complex rRNA tertiary structure formed by helices h24, h27, h44 and h45, and the NpmA  $\beta$ 2/3 linker. This interaction promotes conformational changes in the NpmA  $\beta$ 5/6 and  $\beta$ 6/7 linkers, allowing R207 to capture h44 at the A1408 phosphate, promoting flipping of A1408. Finally, A1408 is sequestered in an intimate binding pocket completed by W107 and W197 closure onto the adenosine ring in an induced fit mechanism that precisely orients it for attack of the  $\epsilon$ -methyl of SAM. In support of this model, recent studies of the DNA methyltransferase M.HhaI offer a precedent for base flipping before active site closure (21).

DNA methyltransferases promote base flipping by destabilizing the helix around the target nucleotide and stabilizing the flipped state by replacement of DNA base pairing and stacking with protein-DNA interactions (22). In contrast to the Watson-Crick base paired target of DNA methyltransferases, A1408 is located in h44 opposite A1492/A1493 but forms only a single hydrogen bond to A1493. Nucleotides A1492/A1493 are essential to the high fidelity of decoding and are themselves conformationally dynamic to allow for inspection of the mRNA-tRNA pair (8). Thus, A1408 may be more readily flipped by virtue of the inherent dynamics in this region of h44 such that the major role of NpmA is to capture and stabilize the flipped conformation by the concerted action of initial docking and the critical molecular interactions mediated by NpmA residues R207, W107 and W197.

**Mechanistic conservation and variation among aminoglycoside-resistance 16S rRNA methyltransferases.** As the A1408 aminoglycoside-resistance methyltransferases are highly divergent in sequence, we asked whether the 30S recognition and base flipping mechanisms revealed by our structure might be conserved among these enzymes. Despite having only ~30% identity in amino acid sequence, the NpmA and KamB structures are essentially identical, with the only significant conformational differences found in the  $\beta$ 5/6 linker (15). Mutagenesis of KamB implicated the  $\beta$ 2/3 and  $\beta$ 6/7 linkers in a putative 30S binding surface, and alignment of KamB onto the 30S-bound NpmA structure confirms that these regions are positioned to interact with the same complex rRNA surface formed by h24, h27, h44 and h45 (**Figs. S3B & S7 and Table S2**). The strong functional conservation of residues important for both NpmA and KamB activity indicates that the 30S docking and target nucleotide recognition mechanisms, mediated primarily by the  $\beta$ 2/3 and  $\beta$ 6/7 linkers, respectively, are common to all A1408 methyltransferases. Absolute conservation of the functionally critical Trp residues (107 and 197 in NpmA) also indicates that A1408 base flipping is a common mechanistic feature.

Although these global recognition features are likely conserved, comparison of the 30S-NpmA structure and 30S-KamB model, taken with functional data on both enzymes, suggests that they differ in the specific molecular details of their action. For example, we identify here a single NpmA residue (R207) that is critical for base flipping via its interaction with the A1408 phosphate group but mutation of the equivalent residue in KamB (R203) has minimal effect on activity (**Table S2**). Additionally, there is no obvious equivalent in the KamB  $\beta$ 5/6 linker of NpmA residue E146, which supports

R207 in its role in A1408 base flipping. Instead, KamB activity is ablated by mutation of R196 or R201 (15), suggesting that in KamB they act in concert to fulfill the role of NpmA R207. Thus, while these enzymes are functionally equivalent, in that they both methylate N1 of A1408 and they exploit the same 30S features for substrate recognition, they differ in the molecular details of their action. Whether the A1408 methyltransferase family adopts further heterogeneous molecular mechanisms built upon a common mode of global recognition will require detailed structural and functional analyses of additional enzymes in this family.

The G1405 subfamily of aminoglycoside-resistance 16S rRNA methyltransferases differ substantially in their structures compared to enzymes targeting A1408. While these enzymes are built upon the same SAM-binding core fold, they lack equivalents of the NpmA  $\beta$ 5/6 and  $\beta$ 6/7 extensions that are critical for 30S recognition by A1408 methyltransferases. Additionally, although the  $\alpha$  helix of the  $\beta$ 2/3 linker is preserved, it is occluded by the large N-terminal extension in the G1405 enzymes that appears to direct 30S interactions (14, 16). Nonetheless, given the proximity of G1405 and A1408 and their common requirement for the intact 30S as substrate, the G1405 enzymes must presumably exploit similar features of the conserved 16S rRNA tertiary surface.

**Modification enzymes may target nucleotides in the decoding center by a common mechanism.** Modification of 16S rRNA confers antibiotic resistance, but also serves to regulate ribosome biogenesis and fine tune protein synthesis (23). 16S rRNA contains 10 mono- or dimethylated nucleotides and a single pseudouridine that form two distinct clusters within the 30S subunit (24, 25): lining the mRNA tunnel and the decoding center,

adjacent to the aminoglycoside-resistance modifications (Fig. S8). There is an apparent dichotomy in substrate requirement between the enzymes responsible for these two modification clusters. Enzymes acting around the mRNA tunnel typically methylate naked 16S RNA or some form of pre-30S subunit. In contrast, like the aminoglycoside-resistance methyltransferases, the six enzymes responsible for the cluster of methylations within the decoding center require a fully assembled 30S subunit. We predict that each of these enzymes will exploit features of the h24, h27, h44/h45 tertiary surface to achieve their target recognition and specificity. Our results thus provide the first molecular basis for what may be a common mechanism of 30S particle recognition in a sequence-independent but tertiary structure-dependent manner.

The cryo-EM structure of one of these intrinsic 16S rRNA methyltransferases, RsmA (formerly KsgA), bound to the 30S was determined recently (26). RsmA acts late in 30S biogenesis, dimethylating A1518 and A1519 in h45 in a step that has been proposed to signal the end of subunit assembly (27). The cryo-EM structure of the 30S-RsmA complex offered the first structural evidence that specificity may be governed by the juxtapositioning of multiple rRNA helices. However from this low resolution analysis, it was not possible to judge whether sequence-dependent contacts are made in addition to the recognition of RNA tertiary structure. In RsmA, the core SAM-binding fold is embellished with a large C-terminal domain that is positioned to interact with h24 and h27 of 16S rRNA and may direct specificity by orienting the enzyme active site over the target nucleotides. Our structure of the 30S-NpmA complex provides a precedence for specific recognition in the absence of any sequence specific contacts and reliance solely on interactions with the sugar-phosphate backbone of juxtaposed rRNA helices

that form in the mature particle. Steric accessibility of the target site may explain why NpmA and RsmA rely on recognition of tertiary features while other modification enzymes that act early in ribosome biogenesis, recognize sequence. Further structural studies will need to be determined to verify whether this theme linking recognition with the stage of ribosome maturity generally holds true.

**Feasibility of horizontal gene transfer to other pathogens.** Extensive evidence indicates that antibiotic resistance genes are ancient and exist within microbial communities in pristine environments (28-30). Acquired resistance genes in pathogens are presumed to originate from these sources, with their prevalence enriched by exposure to antibiotic (mis)use in agriculture and medicine. This raises the important question of how easily might other pathogenic microbes acquire and exploit resistance determinants like NpmA.

The strong conservation of the complex tertiary surface exploited by NpmA suggests it is very likely to be active in all bacterial species without significant adaptation. Indeed A1408 and G1405 enzymes have been found to be fully active in all heterologous systems tested to date (31-33). Together, these data and our new mechanistic insights into NpmA action suggests that there exists no major impediment to the rapid spread of A1408 aminoglycoside-resistance activity among pathogenic bacterial populations. However, the highly conserved nature of the A1408 methyltransferase docking site also presents a novel target for development of specific inhibitors of these resistance determinants.

## Materials and Methods

**Fe-BABE-directed 16S rRNA Structure Probing.** Directed hydroxyl radical probing of 16S rRNA using single cysteine NpmA mutants derived with Fe(II)-1-(p-bromoacetamidobenzyl)-EDTA (Fe-BABE) was performed essentially as previously described (27, 34). Further details can be found in SI Materials and Methods.

### **NpmA Mutagenesis and Kanamycin Minimum Inhibitory Concentration (MIC)**

**Assays.** The ability of NpmA mutants to support bacterial growth in the presence of kanamycin (0-1024  $\mu\text{g/mL}$ ) was measured in liquid culture. The MIC was determined as the lowest kanamycin concentration that fully inhibited growth. Further details can be found in SI Materials and Methods.

**Structural determination of the 30S -NpmA-sinefungin complex.** Tth 30S subunits were purified, crystallized and cryoprotected, and *E. coli* NpmA protein was purified as previously described (20, 35). NpmA-sinefungin (SFG) complex was incubated with pre-formed 30S crystals and flash frozen in liquid nitrogen. X-ray diffraction data were collected from two well-diffracting crystals at the Northeastern Collaborative Access Team (NE-CAT) beamline 24-ID-C of the Advanced Photon Source (Argonne, IL) (**Table S1**). Data reduction and merging were completed with XDS (36).

Crystallographic refinement was performed in PHENIX (37) followed by iterative rounds of manual rebuilding in Coot (38). Figure preparation was performed in PyMOL (39).

**ACKNOWLEDGMENTS** We thank J. Marquez for technical assistance and D. Reines and X. Cheng for discussion and comments. This work was funded by NIH-NIAID (R01-AI088025 to GLC) and in part by the NIH-NIGMS (R01-GM093279 to CMD). CMD is a Pew Scholar in the Biomedical Sciences. This work is based on research conducted at the Advanced Photon Source on the NE-CAT beamlines, which is supported by NIH-NCRR Award RR-15301, and at the SER-CAT beamline. Use of the Advanced Photon Source, an Office of Science User Facility operated for the US Department of Energy (DOE) Office of Science by Argonne National Laboratory, was supported by the US DOE under Contract DE-AC02-06CH11357.

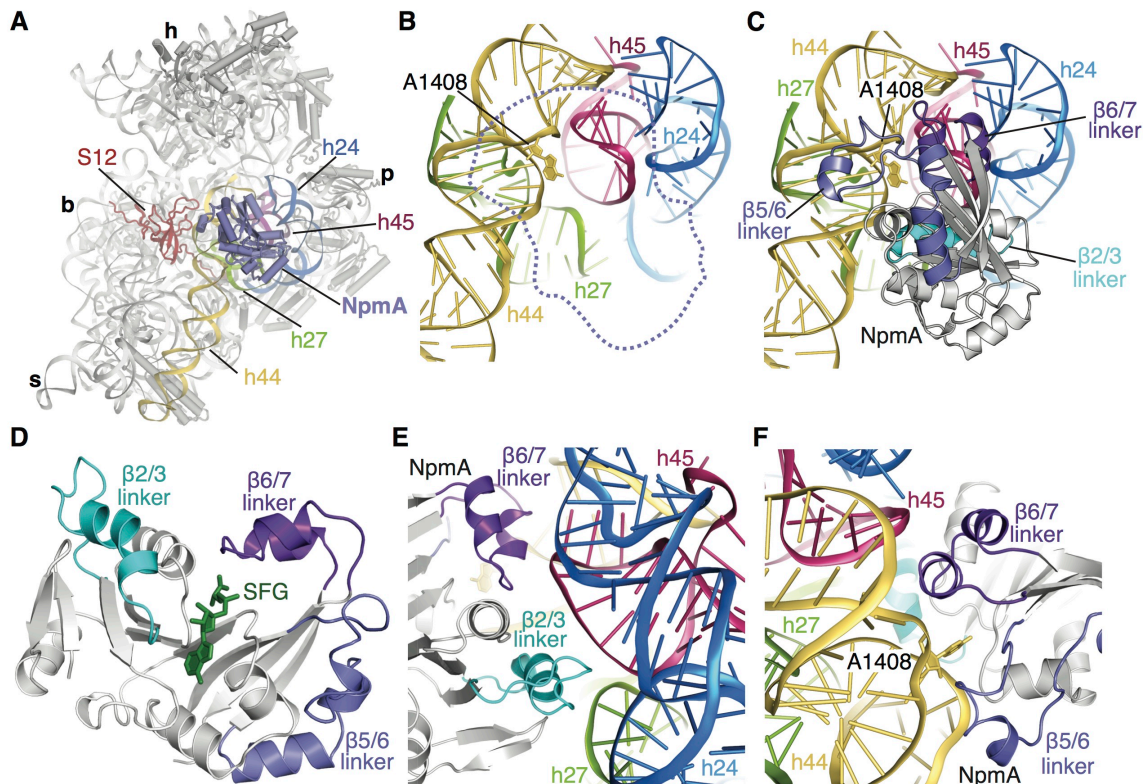


**Figure 1. X-ray crystal structure of the 30S subunit-NpmA complex.**

(A) NpmA (purple) binds at the 30S decoding center and interacts with four 16S rRNA helices: h24 (blue), h27 (green), h44 (yellow) and h45 (magenta). Features of the 30S are labeled as head (h), platform (p), spur (s), and body (b).

(B) Close-up view of the complex 16S rRNA tertiary structure recognized by NpmA indicated by a dotted purple line. The A1408 target nucleotide is shown as sticks.

(C) Same view of the 16S rRNA surface but with the bound NpmA shown as a cartoon.

(D) NpmA regions mediating most contacts with 16S rRNA highlighted:  $\beta$ 2/3 linker (cyan),  $\beta$ 5/6 linker (slate) and  $\beta$ 6/7 linker (purple). Sinefungin (SFG) is shown as sticks (green).

**(E),(F)** The rigid  $\beta$ 2/3 linker makes intimate contacts with h24, h27 and h45 while the  $\beta$ 6/7 linker recognizes the junction of h44 and h45. The  $\beta$ 5/6 linker makes an additional contact to h44 below the A1408 target nucleotide.

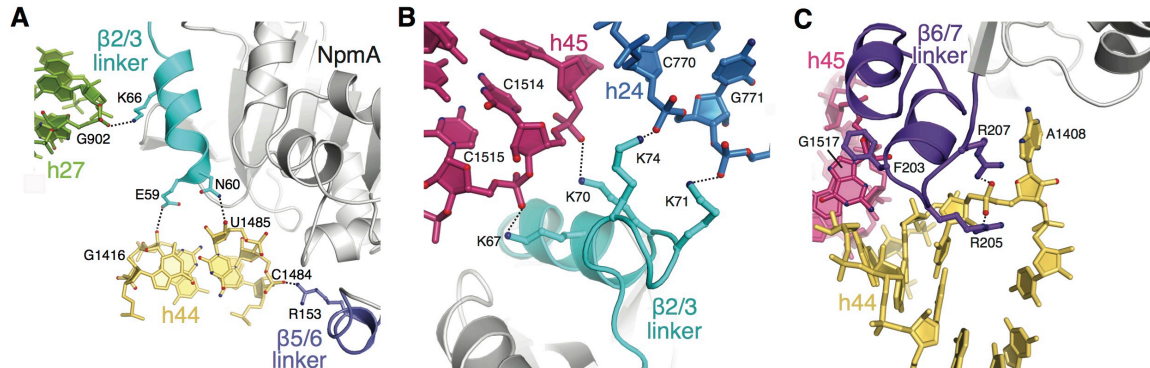


**Figure 2. NpmA makes multiple contacts across the complex 16S rRNA surface formed by h24, h27, h44 and h45.**

**(A)** The NpmA  $\beta$ 2/3 linker (cyan) forms an electrostatic contact with h27 (green) and hydrogen bonding interactions to a ribose group on each strand of h44 (yellow) that measure the minor groove width. An additional electrostatic contact is formed at an adjacent h44 residue by the  $\beta$ 5/6 linker (slate).

**(B)** A highly basic loop in the NpmA  $\beta$ 2/3 linker recognizes the juxtaposition of h45 (magenta) and h24 (blue) through multiple electrostatic interactions with rRNA backbone.

**(C)** The NpmA  $\beta$ 6/7 linker (purple) reaches into a narrow cleft between h44 and h45 of 16S rRNA. F203 stacks with the tetraloop of h45, while R205 and R207 reach into the h44 minor groove to make electrostatic interactions with the phosphate group of the target nucleotide A1408 which is flipped out of the h44 base stack.

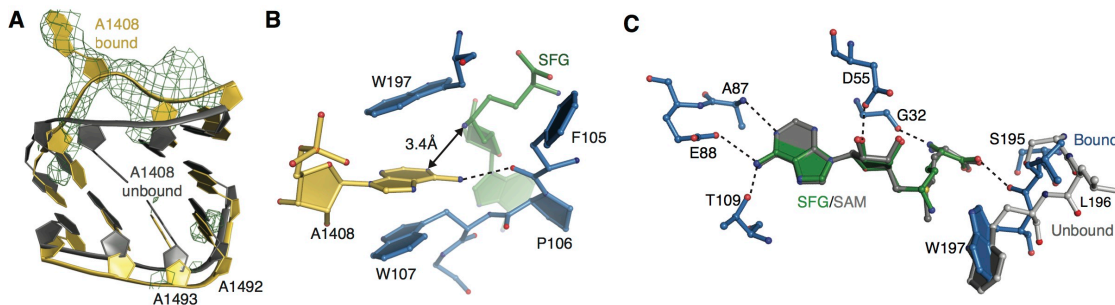


**Figure 3. A1408 is flipped from h44 and sequestered in a remodeled NpmA active site.**

**(A)** When NpmA is bound (yellow), A1408 is flipped from h44 as shown by the isomorphous difference electron density (green mesh), contoured at  $3\sigma$ . The structure of the same region of h44 in the absence of NpmA is shown for comparison (PDB ID 1J5E; gray).

**(B)** A1408 is intimately sequestered within the NpmA active site (blue sticks). Residues W107 and W197 form  $\pi$ -stacking interactions with A1408 and the carbonyl of F105 forms a hydrogen bond to the adenine N6.

**(C)** Comparison of the cofactor binding pocket with SFG (green) in the 30S-NpmA-SFG complex structure and SAM (gray) in the free NpmA-SAM complex (PDB ID 3MTE). The cofactor orientation (RMSD 0.3 Å) and interactions with amino acids are maintained. One additional hydrogen bonding interaction between the carbonyl of L196 and the SFG carboxyl group specific to the co-factor mimic in the 30S-bound structure results from the local reorganization of the  $\beta$ 6/7 linker.

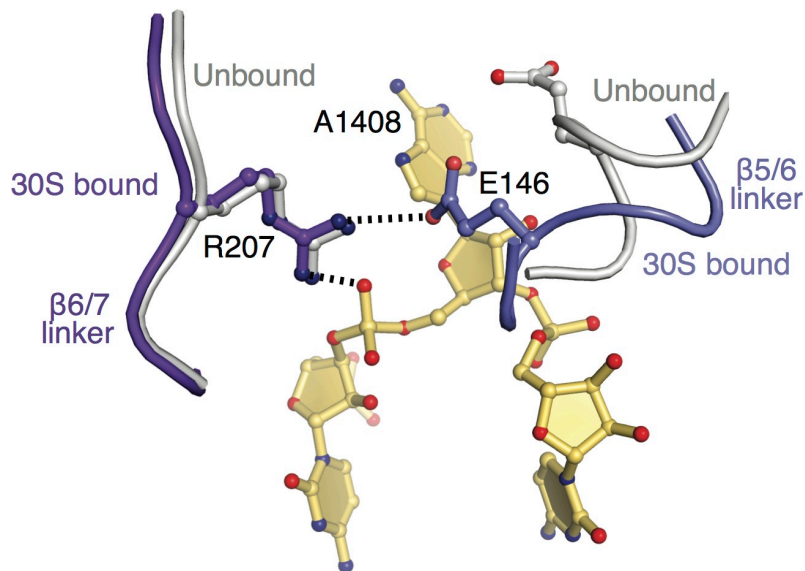


**Figure 4. A conformational change in the  $\beta$ 5/6 linker positions E146 to support the role of R207 in A1408 base flipping.** Arginine 207 is conformationally static in the 30S-bound (purple) and free (gray) forms (PDB ID 3MTE) of NpmA but would sterically clash with the phosphate group of A1408 in the absence of base flipping. Rearrangement of the  $\beta$ 5/6 linker (slate) brings E146 into position to form a charged hydrogen bond with R207 that acts as a buttress, forcing A1408 to flip to avoid the steric clash.

## References

1. Wilson DN (2014) Ribosome-targeting antibiotics and mechanisms of bacterial resistance. *Nat Rev Micro* 12(1):35-48.
2. Franceschi F (2007) Back to the future: the ribosome as an antibiotic target. *Future Microbiol.* 2(6):571-574.
3. Moazed D & Noller HF (1987) Interaction of antibiotics with functional sites in 16S ribosomal RNA. *Nature* 327(6121):389-394.
4. Davies J, Gorini L, & Davis BD (1965) Misreading of RNA codewords induced by aminoglycoside antibiotics. *Mol. Pharmacol.* 1(1):93-106.
5. Fourmy D, Recht MI, Blanchard SC, & Puglisi JD (1996) Structure of the A site of *Escherichia coli* 16S ribosomal RNA complexed with an aminoglycoside antibiotic. *Science* 274(5291):1367-1371.
6. Carter AP, et al. (2000) Functional insights from the structure of the 30S ribosomal subunit and its interactions with antibiotics. *Nature* 407(6802):340-348.
7. Vicens Q & Westhof E (2002) Crystal structure of a complex between the aminoglycoside tobramycin and an oligonucleotide containing the ribosomal decoding a site. *Chem. Biol.* 9(6):747-755.
8. Ogle JM, et al. (2001) Recognition of cognate transfer RNA by the 30S ribosomal subunit. *Science* 292(5518):897-902.
9. Falagas ME, Grammatikos AP, & Michalopoulos A (2008) Potential of old-generation antibiotics to address current need for new antibiotics. *Expert Rev. Anti Infect. Ther.* 6(5):593-600.

10. Jackson J, Chen C, & Buising K (2013) Aminoglycosides: how should we use them in the 21st century? *Curr. Opin. Infect. Dis.* 26(6):516-525.
11. Ramirez MS & Tolmasky ME (2010) Aminoglycoside modifying enzymes. *Drug Resist Updat* 13(6):151-171.
12. Conn GL, Savic M, & Macmaster R (2009) Resistance to antibiotics in bacteria through modification of nucleosides in 16S ribosomal RNA. *DNA and RNA Modification Enzymes: Comparative Structure, Mechanism, Functions, Cellular Interactions and Evolution*, ed Grosjean H (Landes Bioscience, Austin, TX).
13. Wachino J & Arakawa Y (2012) Exogenously acquired 16S rRNA methyltransferases found in aminoglycoside-resistant pathogenic Gram-negative bacteria: an update. *Drug Resist Updat* 15(3):133-148.
14. Schmitt E, Galimand M, Panvert M, Courvalin P, & Mechulam Y (2009) Structural bases for 16 S rRNA methylation catalyzed by ArmA and RmtB methyltransferases. *J. Mol. Biol.* 388(3):570-582.
15. Macmaster R, Zelinskaya N, Savic M, Rankin CR, & Conn GL (2010) Structural insights into the function of aminoglycoside-resistance A1408 16S rRNA methyltransferases from antibiotic-producing and human pathogenic bacteria. *Nucleic Acids Res.* 38(21):7791-7799.
16. Husain N, et al. (2010) Structural basis for the methylation of G1405 in 16S rRNA by aminoglycoside resistance methyltransferase Sgm from an antibiotic producer: a diversity of active sites in m7G methyltransferases. *Nucl. Acids Res.*:doi:10.1093/nar/gkq1122

17. Husain N, et al. (2011) Structural basis for the methylation of A1408 in 16S rRNA by a panaminoglycoside resistance methyltransferase NpmA from a clinical isolate and analysis of the NpmA interactions with the 30S ribosomal subunit. *Nucleic Acids Res.* 39(5):1903-1918.
18. Zarubica T, Baker MR, Wright HT, & Rife JP (2011) The aminoglycoside resistance methyltransferases from the ArmA/Rmt family operate late in the 30S ribosomal biogenesis pathway. *RNA* 17(2):346-355.
19. Wachino J, et al. (2007) Novel plasmid-mediated 16S rRNA m1A1408 methyltransferase, NpmA, found in a clinically isolated *Escherichia coli* strain resistant to structurally diverse aminoglycosides. *Antimicrob. Agents Chemother.* 51(12):4401-4409.
20. Clemons WM, et al. (2001) Crystal structure of the 30 S ribosomal subunit from *Thermus thermophilus*: Purification, crystallization and structure determination. *J. Mol. Biol.* 310(4):827-843.
21. Matje DM, Krivacic CT, Dahlquist FW, & Reich NO (2013) Distal Structural Elements Coordinate a Conserved Base Flipping Network. *Biochemistry.*
22. Huang N, Banavali NK, & MacKerell AD, Jr. (2003) Protein-facilitated base flipping in DNA by cytosine-5-methyltransferase. *Proc. Natl. Acad. Sci. U. S. A.* 100(1):68-73.
23. Decatur WA & Fournier MJ (2002) rRNA modifications and ribosome function. *Trends Biochem. Sci.* 27(7):344-351.
24. Dunin-Horkawicz S, et al. (2006) MODOMICS: a database of RNA modification pathways. *Nucleic Acids Res.* 34(Database issue):D145-149.

25. Machnicka MA, et al. (2013) MODOMICS: a database of RNA modification pathways--2013 update. *Nucleic Acids Res.* 41(Database issue):D262-267.
26. Boehringer D, O'Farrell HC, Rife JP, & Ban N (2012) Structural insights into methyltransferase KsgA function in 30S ribosomal subunit biogenesis. *J. Biol. Chem.* 287(13):10453-10459.
27. Xu Z, O'Farrell HC, Rife JP, & Culver GM (2008) A conserved rRNA methyltransferase regulates ribosome biogenesis. *Nat. Struct. Mol. Biol.* 15(5):534-536.
28. Allen HK, et al. (2010) Call of the wild: antibiotic resistance genes in natural environments. *Nat Rev Microbiol* 8(4):251-259.
29. D'Costa VM, et al. (2011) Antibiotic resistance is ancient. *Nature* 477(7365):457-461.
30. Pruden A, Arabi M, & Storteboom HN (2012) Correlation between upstream human activities and riverine antibiotic resistance genes. *Environ. Sci. Technol.* 46(21):11541-11549.
31. Holmes DJ, Drocourt D, Tiraby G, & Cundliffe E (1991) Cloning of an aminoglycoside-resistance-encoding gene, kamC, from *Saccharopolyspora hirsuta*: comparison with kamB from *Streptomyces tenebrarius*. *Gene* 102(1):19-26.
32. Galimand M, Sabtcheva S, Courvalin P, & Lambert T (2005) Worldwide disseminated armA aminoglycoside resistance methylase gene is borne by composite transposon Tn1548. *Antimicrob. Agents Chemother.* 49(7):2949-2953.

33. Savic M, Lovric J, Tomic TI, Vasiljevic B, & Conn GL (2009) Determination of the target nucleosides for members of two families of 16S rRNA methyltransferases that confer resistance to partially overlapping groups of aminoglycoside antibiotics. *Nucleic Acids Res.* 37(16):5420-5431.
34. Culver GM & Noller HF (2000) Directed hydroxyl radical probing of RNA from iron(II) tethered to proteins in ribonucleoprotein complexes. *Methods Enzymol.* 318:461-475.
35. Zelinskaya N, Rankin CR, Macmaster R, Savic M, & Conn GL (2011) Expression, purification and crystallization of adenosine 1408 aminoglycoside-resistance rRNA methyltransferases for structural studies. *Protein Expr. Purif.* 75(1):89-94.
36. Kabsch W (2010) Integration, scaling, space-group assignment and post-refinement. *Acta Crystallogr. D Biol. Crystallogr.* 66(Pt 2):133-144.
37. Echols N, et al. (2012) Graphical tools for macromolecular crystallography in PHENIX. *J Appl Crystallogr* 45(Pt 3):581-586.
38. Emsley P, Lohkamp B, Scott WG, & Cowtan K (2010) Features and development of Coot. *Acta Crystallogr. D Biol. Crystallogr.* 66(Pt 4):486-501.
39. Schrodinger, LLC (2010) The PyMOL Molecular Graphics System, Version 1.3r1.

## Supplemental Materials and Methods

**Fe-BABE-directed 16S rRNA Structure Probing.** Directed hydroxyl radical probing of 16S rRNA using NpmA proteins site-specifically derived with Fe(II)-1-(p-bromoacetamidobenzyl)-EDTA (Fe-BABE) to initiate Fenton chemistry was performed essentially as described previously (1, 2). As NpmA contains no natural cysteines, single-Cys mutants were generated by mutation of NpmA at 15 unique surface sites. The accessibility of each introduced Cys residue for derivatization was assessed by modification with 7-diethylamino-3-([4'-(iodoacetyl) amino]phenyl)-4-methylcoumarin (DCIA). Methyltransferase activity was assessed using bacterial growth assays with kanamycin (MIC measurements), and [3H]-SAM in vitro methylation assays with purified mutant protein before and after derivatization with Fe-BABE. Mutants displaying reduced activity or poor labeling efficiency were excluded from analysis. Finally, a total of five residues with the Fe-BABE probe well distributed across the NpmA surface were selected for detailed analysis.

*E. coli* 30S subunits (140 pmol) were incubated with five-fold molar excess of Fe(II)BABE-labeled NpmA and excess unbound protein removed using a Sephacryl S200 spin column. Fenton chemistry was initiated by rapid addition of ascorbic acid and H<sub>2</sub>O<sub>2</sub> to 30S-NpmA complex (40 pmol) in 120 µl final volume and the reaction incubated on ice for 10 minutes. Following addition of thiourea (20 mM) quencher, the reaction was diluted to 250 µl with H<sub>2</sub>O, extracted with two volumes of phenol/ chloroform/ isoamylalcohol (25:24:1) and RNA precipitated with ethanol. Sites of Fe-BABE-induced rRNA strand scission were identified by reverse transcription using AMV reverse

transcriptase and <sup>32</sup>P-labeled DNA oligonucleotide primers designed to report on an extensive region of 16S rRNA surrounding the A1408 target site, including all of h44 and the 30S platform and head regions (**Figure S2B**). Sequencing lanes were obtained using unmodified 16S rRNA and inclusion of the appropriate ddNTP.

### **NpmA Mutagenesis and Kanamycin Minimum Inhibitory Concentration (MIC)**

**Assays.** A previously described pET44a-NpmA expression construct (3) was modified to contain an N-terminal hexahistidine tag and thrombin cleavage site and point mutants generated using the megaprimer whole-plasmid PCR method (4). The presence of each desired NpmA mutation and absence of other changes was confirmed by automated DNA sequencing. MIC assays were conducted in 96-well plate format using *E. coli* BL21(DE3) harboring plasmids expressing wild-type or mutant NpmA protein grown on two-fold dilutions of kanamycin over the range 2-1024 µg/mL. Each well containing 100 µl LB medium, 5 µM IPTG and kanamycin was inoculated with 1 x10<sup>5</sup> cfu/mL in 100 µl of LB medium. Plates were incubated at 37 °C with shaking for 24 hours. The MIC was defined as the lowest concentration of kanamycin that inhibited growth (OD<sub>600</sub> < 0.05).

**Superpositions of 30S-bound and free NpmA.** The structure of NpmA has been solved with no cofactor, bound to SAM cofactor, and bound to the reaction product SAH (5, 6). In total there are five entries in the Protein Data Bank for NpmA, four with two chains per asymmetric unit and one entry with a tetramer in the asymmetric unit, summing to 12 unique coordinate sets. To identify conformational changes associated with NpmA binding, each conformation was superpositioned onto bound NpmA using the align

command in PyMOL. Detailed comparisons and RMSD calculations for the  $\beta$ 2/3 linker (residues 56-79),  $\beta$ 5/6 linker (residues 140-176) and the  $\beta$ 6/7 linker (186-208) were made in the same manner. Chain A of PDB entry 3MTE is most similar to 30S-bound NpmA and was used for all comparisons.

## Supplemental Figures

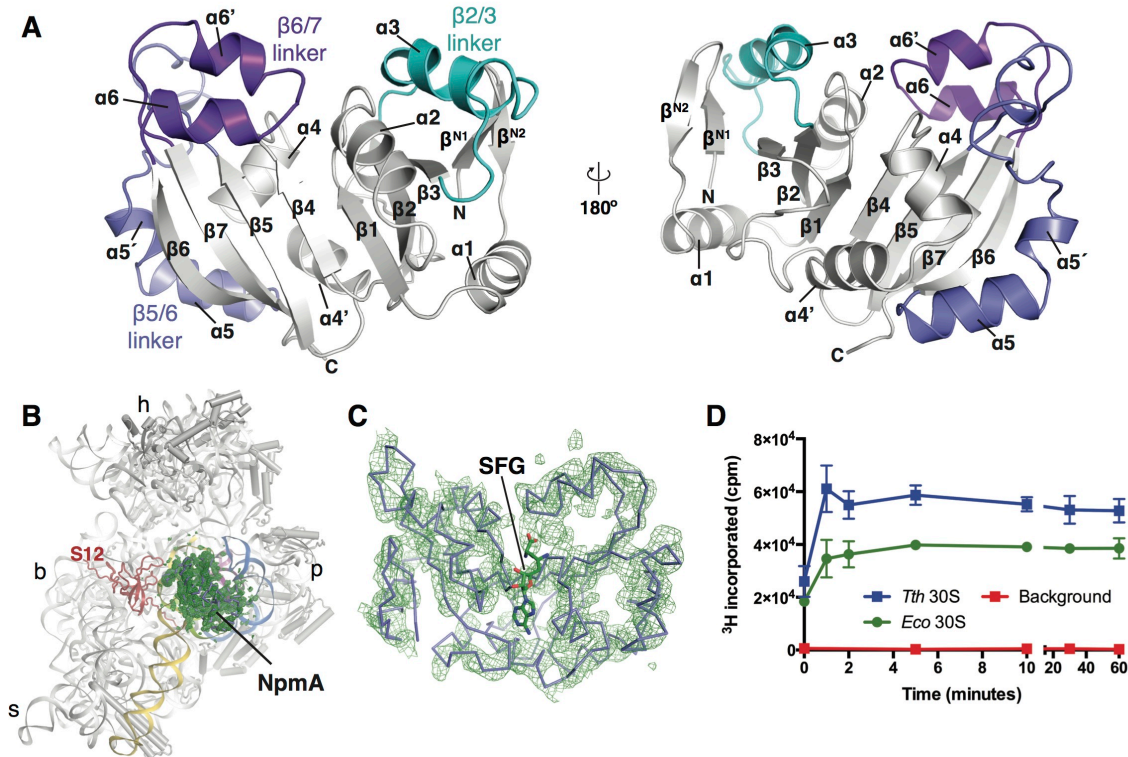


**Figure S1. *E. coli* NpmA structure and elements that mediate interaction with the 30S subunit.**

**(A)** Two views of the NpmA structure (5) related by a 180° rotation about the vertical axis. NpmA adopts a Class I methyltransferase SAM-binding fold comprising a  $\beta$ -sheet core of seven strands with a characteristic  $6 \uparrow 7 \downarrow 5 \uparrow 4 \uparrow \cdot 1 \uparrow 2 \uparrow 3 \uparrow$  topology, common to both aminoglycoside-resistance methyltransferase subfamilies. Linker regions specific to A1408 methyltransferases that interact with the 30S subunit highlighted:  $\beta$  2/3 linker (cyan),  $\beta$ 5/6 linker (slate) and  $\beta$ 6/7 linker (purple). The latter two extended regions are characteristic of the A1408 methyltransferase family (5, 6). The view of NpmA shown on

the right is similar to the orientation of **Figure 1D** (rotated  $\sim 45^\circ$  around the horizontal axis).

**(B)** X-ray diffraction data for the 30S-NpmA-sinefungin (SFG) complex was used to calculate  $F_o - F_c$  difference electron density using structure factors for the 30S in the absence of NpmA (PDB ID 1J5E). The resulting electron density map (green mesh), contoured at  $2.5 \sigma$ , clearly reveals the position of NpmA on the 30S subunit. The complex is shown in the same orientation, and with 30S features labeled and rRNA helices (h24, h27, h44 and h45) colored as in **Figure 1A**.

**(C)** A close-up view of NpmA shown as a  $C\alpha$  backbone trace (purple) and with the bound SAM analog SFG (green sticks with atom colors). **(D)** In vitro methylation assays monitoring tritium incorporation from [ $^3\text{H}$ ]-SAM into 16S rRNA reveal both *E. coli* and *Tth* 30S ribosomes are equivalent as NpmA substrates. Assays were performed as described previously (3) except that *Tth* 30S were preheated at  $55^\circ\text{C}$  before addition to the reaction mixture.

**(D)** *In vitro* methylation assays monitoring tritium incorporation from [ $^3\text{H}$ ]-SAM into 16S rRNA reveal both *E. coli* and *Tth* 30S ribosomes are equivalent as NpmA substrates. Assays were performed as described previously (3) except that *Tth* 30S were preheated at  $55^\circ\text{C}$  before addition to the reaction mixture.

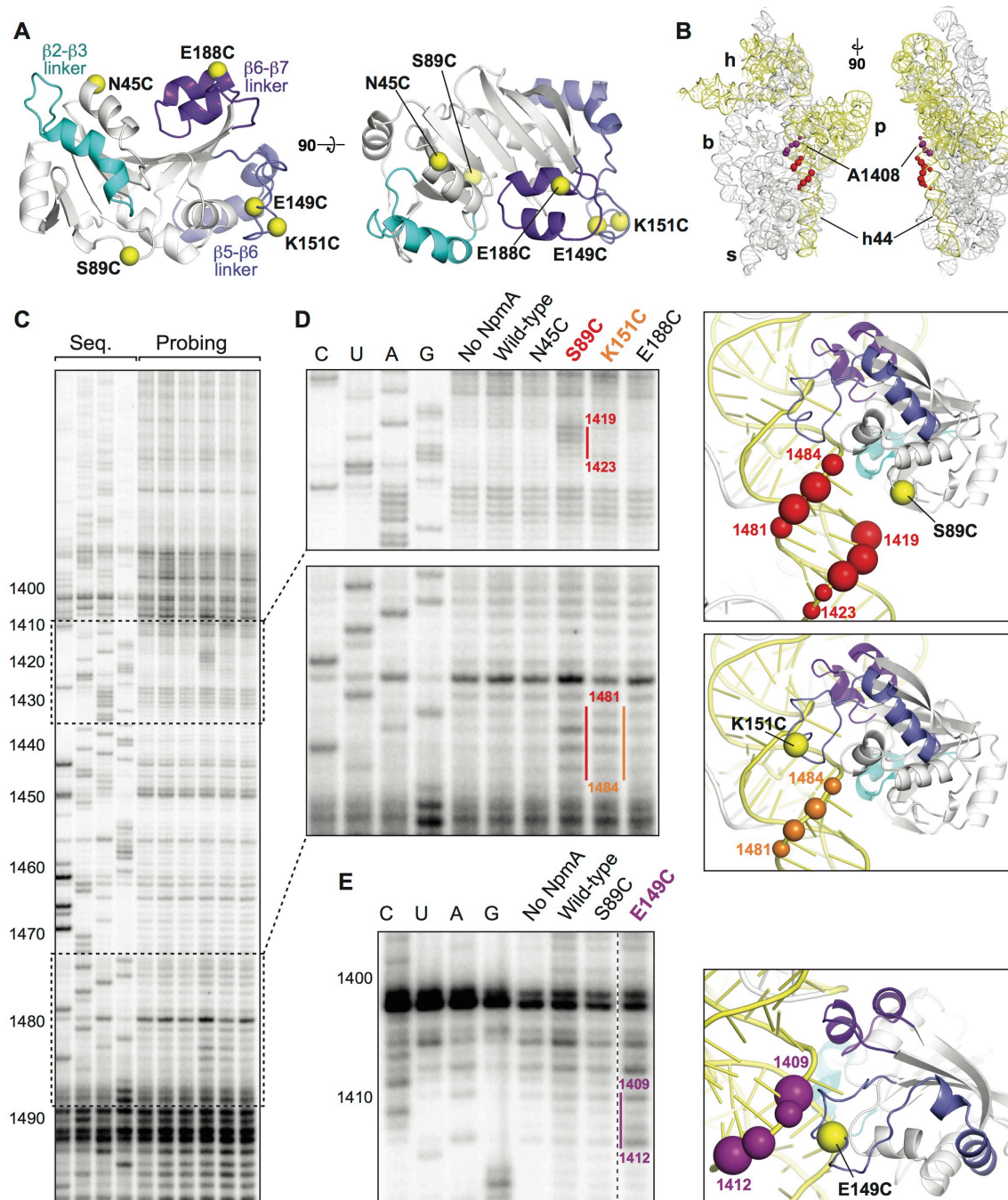


**Figure S2. Determination of the Npm docking site on *E. coli* 30S in solution using Fe-BABE-derived NpmA probing of 16S rRNA.**

**(A)** Sites of incorporation of Fe-BABE into NpmA at five single cysteine residues introduced by site-directed mutagenesis (yellow spheres). The NpmA  $\beta$ 2/3 (cyan),  $\beta$ 5/6

(slate) and  $\beta 6/7$  (purple) linkers, identified in the 30S-NpmA crystal structure as critical for 30S-NpmA interaction, are highlighted here to allow direct comparison with these solution-probing studies.

**(B)** Two views of the 16S rRNA with regions mapped using reverse transcription following directed probing experiments highlighted (yellow). Colored spheres indicate the location of backbone cleavages induced by Fe-BABE at NpmA residues 89 (red) and 149 (purple) shown in panels D and E.

**(C)** Example of a full sequencing gel used to detect Fe-BABE-induced backbone cleavage using reverse transcriptase and a  $^{32}\text{P}$ -labeled DNA primer. 16S rRNA nucleotide numbering derived from the sequencing lanes is shown, left. Sequencing lanes (C, A, U and G, detailed in panel D) correspond to sequencing reactions with the complementary ddNTP.

**(D)** Zoomed views (left) of two regions of the gel in panel C and the corresponding sites of RNA cleavage (right) induced by Fe-BABE at NpmA residues 89 (red; top) and 151 (orange; bottom). Cleavage sites are shown as color-coded spheres, scaled corresponding to band intensity (strong, medium and weak). Lanes C, A, U and G correspond to sequencing reactions with the complementary ddNTP.

**(E)** Cleavage sites arising from Fe-BABE tethered at NpmA residue 149 (purple) depicted as described in panel D.

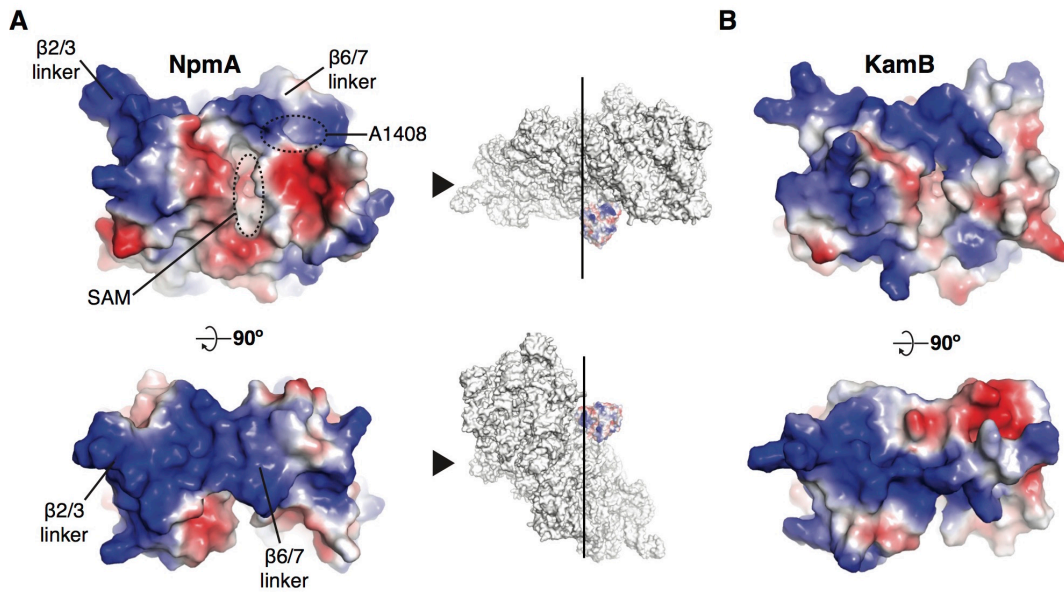


**Figure S3. Surface electrostatic potential of A1408 methyltransferase regions involved in binding the 30S subunit.**

**(A)** The  $\beta 2/3$  and  $\beta 6/7$  linkers of NpmA form an extensive positively charged (blue) surface for interaction with the 30S subunit. The line and arrow on the 30S-NpmA complex depict the plane and point of view, respectively for each protein orientation.

**(B)** The same regions in the aminoglycoside-producer ortholog KamB maintain the overall charge of this surface despite extensive variation in sequence.

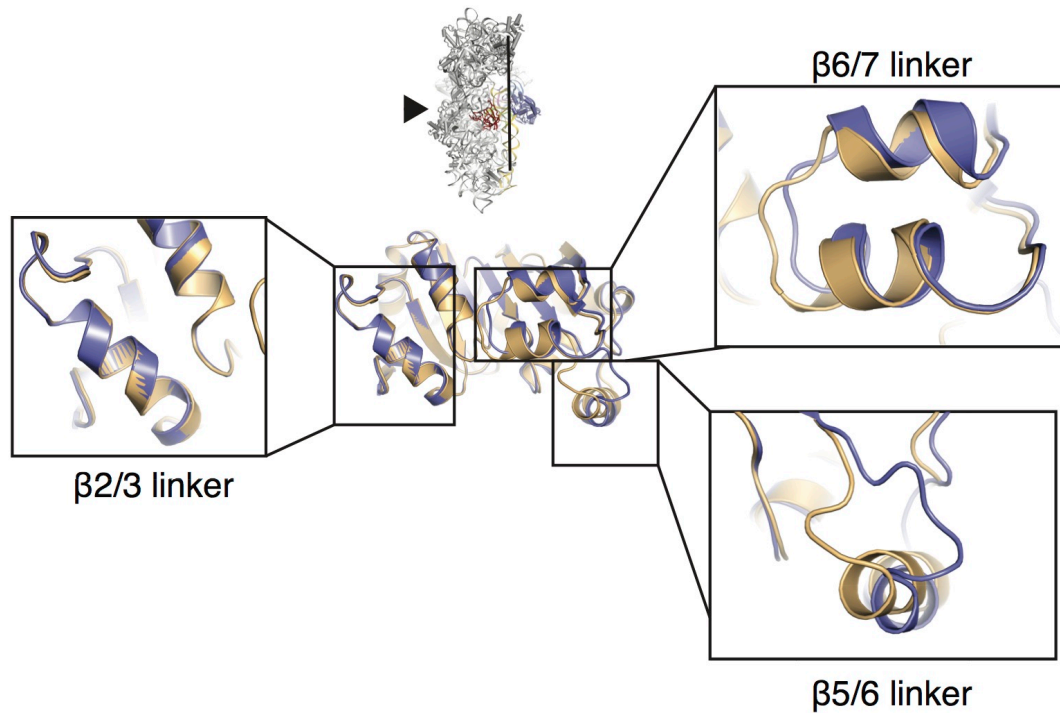


**Figure S4. NpmA conformational changes that occur upon 30S subunit binding.** An all-atom alignment performed in PyMOL of free (PDB ID 3MTE; orange) and 30S bound (purple) NpmA is shown (center) with zoomed views of the three regions primarily mediating interactions with the 30S subunit. An icon of NpmA bound to the 30S subunit (top) depicts the point of view (arrowhead). The most significant conformational change occurs in the  $\beta 5/6$  linker which reorganizes to avoid a steric clash with the 30S subunit. The  $\beta 6/7$  linker moves towards the active site upon 30S subunit binding through a localized conformational change while the  $\beta 2/3$  linker is rigid and does not change conformation.

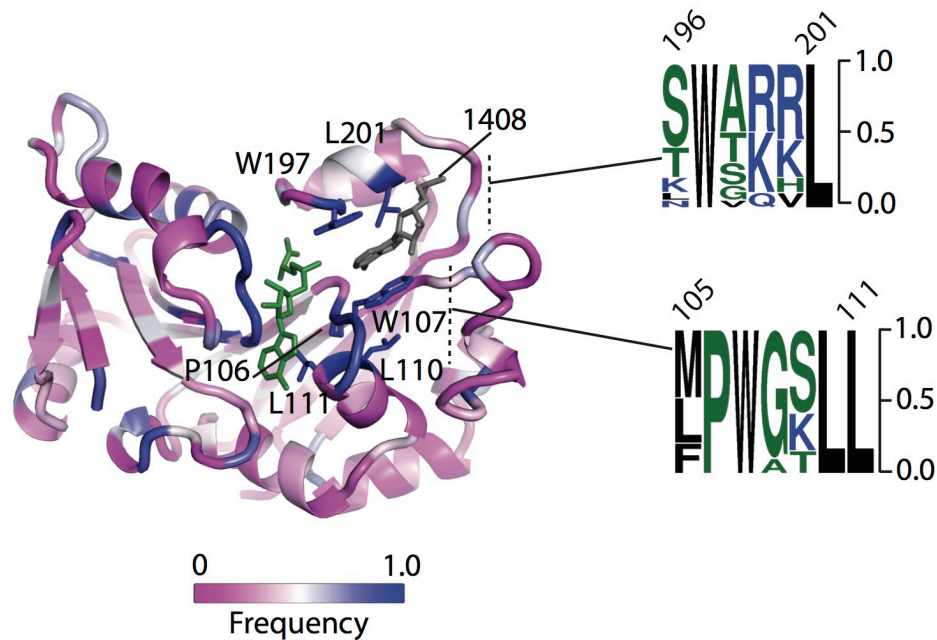


**Figure S5. Sequence conservation across A1408 methyltransferases indicates the mechanism of A1408 positioning is highly conserved.** A BLASTP search of the UniProtKB database using the NpmA amino acid sequence produced 19 unique putative A1408 methyltransferases (E-values  $2 \times 10^{-44}$  to  $2 \times 10^{-5}$ ) that were well separated from tRNA methyltransferase relatives (E-Value  $1 \times 10^{-3}$ ) (7). Multiple sequence alignment was performed in T-Coffee (8). NpmA amino acids are colored by percent identity across nineteen A1408 methyltransferases with blue indicating highly conserved and magenta indicating divergent amino acids. Residues conserved >90% are shown as sticks. The cofactor analog sinefungin is shown in green. A sequence logo (9) displaying the conservation of two motifs involved in A1408 positioning is shown with amino acids colored by hydrophobicity.

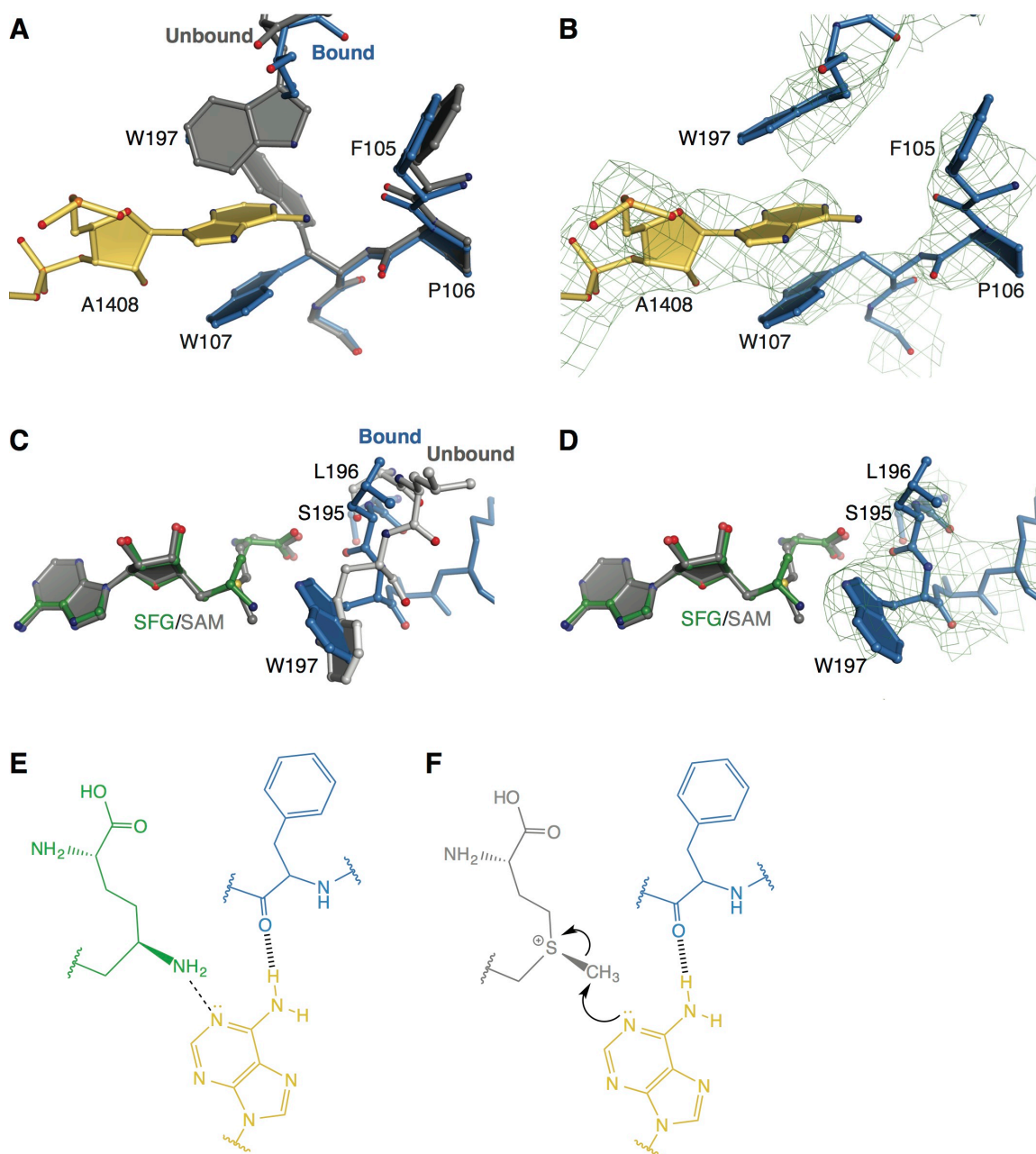


**Figure S6. Conformational changes direct positioning of A1408 for methyl transfer by NpmA.**

(A) Comparison of the free NpmA-SAM (grey) and 30S-bound NpmA-SFG (blue) complexes reveals the conformational changes of two active site tryptophans that position A1408 upon binding to 30S.

**(B)** The 30S-bound conformation of NpmA with unbiased isomorphous difference electron density map (Fo-Fo at 2.5  $\sigma$ ; green mesh) supporting the modeled reorganization of the active site tryptophans.

**(C)** Comparison of the free NpmA-SAM (grey) and 30S-bound NpmA-SFG (blue) complexes reveals conformational changes in NpmA residues 195-197 upon binding.

**(D)** The 30S-bound conformation of NpmA with unbiased isomorphous difference electron density map (Fo-Fo at 2.0  $\sigma$ ; green mesh) supporting the modeled reorganization of the residues 195-197 within the  $\beta$ 6/7 linker.

**(E)** NpmA active site is shown with sinefungin (SFG) bound (as in the crystal structure) and **(F)** the authentic methyl group donor SAM. Modification of A1408 is prevented in the crystal by the presence of a carbon-linked amino moiety of SFG in place of the S-methyl group of SAM. With SAM in the active site A1408 would be positioned for nucleophilic attack by the reactive methyl group via an SN2 mechanism.

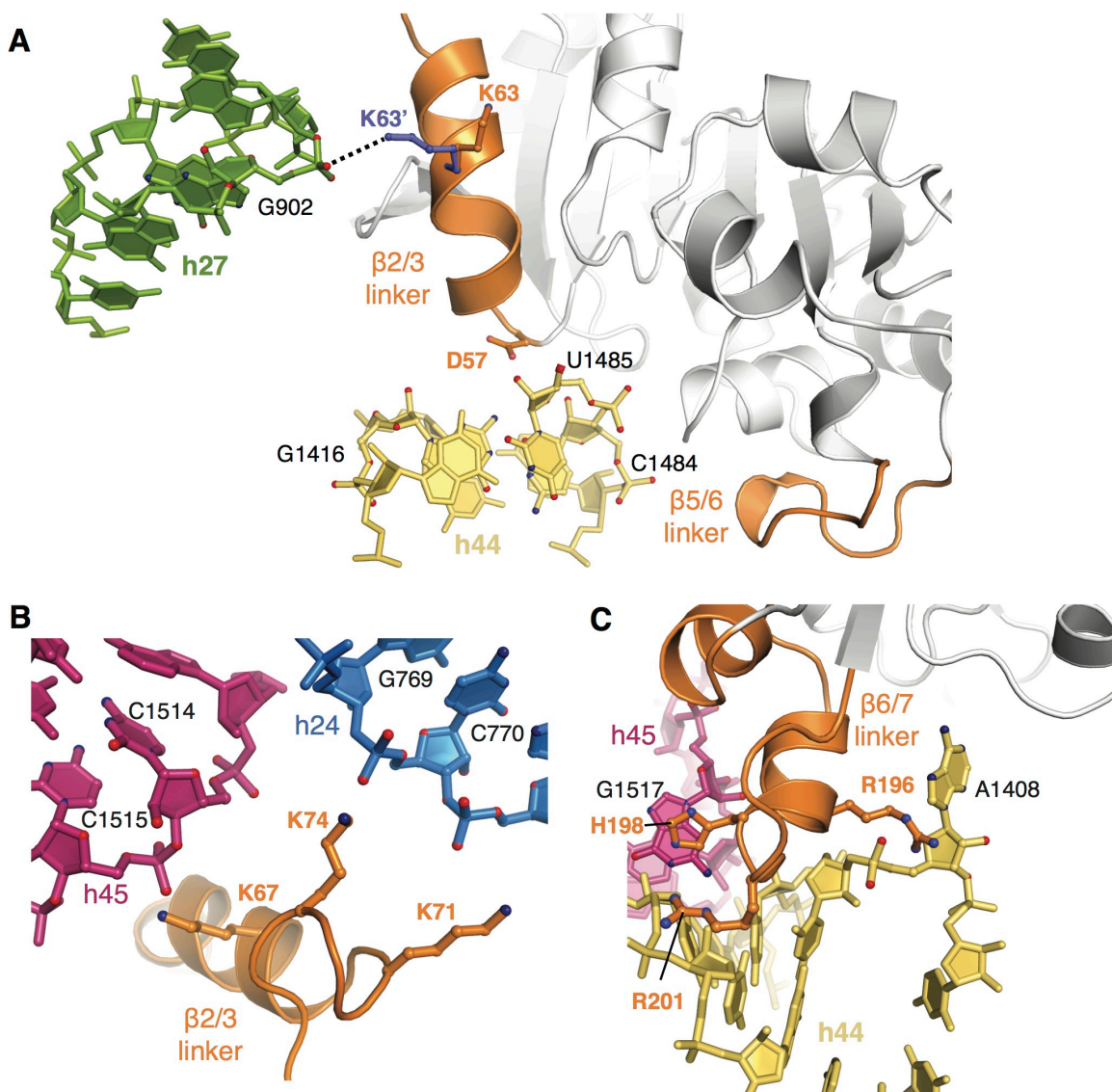


**Figure S7. Superposition of KamB (orange; PDB ID 3MQ2) onto the 30S-bound NpmA structure identifies likely common features of 30S subunit recognition among the family of A1408 methyltransferases.**

(A) Like NpmA, the KamB  $\beta$ 2/3 linker is positioned to interact with h27 and h44. While KamB lacks K66 (which is unique to NpmA), the same contact with the G902 phosphate could be made by K63 in an alternate side chain conformer (K63'; purple).

**(B)** Three of the four NpmA  $\beta$ 2/3 linker lysine residues that make electrostatic interactions with h24 and h45 are conserved in KamB.

**(C)** The stacking interaction of NpmA F203 with h45 may be substituted by KamB H198. Conformational changes in the KamB  $\beta$ 6/7 linker must also occur upon 30S binding but the two functionally critical arginine residues in this region, R196 and R201, are positioned in close proximity to the target nucleotide phosphate and may share the role of stabilizing the flipped backbone conformation. The views shown correspond approximately to those of 30S-NpmA interactions in **Figure 2**.

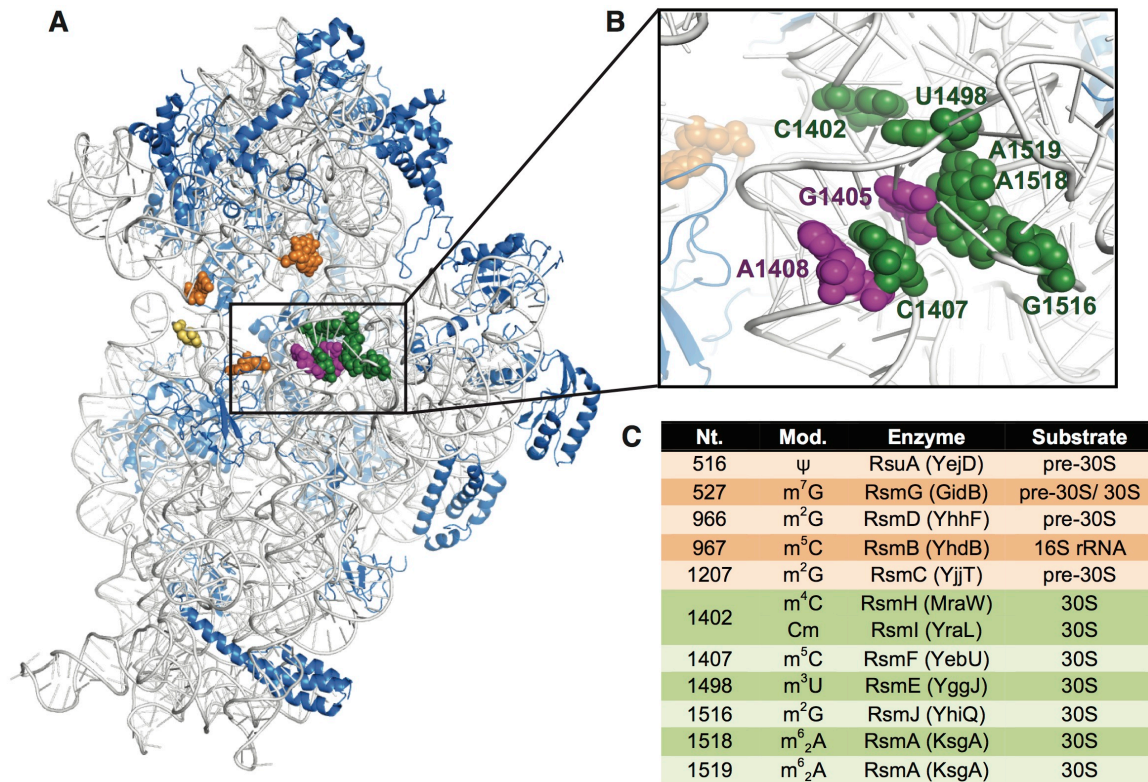


**Figure S8. Incorporation of nucleotide modifications clustered in the decoding center requires the intact 30S subunit as substrate.**

(A) The *E. coli* 30S subunit with its 11 modified nucleotides (shown as spheres). Nucleotides are colored according to their associated modification enzyme and its substrate requirement: *E. coli* enzymes acting on 16S rRNA or pre-30S particles (orange/yellow), *E. coli* enzymes acting on complete 30S subunits (green) and aminoglycoside-resistance enzymes (magenta). The modification by RsmD at 527 is highlighted (yellow) as its substrate requirement apparently differ between *E. coli*, which requires intact 30S (10), and other bacteria, e.g. pre-30S in *T. thermophilus* (11).

(B) Zoomed view of the cluster of methylated nucleotides around the decoding center.

**(C)** Summary of *E. coli* nucleotide modifications and their associated modification enzymes. Enzymes are named according to the current nomenclature with common synonym (prior name) in parenthesis. Enzymes incorporating modifications clustered around the decoding center universally require the complete 30S as substrate. Data used to prepare this figure was retrieved from the MODOMICS website:  
<http://modomics.genesilico.pl/> (12, 13).

## Supplemental References

1. Culver GM & Noller HF (2000) Directed hydroxyl radical probing of RNA from iron(II) tethered to proteins in ribonucleoprotein complexes. *Methods Enzymol.* 318:461-475.
2. Xu Z, O'Farrell HC, Rife JP, & Culver GM (2008) A conserved rRNA methyltransferase regulates ribosome biogenesis. *Nat. Struct. Mol. Biol.* 15(5):534-536.
3. Zelinskaya N, Rankin CR, Macmaster R, Savic M, & Conn GL (2011) Expression, purification and crystallization of adenosine 1408 aminoglycoside-resistance rRNA methyltransferases for structural studies. *Protein Expr. Purif.* 75(1):89-94.
4. Miyazaki K & Takenouchi M (2002) Creating random mutagenesis libraries using megaprimer PCR of whole plasmid. *Biotechniques* 33(5):1033-1034.
5. Macmaster R, Zelinskaya N, Savic M, Rankin CR, & Conn GL (2010) Structural insights into the function of aminoglycoside-resistance A1408 16S rRNA methyltransferases from antibiotic-producing and human pathogenic bacteria. *Nucleic Acids Res.* 38(21):7791-7799.
6. Husain N, et al. (2011) Structural basis for the methylation of A1408 in 16S rRNA by a panaminoglycoside resistance methyltransferase NpmA from a clinical isolate and analysis of the NpmA interactions with the 30S ribosomal subunit. *Nucleic Acids Res.* 39(5):1903-1918.

7. Altschul SF, Gish W, Miller W, Myers EW, & Lipman DJ (1990) Basic local alignment search tool. *J. Mol. Biol.* 215(3):403-410.
8. Di Tommaso P, et al. (2011) T-Coffee: a web server for the multiple sequence alignment of protein and RNA sequences using structural information and homology extension. *Nucleic Acids Res.* 39(Web Server issue):W13-17.
9. Crooks GE, Hon G, Chandonia JM, & Brenner SE (2004) WebLogo: a sequence logo generator. *Genome Res.* 14(6):1188-1190.
10. Okamoto S, et al. (2007) Loss of a conserved 7-methylguanosine modification in 16S rRNA confers low-level streptomycin resistance in bacteria. *Mol. Microbiol.* 63(4):1096-1106.
11. Gregory ST, et al. (2009) Structural and functional studies of the *Thermus thermophilus* 16S rRNA methyltransferase RsmG. *RNA* 15(9):1693-1704.
12. Dunin-Horkawicz S, et al. (2006) MODOMICS: a database of RNA modification pathways. *Nucleic Acids Res.* 34(Database issue):D145-149.
13. Machnicka MA, et al. (2013) MODOMICS: a database of RNA modification pathways--2013 update. *Nucleic Acids Res.* 41(Database issue):D262-267.

**CHAPTER 3:****Substrate recognition and modification by a pathogen-associated aminoglycoside-  
resistance 16S rRNA methyltransferase**

**Substrate recognition and modification by a pathogen-associated aminoglycoside-  
resistance 16S rRNA methyltransferase**

by

Kellie Vinal<sup>1,2</sup> and Graeme L. Conn<sup>1,\*</sup>

<sup>1</sup>Department of Biochemistry, Emory University School of Medicine, 1510 Clifton Road  
NE, Atlanta GA 30322, USA.

<sup>2</sup>Graduate Program in Microbiology and Molecular Genetics (MMG), Graduate Division  
of Biological and Biomedical Sciences, Emory University

Manuscript in preparation for submission to Proceedings of the National Academy of  
Sciences

## Abstract

Site-specific methylation of ribosomal RNA (rRNA) can confer exceptionally high-level resistance to diverse ribosome-targeting antibiotics. The pathogen-derived 16S rRNA methyltransferase NpmA, for example, catalyzes m<sup>1</sup>A1408 modification conferring exceptionally high levels of resistance to structurally diverse aminoglycosides. Here we describe the development of a fluorescence polarization binding assay and its use, together with biochemical assays, to dissect the mechanism of NpmA substrate recognition and control of catalytic activity. These studies reveal that electrostatic interactions made by the NpmA  $\beta$ 2/3 linker are collectively critical for docking of NpmA on the conserved tertiary surface. In contrast, the NpmA regions containing the major augmentations to the core S-adenosyl-L-methionine (SAM)-dependent methyltransferase fold, the  $\beta$ 5/ $\beta$ 6 and  $\beta$ 6/ $\beta$ 7 linkers, are largely dispensable for binding affinity. However, these regions contain several residues critical for optimal positioning of A1408 for modification. In sum, our data support a model for NpmA action in which 30S binding and adoption of a catalytically competent state on the substrate are distinct, with docking on the 16S rRNA surface via the  $\beta$ 2/3 linker necessarily preceding adoption of a catalytically competent state. Our model for NpmA action is also consistent with catalysis of methyl transfer being completely positional in nature, as the most significant impact on NpmA activity occurs upon introduction of defects that impact binding or stabilization of the flipped conformation. Our data provide a molecular framework for aminoglycoside-resistance rRNA methyltransferases that might serve as a functional

paradigm for related enzymes and provide a starting point for inhibitor development to ultimately extend the efficacy of aminoglycosides in the clinic.

## **Introduction**

Bacteria exploit diverse resistance mechanisms to counter the effect of antibiotics. In response to continued exposure to their own bioactive molecules, antibiotic-producing bacteria have evolved the requisite effective self-protective mechanisms, such as the expression of ribosomal RNA (rRNA) methyltransferases which block binding of ribosome-targeting drugs (1-3). Similarly, while human and animal pathogens may have acquired or developed resistance due to the overuse of antibiotics in the clinic and in agriculture (4, 5), broadly disseminated resistance also likely far predates the human antibiotic era (6). Regardless of the origin of clinical resistance, the continued emergence of increasingly resistant bacterial pathogens necessitates a deeper understanding of resistance mechanisms foster identification of new antimicrobial targets to revive existing drugs and develop novel antimicrobial compounds.

Aminoglycosides are potent antimicrobial agents used for clinical treatment of life-threatening infections of both gram-positive and gram-negative bacteria, and are also routinely for both veterinary and growth promotion applications in agricultural settings (7, 8). Most aminoglycosides bind 16S rRNA helix 44 (h44) to induce conformational changes in the universally conserved nucleotides A1492 and A1493 in the ribosome decoding center. As a result, the bacterial ribosome is rendered unable to accurately discern cognate mRNA:tRNA pairing thus impairing translational fidelity (2, 3, 9-13).

More recent evidence has also suggested an additional 23S rRNA binding site for some aminoglycosides which disrupts intersubunit bridge B2, impacting a ribosomal conformational change required during elongation (14).

Both aminoglycoside-producing and human pathogenic bacteria can achieve high levels of resistance to aminoglycosides by reducing drug permeability or increasing efflux from the cell, enzymatic chemical modification of the drug, or mutation or chemical modification of the aminoglycoside binding site (1, 3, 15). In particular, S-adenosyl-L-methionine (SAM)-dependent 16S rRNA methyltransferases are the predominant resistance mechanism found in aminoglycoside-producing bacteria and are an increasing clinical concern with their continued emergence in major human pathogens (8, 16). These enzymes site-specifically methylate 16S rRNA in the ribosome decoding center to prevent aminoglycoside binding and thus confer exceptionally high levels of resistance to this class of drug (2, 16-18). Genes encoding aminoglycoside-resistance 16S rRNA methyltransferases are often located on plasmids or within other mobile genetic elements, frequently in conjunction with other antimicrobial resistance genes, and appear to be globally disseminated (8, 19). Together, the conserved nature of the ribosomal target of these methyltransferase enzymes, as well as the apparent transmissibility of their activity to both gram-positive and pathogenic gram-negative bacteria, underscore the need to develop potent inhibitors of these resistance determinants (8, 20).

The structure of the pathogen-derived m<sup>1</sup>A1408 aminoglycoside-resistance methyltransferase NpmA bound to the 30S ribosomal subunit provided a first snapshot of this enzyme-substrate complex in a “pre-catalytic” state (21). Comparison of free and 30S-bound NpmA revealed structural differences that suggested substrate recognition and

methyltransferase activity are potentially controlled by a combination of rigid docking of complementary surfaces and binding-induced conformational changes in both enzyme and substrate. However, the molecular mechanisms underpinning precise substrate recognition and modification cannot be discerned from the structures alone. Here, we describe the development of a fluorescence-based binding assay for 30S-NpmA interaction and its application in defining the mechanism of 30S substrate recognition and modification by the pathogen-derived aminoglycoside-resistance methyltransferase NpmA.

## **Materials and Methods**

**NpmA mutagenesis, expression, and purification.** Amino-terminally hexahistidine-tagged (6xHis) wild-type and variant NpmA proteins were expressed from a previously described pET44a expression construct containing an *E. coli* codon-optimized NpmA gene obtained by chemical synthesis (21, 22). NpmA amino acid substitutions were generated in the pET44a-NpmA plasmid using the megaprimer whole-plasmid PCR method (23) and confirmed by automated DNA sequencing.

Wild-type and variant NpmA proteins were expressed in *E. coli* BL21(DE3) cells grown at 37 °C in Terrific Broth containing 100 µg/mL ampicillin, with induction of protein expression at mid-log phase (OD<sub>600</sub> = 0.6-0.8) using 1 mM isopropyl β-D-1-thiogalactopyranoside (IPTG). Cells were grown a further 2.5 hours post-induction at 37 °C (except for NpmA Δβ6/7, which was grown at 20 °C overnight), harvested by centrifugation, and lysed by sonication in 50 mM sodium HEPES (pH 7.5) buffer

containing 1 M NaCl, 10 mM imidazole, 10% glycerol, 0.5% Triton-X100, 6 mM  $\beta$ -mercaptoethanol ( $\beta$ -Me), 0.27 units/ml DNase I, 1 mM benzamidine, and 1 mM phenylmethylsulfonyl fluoride (PMSF). Soluble cell lysate was dialyzed against 50 mM sodium HEPES buffer (pH 7.5) containing 2 M NaCl and 10 mM  $\beta$ -ME and 6xHis-NpmA proteins purified by  $\text{Ni}^{2+}$ -affinity chromatography using a HisTrap Fast Flow column (GE Healthcare). Bound protein was eluted using a linear gradient of imidazole (25-500 mM) in 50 mM sodium HEPES buffer (pH 7.5) containing 0.5 M NaCl and 10 mM  $\beta$ -Me. Pooled NpmA-containing fractions were further purified by gel filtration chromatography on a Superdex 75 column equilibrated with 50 mM sodium HEPES buffer (pH 7.5) containing 150 mM NaCl and 6 mM  $\beta$ -ME. Purified proteins were either used in experiments immediately or stored at  $-80\text{ }^{\circ}\text{C}$  following flash freezing.

**Kanamycin minimum inhibitory concentration (MIC) assays.** MIC assays were conducted in 96-well plate format using *E. coli* BL21(DE3) harboring plasmids expressing wild-type or variant NpmA grown in lysogeny broth (LB) medium containing two-fold dilutions of kanamycin over the range 2-1024  $\mu\text{g}/\text{mL}$ . Each well containing 100  $\mu\text{L}$  LB medium, 5  $\mu\text{M}$  IPTG, and kanamycin was inoculated with  $1 \times 10^5$  colony forming units/mL in an additional 100  $\mu\text{L}$  of LB medium. Plates were incubated at  $37\text{ }^{\circ}\text{C}$  with shaking for 24 hours. The MIC was defined as the lowest concentration of kanamycin that inhibited growth ( $\text{OD}_{600} < 0.05$  above background).

**Isothermal titration calorimetry (ITC).** Purified NpmA protein (60-80  $\mu\text{M}$ ) was exhaustively dialyzed against 50 mM sodium HEPES buffer (pH 7.5) containing 150 mM

NaCl. Final dialysis buffer was used to prepare solutions of SAM (2 mM) and SAH (0.6-0.8 mM). Titration experiments were performed at 25 °C using an Auto-iTC<sub>200</sub> microcalorimeter (Malvern/MicroCal) with 16 × 2.4 μL injections of SAM or SAH into each protein. Data were fit using Origin 7 software with a single binding site model to extract the binding affinity ( $K_d$ ) for each protein-ligand pair. All experiments were performed in parallel with a control experiment with wild-type NpmA for each preparation protein and ligands.

**Fluorescence assay to monitor 30S-NpmA interaction.** 30S subunits were purified from *E. coli* (MRE600) grown to mid-log phase ( $OD_{600} = 0.6-0.7$ ), essentially as previously described (24). Single-Cys variants of NpmA were fluorescein labeled by incubation of purified protein in the dark overnight at 25 °C with five-fold excess of fluorescein-5-maleimide (AnaSpec, Inc.). Excess dye reagent was removed using a dye removal column (Thermo Scientific), and fluorescently labeled proteins (denoted as \*) were analyzed by SDS-PAGE with visualization on a Typhoon Trio imaging system. Pilot FP experiments were conducted at 25 °C in 100 μL reactions containing 50 nM fluorescently labeled protein (NpmA-S89C\*, NpmA-K131C\*, NpmA-E184C\*, or NpmA-E188C\*) and 50 nM *E. coli* (MRE600) 30S ribosomal subunits in 20 mM HEPES/KOH buffer (pH 7.0) containing 10 mM NH<sub>4</sub>Cl, 50 mM KCl, 5 mM Mg(OAc)<sub>2</sub>, and 3 mM β-ME. Fluorescence polarization (FP) was monitored using a BioTek Synergy4 plate reader.

FP experiments to measure 30S-NpmA binding affinity ( $K_d$ ) were performed in the same solution conditions as used for the pilot FP experiments and contained NpmA-

E184C\* (20 nM) and *E. coli* (MRE600) 30S ribosomal subunit (over the concentration range 0-256 nM) in each 100  $\mu$ L reaction. Binding reactions were incubated at 25 °C for 15 minutes before FP measurement. Experiments were performed in triplicate and data fit using a one site – total binding equation in GraphPad Prism6 to determine the  $K_d$ .

Measurements of  $K_i$  for each NpmA variant were made using competition binding assays performed in at least triplicate. Each 100  $\mu$ L reaction contained 30S subunits (50 nM), NpmA-E184C\* (50 nM), and the variant NpmA protein (over the concentration range 0.002-10  $\mu$ M) in 20 mM HEPES/KOH buffer (pH 7.0) containing 10 mM  $\text{NH}_4\text{Cl}$ , 75 mM KCl, 5 mM  $\text{Mg}(\text{OAc})_2$ , and 3 mM  $\beta$ -Me. 30S subunits and NpmA-E184C\* were pre-incubated for 10 minutes at 25 °C before addition of unlabeled competitor protein. Samples were incubated at 25 °C for 12 minutes, before measurement of FP as above. Data were fit in GraphPad Prism6 to determine  $K_i$  using the one binding site competition binding equation.

**Reverse transcription analysis of A1408 methylation.** Reverse transcription (RT) assays were used to determine the extent of  $\text{m}^1\text{A1408}$  modification by wild-type and variant NpmA in both *in vitro* methylation assays and in cells expressing the proteins. For *in vitro* assays, NpmA protein (100 pmol) was incubated with a fixed amount of *E. coli* 30S subunits (100 pmol, pre-heated at 42 °C for 5 minutes) for 5 minutes at 37 °C in methylation reaction buffer containing 50 mM HEPES/KOH (pH 7.5), 10 mM  $\text{MgCl}_2$ , 50 mM  $\text{NH}_4\text{Cl}$ , 5 mM  $\beta$ -Me, and 10 mM SAM. Each reaction was terminated by phenol-chloroform extraction followed by ethanol precipitation of 16S rRNA. For analysis of A1408 methylation in cells, *E. coli* BL21(DE3) harboring a plasmid expressing wild-type

or variant NpmA were grown to mid-log phase in LB medium containing 5  $\mu$ M IPTG and total RNA extracted using an RNeasy mini kit (QIAGEN).

For RT analysis of 16S RNA methylation from both methylation assays, a  $^{32}$ P-labeled DNA primer complementary to *E. coli* 16S rRNA nucleotides 1459-1479 was used for primer extension at 37 °C using AMV Reverse Transcriptase (Promega). Primer extension products were run on denaturing (8M urea) 10% PAGE sequencing-style gels and visualized on a Typhoon Trio imaging system.

## Results

### A fluorescence assay to probe 30S-NpmA interaction

To examine the 30S-NpmA subunit substrate interaction, we sought to develop a quantitative, fluorescence polarization (FP)-based assay using a single fluorescent probe incorporated site-specifically into NpmA. We reasoned that this labeled NpmA probe should retain both 30S binding affinity and catalytic activity in this *in vitro* assay, *i.e.* exhibit methylation of A1408 in the presence of SAM and subsequent release from 30S. As a starting point, we used four previously created single-cysteine substituted NpmA proteins (S89C, K131C, E184C, and E188C; **Fig. 1A,B**) which each retained wild-type ability to confer resistance to kanamycin (MIC >1000  $\mu$ g/mL) (21). These substitutions are distributed across the solvent-exposed surface of NpmA when bound to the 30S and were thus predicted to have minimal impact on 30S-NpmA interaction upon covalent attachment of a fluorescein dye.

Each of the four fluorescein-labeled NpmA variants was assessed in pilot FP experiments to determine which dye location might provide the optimal probe of 30S-NpmA interaction. Labeling of NpmA at residue 131 (NpmA-K131C\*) appeared to block 30S-NpmA interaction as no difference in FP was observed in the presence of 30S compared to the free protein (**Fig. 1C, top**). In contrast, both NpmA-S89C\* and NpmA-E188C\* bound to 30S, as indicated by increase in FP in the presence of 30S (**Fig. 1C, center**, and data not shown). However, both labeled proteins failed to dissociate upon addition of SAM suggesting these labeled proteins were either defective in catalysis, unable to release the methylated 30S, or bound with comparable affinity to other site(s) on the 30S. Finally, NpmA-E184C\* also bound 30S and, critically, dissociated from the substrate following addition of SAM (**Fig. 1C, bottom**). Additionally, we found that NpmA-E184C\* could be competed off 30S by unlabeled wild-type NpmA and that FP from untreated 30S-NpmA-E184C\* remained stable over the full time course of these experiments (**Supplementary Fig. S1**). Thus, NpmA-E184C\* fulfills the criteria to be a useful probe of 30S-NpmA interaction and this protein was selected for use in all subsequent experiments.

The binding affinity of NpmA for the 30S ribosomal subunit was first estimated by FP measurement using NpmA-E184C\* and a range of 30S subunit concentrations. Although complicated by apparent non-specific binding at the highest 30S concentrations, this analysis yielded an approximate  $K_d$  for 30S-NpmA interaction of 25 nM (**Fig. 2A**). A competition assay was next established to simplify analysis of numerous NpmA variants. Unlabeled NpmA protein (0.002-10  $\mu$ M) was used to compete off pre-bound NpmA-E184C\* from 30S subunits (both at 0.05  $\mu$ M) and a range of NaCl and

Mg<sup>2+</sup> concentrations were tested to identify conditions that provided the optimal initial FP signal while minimizing non-specific 30S-NpmA interaction (*i.e.* increased FP above free NpmA-E184C\* at the highest competitor concentration; **Supplementary Fig. S2**). Under the final conditions used, this assay yielded a K<sub>i</sub> of 62 nM for unlabeled wild-type NpmA competitor (**Fig. 2B**) to serve as a benchmark for analyses of variant NpmA protein interactions with the 30S subunit.

The previously reported 30S-NpmA complex structure (21) revealed the predominant sites of interaction between NpmA and its substrate to reside in the regions linking  $\beta$ -strands 2 and 3 ( $\beta$ 2/ $\beta$ 3 linker), 5 and 6 ( $\beta$ 5/ $\beta$ 6 linker) and 6 and 7 ( $\beta$ 6/ $\beta$ 7 linker) of the conserved Class I methyltransferase core fold. As described in the following sections, the new competition FP assay was used in combination with complementary analyses of NpmA function to define the contributions of these linker regions, and putative key residues within them, to specific 30S-NpmA substrate binding and recognition.

### **The NpmA $\beta$ 2/3 linker drives interaction with the 30S subunit**

In the 30S-NpmA complex structure, the largely  $\alpha$ -helical NpmA  $\beta$ 2/3 linker directly contacts three 16S rRNA helices (h24, h27, and h45) which form a contiguous RNA surface in the assembled 30S structure (21). These interactions with the 16S rRNA phosphate backbone are mediated by four positively charged residues, K66, K67, K70, and K71 (**Fig. 3A**), suggesting that docking of NpmA onto the 30S subunit might be driven by electrostatic interaction between two conformationally rigid surfaces: the positively charged  $\alpha$ -helix of the NpmA  $\beta$ 2/3 linker and the negatively charged 16S

rRNA tertiary surface. Consistent with this idea, the process noted above of optimizing conditions for the NpmA binding experiments revealed a marked sensitivity of the 30S-NpmA interaction to the solution ionic strength (**Supplementary Fig. S2**).

To directly examine the contribution of these  $\beta$ 2/3 linker lysine residue to the 30S-NpmA interaction, we generated single lysine to glutamic acid substitutions and measured binding of each NpmA variant in the competition FP assay (**Fig. 3B**). Each singly substituted variant exhibited a decrease in binding affinity, ranging from approximately 6-fold (K66E, K67E, and K71E) to 14-fold (K70E) reduction compared to wild-type NpmA (**Table 1**). Binding affinities for each doubly substituted NpmA (K66E/K67E or K70E/K71E) and the quadruple variant (K66E/K67E/K70E/K71E) were reduced below the level measurable in this assay with only small reduction in FP at the highest competitor concentrations (**Fig. 3C** and **Table 1**). These results demonstrate the collective importance of the  $\beta$ 2/3 linker lysines for NpmA binding to its 30S substrate. It is noteworthy that each double and the quadruple variant retained essentially identical affinity for SAM cosubstrate and the reaction by-product SAH to wild-type NpmA (**Table 1** and **Supplementary Fig. S3**), indicating that each variant is correctly folded and the lysine substitutions exclusively affect NpmA interaction with the 30S substrate.

Previous analysis of resistance to kanamycin conferred by each NpmA  $\beta$ 2/3 linker variant in *E. coli* revealed no detectable effect for any single substitution (21), whereas both the double variants had a reproducible but modest impact and the quadruple-substituted NpmA conferred essentially no resistance (**Table 1**). Our direct measurements of 30S-NpmA affinity therefore suggest that there is sufficient redundancy in this set of electrostatic interactions that considerable loss of affinity (up to ~14-fold with single

substitutions) may be tolerated in the context of the bacterial cell. Although each doubly substituted variant conferred an intermediate resistance in *E. coli* indicating some 16S rRNA modification must occur, within the limits of *in vitro* binding assay, no interaction could be detected. We therefore performed an *in vitro* analysis of 30S methylation by each NpmA  $\beta$ 2/3 linker variant (**Fig. 3D**, *top*). These experiments revealed that *in vitro*, with equal concentration of enzyme and substrate, each single  $\beta$ 2/3 linker variant can methylate A1408 as effectively as wild-type NpmA. In contrast, the doubly substituted variants reduce the methylation ability of NpmA to ~75-90% and the quadruple-substituted variant reduces methylation ability to ~39% as compared to wild-type NpmA. Thus the extent of 16S rRNA methylation qualitatively mirrors both the *in vitro* binding analysis and kanamycin MIC values in *E. coli*. However, the extent of modification for the multiply substituted variants is significantly higher than might be expected given their reduced ability to confer resistance in cells, particularly for the quadruple variant. We therefore performed an equivalent RT analysis of 16S rRNA modification from subunits extracted from *E. coli* grown under essentially the same conditions as used in the MIC assays (**Fig. 3D**, *bottom*). Each single  $\beta$ 2/3 linker substitution modestly reduced the extent of A1408 methylation (~66-89%), indicating that complete modification of all subunits is not required for a level of resistance (MIC) indistinguishable from that conferred by the wild-type enzyme. In more stark contrast to the *in vitro* analysis, cells expressing the doubly substituted and quadruple-substituted variants were dramatically reduced in their extent of A1408 methylation (to ~11-14% and 4%, respectively; **Fig. 3D**, *bottom*), correlating with the observed MICs.

These analyses reveal that the impact on NpmA activity of increasing charge reversal (K to E) substitutions in the  $\beta$ 2/3 linker correlates well with both 30S-NpmA binding affinity and the enzyme's ability to incorporate the aminoglycoside-resistance  $m^1A1408$  modification. The apparent differences observed in the extent of 16S methylation *in vitro* and in *E. coli* cells likely arise from the high concentration of 30S subunits in the bacterial cell and thus differences in the relative enzyme/ substrate concentrations in the two assays (see *Discussion*). Together, these results demonstrate the collective importance of the  $\beta$ 2/3 linker residues in docking onto the rigid 16S rRNA tertiary surface of the 30S subunit and the subsequent capacity of NpmA to incorporate the  $m^1A1408$  modification and confer aminoglycoside resistance.

#### **Contributions of the NpmA $\beta$ 5/6 and $\beta$ 6/7 linkers to 30S-NpmA binding affinity**

NpmA variants with a complete deletion of either the  $\beta$ 5/6 linker (amino acids 145-155) or  $\beta$ 6/7 linker (amino acids 187-207) were created to examine the overall contribution of each region to 30S-NpmA binding affinity. Despite the size of each deletion, both proteins were solubly expressed and appeared well folded from their elution as a symmetrical peak at the expected volume from a gel filtration column (**Supplementary Fig. S4**). These deletions may be structurally tolerated given their location on the protein surface and the observed structural variability observed in these linker regions in NpmA and related enzymes (25-27).

Deletion of either linker fully ablated the ability of the enzyme to confer resistance in the MIC assay (**Table 1**), confirming the expected overall importance of these regions for NpmA activity. Additionally, in contrast to the case for all  $\beta$ 2/3 linker

variants tested, deletion of the NpmA  $\Delta\beta 5/6$  and  $\Delta\beta 6/7$  linkers also significantly impacted binding of SAM and SAH, with affinities reduced for both ligands  $\sim 100$ - and  $\sim 10$ -fold, respectively (**Table 1**). Remarkably, however, the impact of each linker deletion on interaction with the 30S substrate was much less dramatic and also distinct for each variant (**Fig. 4, Table 1**). While NpmA- $\Delta\beta 6/7$  had slightly reduced 30S-NpmA binding affinity ( $\sim 2.5$ -fold), NpmA lacking the  $\Delta\beta 5/6$  linker binds 30S with modestly ( $\sim 3$ -fold) higher affinity than the wild-type enzyme. Thus, despite making essential contributions to NpmA activity, these regions contribute minimally to 30S substrate binding affinity.

#### **Role of the $\beta 5/6$ linker in 30S substrate recognition**

In its 30S-bound state, the NpmA  $\beta 5/6$  linker forms an  $\alpha$ -helical structure that contacts both strands of 16S rRNA across the h44 major groove. The N-terminal end of the  $\beta 5/6$  linker  $\alpha$ -helix packs against the distorted 16S rRNA backbone between C1409 and the flipped A1408 target nucleotide and undergoes the most pronounced conformational reorganization between the free and 30S-bound states of NpmA (21). The opposite end of the  $\beta 5/6$  linker  $\alpha$ -helix is positioned via an electrostatic interaction between R153 and the phosphate group of C1484 (**Fig. 5A**). As this  $\alpha$ -helical  $\beta 5/6$  linker appears to be unique to NpmA among the known  $m^1A1408$  methyltransferase structures (25-28), we individually substituted two central residues, A148 and E149, with proline to test whether disrupting the  $\alpha$ -helix would impact NpmA activity. However, both variants conferred wild-type MIC (**Table 1**), suggesting that the precise structure formed by the  $\beta 5/6$  linker is not critical for NpmA activity.

We next tested whether  $\beta$ 5/6 linker R153 contributes to 30S binding affinity and found that NpmA-R153E bound ~6-fold more weakly than the wild-type enzyme (**Fig. 5B, Table 1**). This reduction in substrate binding affinity is also consistent with the modestly reduced MIC previously observed for the NpmA-R153E variant (21). These results point to a significant contribution of R153 to 30S-NpmA interaction. This observation and the finding that NpmA lacking the  $\beta$ 5/6 linker binds with higher rather than lower affinity can be reconciled in a mechanism of 30S substrate recognition in which the  $\beta$ 5/6 linker contributes primarily to stabilization of the catalytically competent state of the enzyme with A1408 flipped into its active site (see *Discussion*).

#### **Role of the $\beta$ 6/7 linker in SAM binding and 30S substrate recognition**

The NpmA  $\beta$ 6/7 linker forms two  $\alpha$ -helices connected by a short loop (**Fig. 6A,B**), the second of which contains several residues important for enzyme activity (21). These residues including R200 and R207 which make electrostatic interactions with the 16S rRNA and Trp197 which stacks on the flipped A1408 base in the enzyme active center. Additionally, the  $\beta$ 6/7 linker forms part of the SAM binding pocket and 30S binding appears to induce a local change in the NpmA backbone of L196 to create an additional interaction with the cosubstrate not observed in the free NpmA-SAM complex (21). Thus, the  $\beta$ 6/7 linker potentially contributes to NpmA activity by influencing cosubstrate and substrate binding, as well as precisely orienting the flipped A1408 target base in the enzyme active site for modification.

We first tested whether the secondary structure of the NpmA  $\beta$ 6/7 linker is critical for activity by substituting a single residue in the center of each short  $\alpha$ -helix with proline

(**Fig. 6B**). As for the  $\beta$ 5/6 linker, disrupting the first  $\alpha$ -helix of the  $\beta$ 6/7 linker (residues 186-193) with a V190P substitution had no impact on resistance to kanamycin or SAM/SAH binding affinity (**Table 1**). In contrast, placement of a proline residue in the second  $\beta$ 6/7 linker  $\alpha$ -helix (residues 198-203) with a L201P substitution fully ablated ability of NpmA to confer antibiotic resistance and had the most significant impact of any  $\beta$ 6/7 linker substitution tested here on methylation ability of NpmA both *in vitro* and in the bacterial cell (**Fig. 6C** and **Table 1**). Interestingly, however, the L201P substitution also resulted in a modest (3-fold) increase in 30S-NpmA binding affinity and differentially impacted NpmA interaction with SAM and SAH ( $K_d$  reduced 6- and 30-fold respectively; **Table 1**). These observations suggest that precise structure of only the second  $\alpha$ -helix of the  $\beta$ 6/7 linker is critical for NpmA activity through its optimal positioning of key residues (including W197, R200, R207 and the backbone of L196).

We next created two variants with changes at L196 to test the prediction that this residue may contribute to regulating NpmA interaction with SAM or the reaction by-product SAH, following methylation (21). A L196G substitution was found to have no impact on either SAM or SAH binding affinity or the ability of the NpmA to confer resistance (**Table 1**), consistent with the observed 30S-binding induced interaction between SAM and L196 being mediated by the protein backbone. However, while a L196 deletion (L196 $\Delta$ ) had a modest impact on the kanamycin MIC, a strongly differential impact was observed on SAM and SAH binding affinity ( $K_d$  reduced 2- and 20-fold, respectively), comparable to the effect of the L201P substitution. These observations point to a role for the  $\beta$ 6/7 linker in regulating NpmA activity through its interaction with cosubstrate and the reaction by-product (see *Discussion*).

Finally, we tested the impact of charge-reversal substitution of the two Arg residues on binding affinity for the 30S subunit to assess the  $\beta 6/7$  linker contribution to 30S substrate binding. NpmA-R200E bound 30S with a slightly reduced affinity ( $\sim 2$ -fold reduced  $K_i$ ) comparable to the deficit in substrate binding upon complete  $\beta 6/7$  linker deletion (NpmA- $\Delta\beta 6/7$ ,  $\sim 2.5$ -fold reduced  $K_i$ ). This results suggests that the decrease in 30S affinity in both NpmA variant proteins can largely be attributed to the loss of a single favorable electrostatic interaction mediated by R200 (**Fig. 6E** and **Table 1**). RT analyses additionally revealed that although R200E had no impact on *in vitro* activity,  $m^1A1408$  methylation was substantially reduced *in vivo* (**Fig. 6C**). In contrast, while NpmA-R207E bound 30S with the same affinity as the wild-type enzyme, RT analyses showed significant reduction and almost complete loss of methylation *in vitro* and *in vivo*, respectively (**Fig. 6C,D** and **Table 1**), consistent with the prior observation that the NpmA-R207E variant is unable to confer resistance in the MIC assay (21). These results pinpoint the specific and essential role played by R207 in promoting the A1408 conformation necessary for catalysis of methylation. These observations thus reveal that while R200 contributes modestly to 30S binding affinity, R207 does not contribute to 30S-NpmA binding but instead plays a specific and functionally critical role in stabilization of the flipped conformation of A1408.

## Discussion

Acquired 16S rRNA methyltransferases are a significant emerging threat to the continued clinical use of aminoglycosides (8, 16). In the present study we set out to define the

molecular mechanism of 30S substrate recognition and m<sup>1</sup>A1408 modification by NpmA as a platform for development of effective inhibitors of these resistance determinants.

Our findings reveal that docking of NpmA on the 30S is driven almost exclusively by electrostatic interactions with 16S rRNA made by a group of lysine residues located in a single region of NpmA, the  $\beta$ 2/3 linker. In contrast, the  $\beta$ 5/ $\beta$ 6 and  $\beta$ 6/ $\beta$ 7 linkers, which contain the major augmentations to the core Class I methyltransferase fold, contribute minimally to 30S-NpmA binding affinity but are nonetheless critical for NpmA activity via SAM cosubstrate binding and stabilizing A1408 in a flipped conformation for modification. Overall, our data support a model for NpmA action in which 30S binding and adoption of a catalytically competent state on the substrate are distinct events:

docking on the 16S rRNA surface via the  $\beta$ 2/3 linker must necessarily precede catalysis of methyltransfer but alterations in the NpmA  $\beta$ 5/ $\beta$ 6 or  $\beta$ 6/ $\beta$ 7 linker that ablate activity do not impact 30S binding. This model is also consistent with catalysis of methyltransfer being completely positional in nature, as the most significant impact on NpmA activity occurs upon introduction of defects that impact binding or stabilization of the flipped conformation.

The m<sup>1</sup>A1408 methyltransferases each possess a subset of the equivalent positively charged residues within their  $\beta$ 2/3 linker, with conservation highest at residues equivalent to NpmA Lys71 (always Lys) and Lys67 (always Lys or Arg). The partial conservation of these positively charged surface residues suggests that initial docking on the 16S rRNA surface mediated by electrostatic interactions of the  $\beta$ 2/3 linker is likely a conserved feature of the m<sup>1</sup>A1408 methyltransferases. In contrast, for the m<sup>7</sup>G1405 aminoglycoside-resistance methyltransferases, the  $\beta$ 2/3 linker is partially surface exposed

but also surrounded by the extended  $\alpha$ -helical N-terminal domain which is implicated in substrate recognition by these enzymes (29, 30). Thus, whether these or other 16S rRNA modification enzymes exploit a similar strategy for docking on the conserved 16S rRNA tertiary surface surrounding the 30S subunit A site remains to be determined by further high-resolution structural studies of 30S-enzyme complexes.

Wild-type NpmA binds 30S with very high affinity ( $\sim 25$  nM  $K_D$ ) and individual substitution of each NpmA  $\beta 2/3$  linker lysine residue has only a modest effect on 30S binding affinity and no impact at all on the resistance conferred to bacteria. These observations, coupled with the partial conservation of the  $\beta 2/3$  linker lysines in other  $m^1A1408$  methyltransferases, suggest that significant redundancy exists in the 16S rRNA-  $\beta 2/3$  linker interface. Another 16S rRNA methyltransferase, RsmA (KsgA), binds the 16S rRNA of pre-30S with very high affinity as part of a quality control mechanism in which N6 dimethylation of A1518 and subsequent dissociation of RsmA signal completion of subunit assembly (31, 32). In contrast, other rRNA enzymes appear to have substantially lower affinity for their substrates (33-36). Why NpmA might be “over-evolved” in its ability to bind *E. coli* 30S is unclear. However, the origin of NpmA is unknown and its transfer among diverse bacterial species with subtle alterations of the 16S rRNA binding surface could have promoted accumulation of points of interaction with 30S. Regardless, this inherent redundancy makes NpmA capable of conferring high levels of resistance to a broad range of bacterial species, even where alterations to the 16S rRNA docking surface that might otherwise have reduced its ability to bind and methylate A1408.

The  $\beta 5/6$  linker is a structurally diverse region among the characterized  $m^1A1408$  methyltransferases (21, 26, 27, 37). Consistent with this, we found that the  $\alpha$ -helical structure of the  $\beta 5/6$  linker, found only in NpmA, is likely dispensable for its activity. However, our results do support a role for conformational changes in the NpmA  $\beta 5/6$  linker as an essential functional switch that controls substrate specificity. Comparison of the free and 30S-bound NpmA structures reveals that the  $\beta 5/6$  linker must reorganize upon 30S binding to avoid steric clashes and pack closely against h44, stabilizing the distorted backbone between C1409 and A1408. The  $\beta 5/6$  linker conformational change also repositions residue E146 to play its proposed role in supporting R207 of the  $\beta 6/7$  linker which contacts the phosphate group of A1408 (21). Although NpmA R153 contributes to 30S binding affinity, the overall impact of the  $\beta 5/6$  linker on 30S binding is neutral: deletion of the entire linker (including R153) increased 30S binding affinity to the same extent as R153E substitution decreased affinity. Thus, an energetic cost associated with driving the functionally critical binding-induced conformational change in the  $\beta 5/6$  linker is off-set by the favorable interaction of R153 with 16S rRNA. In the NpmA variant with a  $\beta 5/6$  linker deletion, the cost of binding-induced conformational changes in NpmA is removed, thus increasing 30S binding affinity, but the enzyme cannot confer resistance due to its reduced ability to sufficiently bind or use SAM for methyltransfer and the loss of its contribution to stabilizing the flipped A1408 target nucleotide. Whether a similar mechanism underpins the activity of other  $m^1A1408$  methyltransferases is unclear but the specific molecular details are likely to differ given the structural and sequence diversity of the  $\beta 5/6$  linker.

Although the NpmA  $\beta$ 6/7 linker makes only a modest contribution to 30S binding affinity (mediated by R200), our results delineated crucial roles for both the precise structure and specific residues within this region. Disrupting the local secondary structure by insertion of a proline residue in the second  $\alpha$ -helix of the  $\beta$ 6/7 linker (L201P variant), results in a protein that binds more tightly to 30S but is completely unable to confer resistance. Thus, the precise structure of the  $\beta$ 6/7 linker appears critical for optimal placement of other residues required for cosubstrate binding (see below) and stabilization of the flipped A1408 conformation. For example, substitution of R207 does not impact 30S binding affinity but nonetheless results in an enzyme unable to confer resistance in bacteria despite retaining significant activity in our *in vitro* methylation activity. These observations are consistent with an exclusive role for R207 in stabilization of the distorted phosphate backbone of the flipped A1408 nucleotide. Similarly, disruption of the  $\beta$ 6/7 linker structure would impact the placement of Trp197 which stacks on the flipped A1408 base in the NpmA active site. Each of the m<sup>1</sup>A1408 methyltransferases possesses an equivalent to NpmA Trp197 but there appears to be significant potential variation both in the  $\beta$ 6/7 linker structure and the contributions of positively charged residues in this group of enzymes. For example, while KamB's  $\beta$ 6/7 linker structure is essentially identical to that of NpmA, KamB activity is abrogated by single substitutions of two arginine residues. Even more strikingly, the  $\beta$ 6/7 linkers of Kmr (26) and cacKam (27) are dynamic and dramatically reorganized into a structure incompatible with 30S binding and modification. Whether these features reflect fundamental mechanistic differences in A1408 recognition and modification, or more minor variations on a common theme, will require further structures of 30S-enzyme complexes to tease apart.

Both the  $\beta 5/6$  and  $\beta 6/7$  linker deletions significantly impacted interaction of NpmA with SAM and SAH. The more dramatic ( $\sim 100$ -fold) defect in SAM/SAH binding with the  $\beta 5/6$  linker deletion was unexpected, as this region does not directly contact SAM. Loss of the  $\beta 5/6$  linker could potentially have long range impacts on NpmA structure or conformational dynamics which in turn impact SAM/SAH affinity but gross changes in the deletion variant seem unlikely given its retained ability to bind 30S. NpmA interaction with cosubstrate has been speculated to be influenced by 30S substrate binding (26, 28), based in part on the observation that substitution of  $\beta 6/7$  linker residue S195 decreases SAM/SAH affinity by  $>50$  fold and yet the variant enzyme is still capable of conferring wild-type resistance. In addition to a direct hydrogen bond made by S195 to the SAM carboxylate group, a local 30S binding-induced conformational change also repositions the L196 backbone to directly interact with SAM. While the L196G substitution has no effect on SAM/SAH affinity (consistent with a backbone mediated interaction), L196 $\Delta$  altered binding in an unprecedented manner for NpmA, with SAH affinity more impacted resulting a relative reduction in affinity of  $\sim 10$ -fold. The L201P and R207E substitutions resulted in similar though less pronounced ( $\sim 5$ -fold) relative reductions in SAH binding affinity, underscoring the importance of the precise  $\beta 6/7$  linker structure and connecting 30S-binding induced reorganization, interaction with SAM and control of base flipping.

Finally, our analyses of 16S rRNA methylation *in vitro* and in bacterial cells expressing NpmA variants offer several additional insights. For many NpmA variants we observed significant differences in the extent of 16S methylation between the two assays. We speculate that this likely arises from the relatively higher concentration of 30S

subunits to enzyme concentration in the bacterial cell as well as competition with other 30S-interacting molecules not present in the defined *in vitro* assay. Thus, alterations in NpmA that reduce the efficiency of initial docking or promotion/ stabilization of the flipped A1408 conformation have an exaggerated impact in the bacterial cell, as observed, for example, for the double and quadruple  $\beta$ 2/3 linker variants and the R207E substitution. The measurements of methylation in cells also give initial clues about both the extent 30S needs to be methylated for maximum resistance as well as an approximate threshold for where methylation is no longer protective. Expression of NpmA variants with single substitutions in the  $\beta$ 2/3 linker resulted in >66% methylation and an indistinguishable resistance phenotype from wild-type NpmA. In contrast, ~10-25% methylation conferred an intermediate resistance phenotype ( $\beta$ 2/3 linker double variants and R200E) and <5% methylation conferred no resistance ( $\beta$ 2/3 linker quadruple variant, L201P and R207E). Thus, although growth may have substantially slowed, only a small fraction of 30S subunits need be methylated for bacteria to survive treatment with antibiotic.

In summary, the present study has revealed new mechanistic insights into substrate recognition and modification for the pathogen-derived aminoglycoside-resistance 16S rRNA methyltransferase NpmA. These detailed structure-function studies provide a platform for inhibitor development exploiting unique facets of the enzyme activity. For example, the conserved surface of the 30S could be targeted for development of compounds that block binding of NpmA without impacting ribosome function. Such efforts are urgently needed in order to prolong the use of aminoglycoside antibiotics in the clinic.

**Acknowledgements**

Single-cysteine NpmA variants were generated and their initial functional characterization were performed by Drs. Miloje Savic and Pooja M. Desai. We also thank Dr. Christine Dunham and members of both the Conn and Dunham laboratories for useful discussions during the course of this work and preparation of the manuscript. This work was funded by the National Institutes of Health/ NIAID grant R01-AI088025.

**TABLE 1.** Summary of kanamycin MICs, relative 16S rRNA methylation activity, and 30S and SAM/SAH binding affinities for substituted and linker deletion NpmA proteins.

Region	Substitution	Kan MIC ( $\mu\text{g/mL}$ )	$K_i$ ( $\mu\text{M}$ ) 30S	$K_d$ ( $\mu\text{M}$ )	
				SAM	SAH
	Wild-type	$>1024^a$	0.06	40	0.4
$\beta 2/\beta 3$ linker	K66E	$>1024^a$	0.37	ND	ND
	K67E	$>1024^a$	0.39	ND	ND
	K70E	$>1024^a$	1.5	ND	ND
	K71E	$>1024^a$	0.30	ND	ND
	K66E/K67E	$256^a$	$> 5$	19.2	0.7
	K70E/K71E	$1024^a$	$> 5$	19.0	0.6
	K66E/K67E/K70E/K71E	$16^a$	$> 5$	17.2	0.8
Linker Deletions	$\Delta\beta 5/\beta 6$ linker	8	0.02	2857	24.5
	$\Delta\beta 6/\beta 7$ linker	16	0.15	375	3.8
$\beta 5/\beta 6$ linker	A148P	$>1024$	ND	ND	ND
	E149P	$>1024$	ND	ND	ND
	R153E	$512^a$	0.34	ND	ND
$\beta 6/\beta 7$ linker	V190P	$>1024$	ND	48	0.5
	L196 $\Delta$	1024	ND	84	8.3
	L196G	$>1024$	ND	47.2	0.71
	R200E	$1024^a$	0.11	ND	ND
	L201P	16	0.02	255	13
	R207E	$4\text{-}16^a$	0.07	47	2.3

<sup>a</sup>MICs for these NpmA variants were previously reported in (21).

ND, Not Determined.

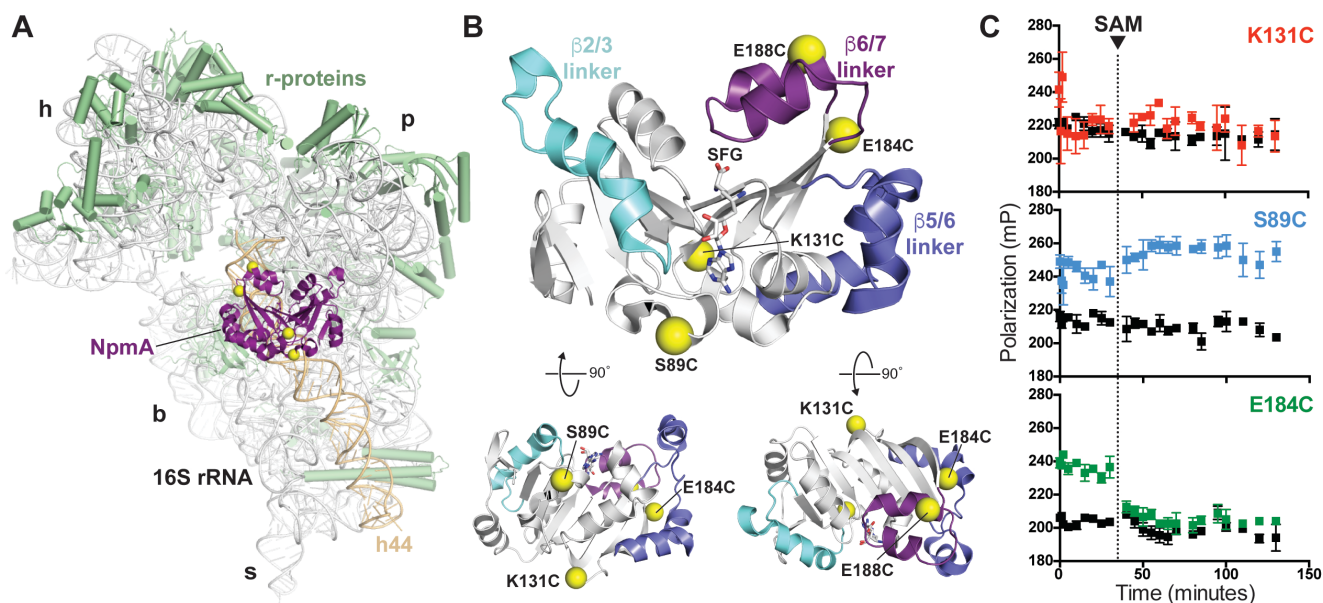


**FIGURE 1. NpmA structure and development of a fluorescence polarization 30S-NpmA binding assay.** *A*, View of NpmA (purple) bound to the 30S subunit. Locations of unique Cys residues in NpmA incorporated for site-specific fluoresce labeling are shown as yellow spheres. Ribosomal proteins are shown in green and 16S rRNA in white, except h44 which is highlighted in tan. 30S features are labeled as head (h), platform (p), base (b) and stalk (s). *B*, NpmA structure in three orthogonal view (top orientation is viewed from the 30S, *i.e.*  $\sim 180^\circ$  rotation around y-axis from *panel A*). Sites of label incorporation are shown as in *panel A*, and the NpmA  $\beta$ 2/3 (cyan),  $\beta$ 5/6 (slate), and  $\beta$ 6/7 (purple) linkers are also highlighted. *C*, Pilot analyses comparing FP signal for labeled NpmA variants before and after addition of SAM (noted by the dotted vertical line), either in the presence of 30S or alone (colored black for all three proteins). Only NpmA E184C\* (green; *bottom plot*), exhibits increased FP in the presence of 30S and decreased FP after SAM addition, indicative of initial binding and subsequent dissociation of the enzyme following catalysis of methyl transfer, respectively.

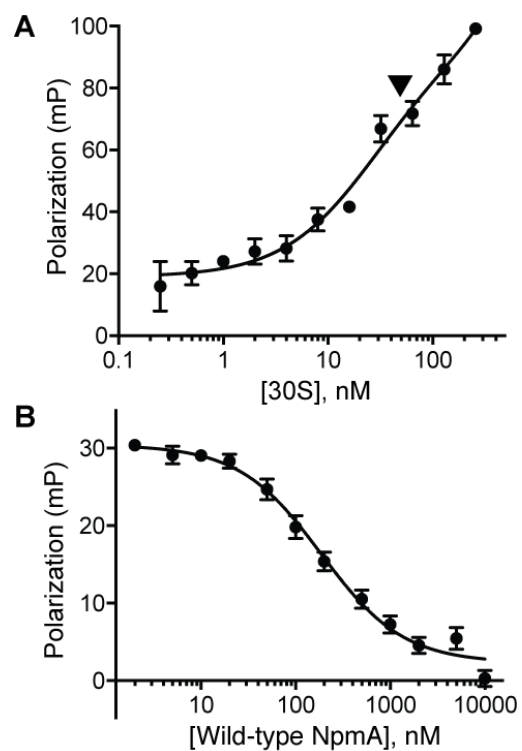


**FIGURE 2. Measurement of 30S-NpmA binding affinity.** *A*, Direct measurement of NpmA-E184C\* binding to the 30S subunit (0-256 nM) by FP. *B*, Competition FP binding experiment using wild-type NpmA (0.002-10  $\mu$ M) to displace the NpmA-E184C\* probe. Analysis of binding ( $K_i$ ) of all NpmA variants was performed using this competition assay.

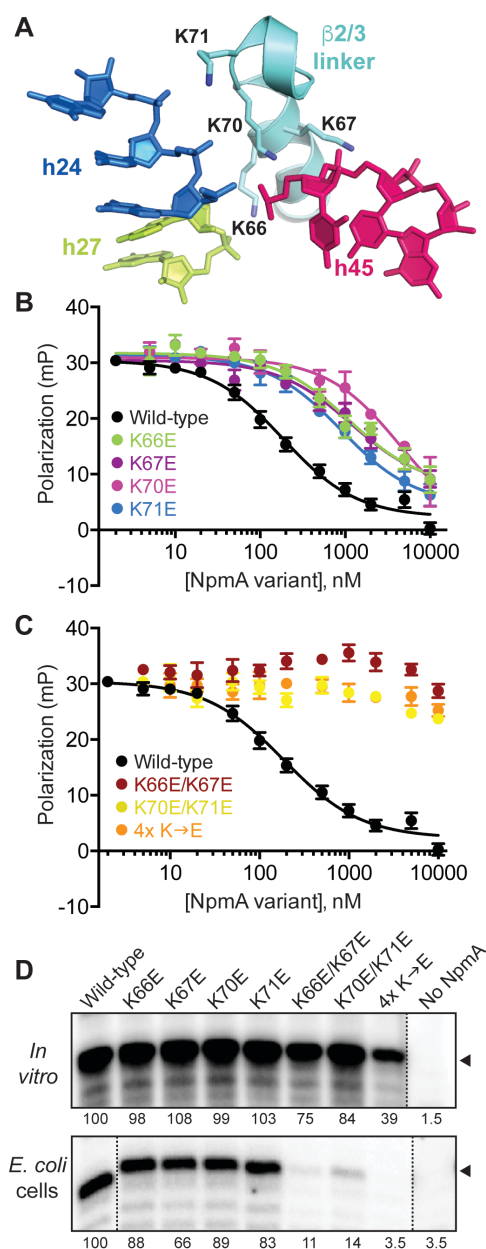


**FIGURE 3.  $\beta$ 2/3 linker residue are critical for 30S-NpmA interaction.** *A*, Four lysine residues of the NpmA  $\beta$ 2/3 linker (cyan) interact with the phosphate backbone of nucleotides in h24, h27, and h45 of 16S rRNA. *B*, Competition FP binding experiments with NpmA-E184C\* and unlabeled NpmA proteins with single Lys to Glu substitutions in the  $\beta$ 2/3 linker. Wild-type NpmA data shown for comparison is the same as in **Fig. 2B**. Binding affinity ( $K_i$ ) for each variant protein derived from these data are shown in **Table 1**. *C*, As for panel B but for the doublely (K66E/K67E and K70E/K71E) and quadruplely (4x K $\rightarrow$ E) substituted NpmA variants. *D*, RT primer extension analysis of m<sup>1</sup>A1408

modification in 16S rRNA extracted from 30S subunits used *in vitro* methylation reactions (*top*) and from *E. coli* cells (*bottom*) expressing the indicated  $\beta$ 2/3 linker variant NpmA proteins.

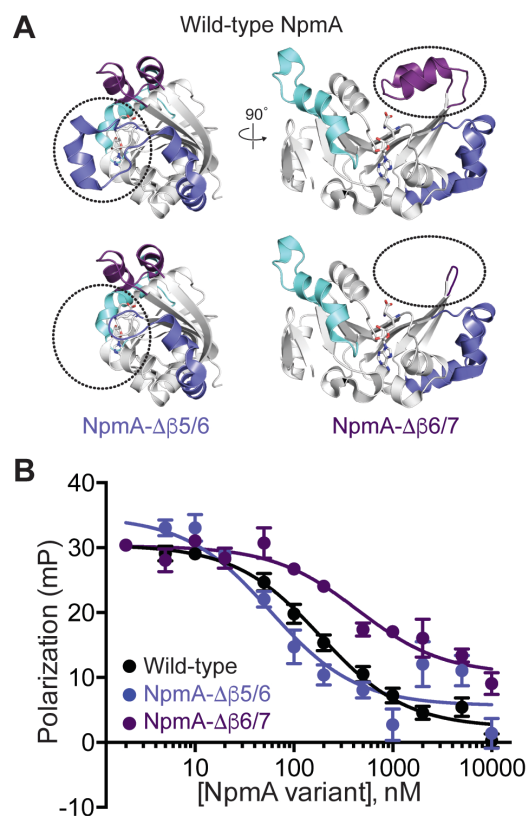


**FIGURE 4. Deletion of the NpmA  $\beta 5/6$  or  $\beta 6/7$  linker has opposite impact on 30S-NpmA affinity.** *A*, Wild-type NpmA structure shown in two orthogonal views (*top*) and the remaining structure after deletion of the  $\beta 5/6$  linker (*bottom left*) and  $\beta 6/7$  linker (*bottom right*) regions. Color coding of the NpmA linkers and the right view of wild-type NpmA are the same as **Fig. 1B**. *B*, Competition FP binding experiments with NpmA-E184C\* and unlabeled NpmA linker deletion variants, NpmA- $\Delta\beta 5/6$  and NpmA- $\Delta\beta 6/7$ . The wild-type NpmA data shown for comparison are the same as in **Fig. 2**. Binding affinity ( $K_i$ ) for each variant protein derived from these data are shown in **Table 1**.

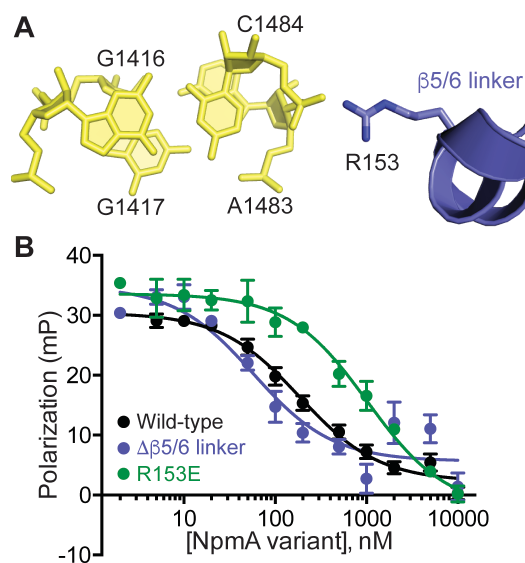


**FIGURE 5.  $\beta$ 5/6 linker residue R153 contributes to 30S-NpmA binding affinity.** *A*, View of NpmA  $\beta$ 5/6 linker residue R153 interaction with the phosphate group bridging 16S rRNA nucleotides A1483 and C1484. *B*, Competition FP binding experiments with NpmA-E184C\* and unlabeled charge reversal substitution of NpmA residue 153 (R153E). The wild-type NpmA and NpmA- $\Delta\beta$ 5/6 data shown for comparison are the same as in **Figs. 2** and **4**, respectively. Binding affinity ( $K_i$ ) for NpmA-R153E derived from these data is shown in **Table 1**.

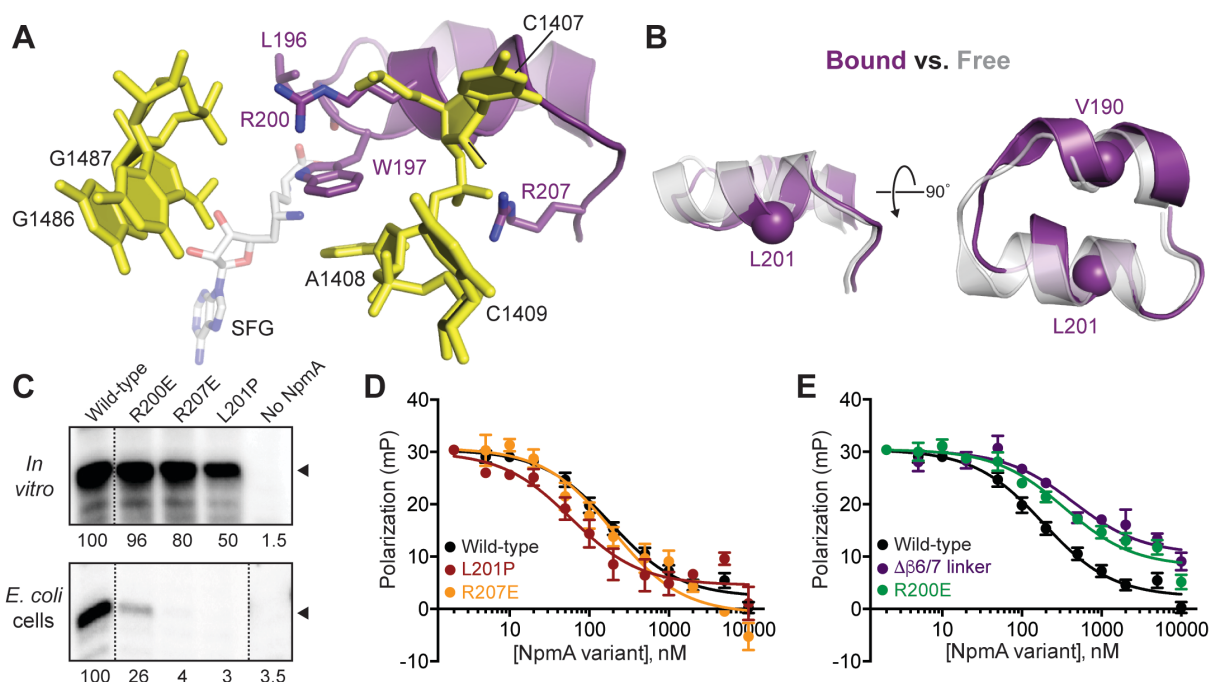


**FIGURE 6. NpmA  $\beta$ 6/7 linker conformational changes impact 30S-NpmA binding affinity.** *A*, View of the NpmA  $\beta$ 6/7 linker and its electrostatic interactions with 16S rRNA via residues R200 and R207. W197 was previously shown to be critical for positioning the A1408 target base in the NpmA active site and the backbone carbonyl of L196 is positioned within hydrogen bonding distance from the bound SAM analog sinefungin (SFG) (21). *B*, Comparison of the NpmA  $\beta$ 6/7 linker in its 30S-bound (purple) and free (semi-transparent gray) forms, revealing a binding-induced, local conformational change centered on L196 (the view shown *left* is the same as *panel A*). Two residues, V190 and L201, substituted with proline are also highlighted by a sphere on their Ca atom. *C*, RT primer extension analysis of m<sup>1</sup>A1408 modification in 16S rRNA extracted from 30S subunits used *in vitro* methylation reactions (*top*) and from *E. coli* cells (*bottom*) expressing the indicated  $\beta$ 6/7 linker variant NpmA proteins. *D*, Competition FP binding experiments with NpmA-E184C\* and unlabeled NpmA with L201P or R207E substitutions. *E*, As panel *D* but for the NpmA-R200E variant. In panels *D* and *E*, the wild-type NpmA and NpmA- $\Delta\beta$ 6/7 data shown for comparison are the same as in **Figs. 2** and **4**, respectively. Binding affinities ( $K_i$ ) derived from these data are shown in **Table 1**.

## References

1. Cundliffe E (1989) How antibiotic-producing organisms avoid suicide. *Annual Review of Microbiology* 43:207-233.
2. Kotra LP, Haddad, J. and Mobashery, S. (2000) Aminoglycosides: perspectives on mechanisms of action and resistance and strategies to counter resistance. *Antimicrobial Agents and Chemotherapy* 44:3249-3256.
3. Jana S, and Deb, J.K. (2006) Molecular understanding of aminoglycoside action and resistance. *Applied Microbiology and Biotechnology* 70:140-150.
4. Neu HC (1992) The Crisis in Antibiotic Resistance. *Science* 257(5073):1064-1073.
5. Khachatourians GG (1998) Agricultural use of antibiotics and the evolution and transfer of antibiotic-resistant bacteria. *CMAJ* 159(9):1129-1136.
6. Wright GD, and Poinar, H. (2012) Antibiotic resistance is ancient: implications for drug discovery. *Trends in Microbiology* 20(4):157-159.
7. Wachino JI, Shibayama, K., Kurokawa, H., Himura, K., Yamane, K., Suzuki, S., Shibata, N., Ike, Y., and Arakawa, Y. (2007) Plasmid-mediated novel m1A1408 methyltransferase NpmA, for 16S rRNA found in clinically isolated *Escherichia coli* resistant to structurally diverse aminoglycosides. *Antimicrobial Agents and Chemotherapy* 51:4401-4409.
8. Wachino JI, Arakawa, Y. (2012) Exogenously acquired 16S rRNA methyltransferases found in aminoglycoside-resistant pathogenic Gram-negative bacteria: an update. *Drug Resist Updat* 15(3):133-148.

9. Magnet S, and Blanchard, J.S. (2005) Molecular insights into aminoglycoside action and resistance. *Chem. Rev.* 105:477-498.
10. Pfister P, Hobbie, S., Vicens, Q., Bottger, E.C., and Westhof, E. (2003) The molecular basis for A-site mutations conferring aminoglycoside resistance: relationship between ribosomal susceptibility and x-ray crystal structures. *ChemBioChem* 4.
11. Carter AP, Clemons, W.M., Brodersen, D.E., Morgan-Warren, R.J., Wimberly, B.T., and Ramakrishnan, V. (2000) Functional insights from the structure of the 30S ribosomal subunit and its interaction with antibiotics. *Nature* 407:340-348.
12. Francois B, Russell, R.J.M., Murray, J.B., Aboul-ela, F., Masquida, B., Vicens, Q., and Westhof, E. (2005) Crystal structures of complexes between aminoglycosides and decoding A site oligonucleotides: role of the number of rings and positive charges in the specific binding leading to miscoding. *Nucleic Acids Research* 33:5677-5690.
13. Vicens Q, and Westhof, E. (2001) Crystal structure of paromomycin docked into the eubacterial ribosomal decoding A site. *Structure* 9:647-658.
14. Wasserman MR, Pulk, A., Zhou, Z., Altman, R.B., Zinder, J.C., Green, K.D., Garneau-Tsodikova, S., Cate, J.H.D., Blanchard, S.C. (2015) Chemically related 4,5-linked aminoglycoside antibiotics drive subunit rotation in opposite directions. *Nature Communications* 6(7896):1-12.
15. Conn GL, Savic, M., and Macmaster, R. (2008) DNA and RNA modification enzymes: structure, mechanism, function, and evolution., (Landes Bioscience).

16. Doi Y, and Arakawa, Y. (2007) 16S ribosomal RNA methylation: emerging resistance mechanisms against aminoglycosides. *Antimicrobial Resistance* 45:88-94.
17. Savic M, Lovric, J. Tomic, T.I., Vasiljevic, B., and Conn, G.L. (2009) Determination of the target nucleosides for members of two families of 16S rRNA methyltransferases that confer resistance to partially overlapping groups of aminoglycoside antibiotics. *Nucleic Acids Research* 37.
18. Galimand M, Courvalin, P., and Lambert, T. (2003) Plasmid-mediated high-level resistance to aminoglycosides in Enterobacteriaceae due to 16S rRNA methylation. *Antimicrobial Agents and Chemotherapy* 47:2565-2571.
19. Cao X, Zhang, Z., Shen, H., Ning, M., Chen, J., Wei, H., and Zhang, K. (2014) Genotypic characteristics of multidrug-resistant *Escherichia coli* isolates associated with urinary tract infections. *APMIS* 122(11):1088-1095.
20. Liou GF, Yoshizawa, S., Courvalin, P., Galimand, M. (2006) Aminoglycoside resistance by ArmA-mediated ribosomal 16S methylation in human bacterial pathogens. *J Mol Biol* 359(2):358-364.
21. Dunkle JA, Vinal, K., Desai, P.M., Zelinskaya, N., Savic, M., West, D.M., Conn, G.L., and Dunham, C.M. (2014) Molecular recognition and modification of the 30S ribosome by the aminoglycoside-resistance methyltransferase NpmA. *PNAS* 59(5):2807-2816.
22. Zelinskaya N, Rankin, C.R., Macmaster, R., Savic, M., and Conn, G.L. (2011) Expression, purification, and crystallization of adenosine 1408 aminoglycoside-

- resistance rRNA methyltransferases for structural studies. *Protein Expression and Purification* 75:89-94.
23. Miyazaki K, and Takenouchi, M. (2002) Creating random mutagenesis libraries using megaprimer PCR of whole plasmid. *Biotechniques* 33:1033-1034.
  24. Moazed D, Stern, S., and Noller, H.F. (1986) Rapid chemical probing of conformation in 16S ribosomal and 30S ribosomal subunits using primer extension. *Journal of Molecular Biology* 187(3):399-416.
  25. Macmaster R, Zelinskaya, N., Savic, M., Rankin, C.R., and Conn, G.L. (2010) Structural insights into the function of aminoglycoside-resistance A1408 16S rRNA methyltransferases from antibiotic-producing and human pathogenic bacteria. *Nucleic Acids Research* 38:7791-7799.
  26. Savic M, Sunita, S. Zelinskaya, N., Desai, P.M., Macmaster, R., Vinal, K., Conn, G.L. (2015) 30S Subunit-Dependent Activation of the *Sorangium cellulosum* So ce56 Aminoglycoside Resistance-Confering 16S rRNA Methyltransferase Kmr. *Antimicrobial Agents and Chemotherapy* 59(5):2807-2816.
  27. Witek MA, Conn, G.L. (2016) Functional Dichotomy in the 16S rRNA (m1A1408) methyltransferase family and control of catalytic activity via a novel tryptophan mediated loop reorganization. *Nucleic Acids Research* 44(1):342-353.
  28. Husain N, Obranic, S., Koscinski, L., Seetharaman, J., Babic, F., Bujnicki, J.M., Maravic-Vlahovicek, G., Sivaraman, J. (2011) Structural basis for the methylation of A1408 in 16S rRNA by a panaminoglycoside resistance methyltransferase NpmA from a clinical isolate and analysis of the NpmA interactions with the 30S ribosomal subunit. *Nucleic Acids Research* 39(5):1903-1918.

29. Husain N, Tkaczuk, K.L., Tulsidas, S.R., Kaminska, K.H., Cubrilo, S., Maravic-Vlahovicek, G., Bujnicki, J.M., Sivaraman, J. (2010) Structural basis for the methylation of G1405 in 16S rRNA by aminoglycoside resistance methyltransferase Sgm from an antibiotic producer: a diversity of active sites in m7G methyltransferases. *Nucleic Acids Research* 38(12):4120-4132.
30. Schmitt E, Galimand, M., Panvert, M., Courvalin, P., Mechulam, Y. (2009) Structural Bases for 16S rRNA Methylation Catalyzed by ArmA and RmtB Methyltransferases. *Journal of Molecular Biology* 388:570-582.
31. O'Farrell HC, Musayev, F.N., Scarsdale, J.N., and Rife, J.P. (2012) Control of substrate specificity by a single active site residue of the KsgA methyltransferase. *Biochemistry* 51:466-474.
32. Connolly K, Rife, J.P., Culver, G. (2008) Mechanistic insight into the ribosome biogenesis functions of the ancient protein KsgA. *Molecular Microbiology* 70(5):1062-1075.
33. Basturea GN, Deutscher, M.P. (2007) Substrate specificity and properties of the *Escherichia coli* 16S rRNA methyltransferase, RsmE. *RNA* 13:1969-1976.
34. Hager J, Staker, B.L., Jakob, U. (2004) Substrate binding analysis of the 23S rRNA methyltransferase RrmJ. *J Bacteriol* 186(19):6634-6642.
35. Maravic G, Bujnicki, J.M., Feder, M., Pongor, S., Flögel, M. (2003) Alanine-scanning mutagenesis of the predicted rRNA-binding domain of ErmC' redefines the substrate-binding site and suggests a model for protein-RNA interactions. *Nucleic Acids Research* 31(16):4941-4949.

36. Ero R, Leppik, M., Liiv, A., Remme, J. (2010) Specificity and kinetics of 23S rRNA modification enzymes RlmH and RluD. *RNA* 16:2075-2084.
37. Witek MA, Conn, G.L. (2014) Expansion of the aminoglycoside-resistance 16S rRNA (m(1)A1408 methyltransferase family: expression and functional characterization of four hypothetical enzymes of diverse bacterial origin. *Biochimica et Biophysica Acta* 1844(9):1648-1655.

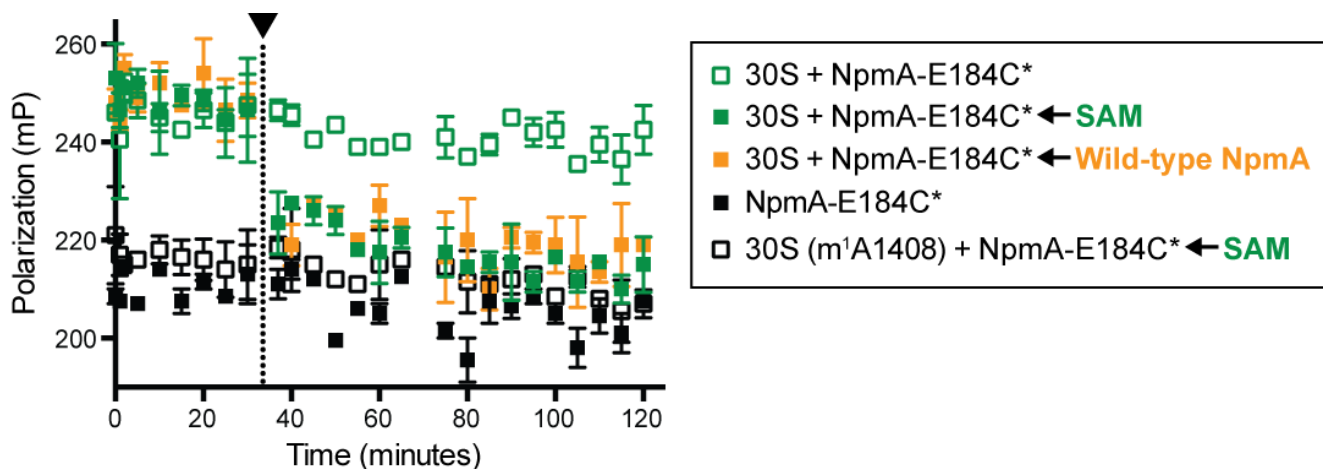


**FIGURE S1. NpmA-E184C\* binds only 30S subunits with unmodified A1408 and is displaced by addition of SAM and/or wild-type NpmA.** NpmA-E184C\* alone (black) and pre-methylated 30S with NpmA-E184C\* (open black squares) in comparison with reactions containing 30S and NpmA-E184C\* (green open squares) with either SAM (green closed squares) or wild-type NpmA (orange closed squares) added at the point indicated by the arrowhead and dotted vertical line.

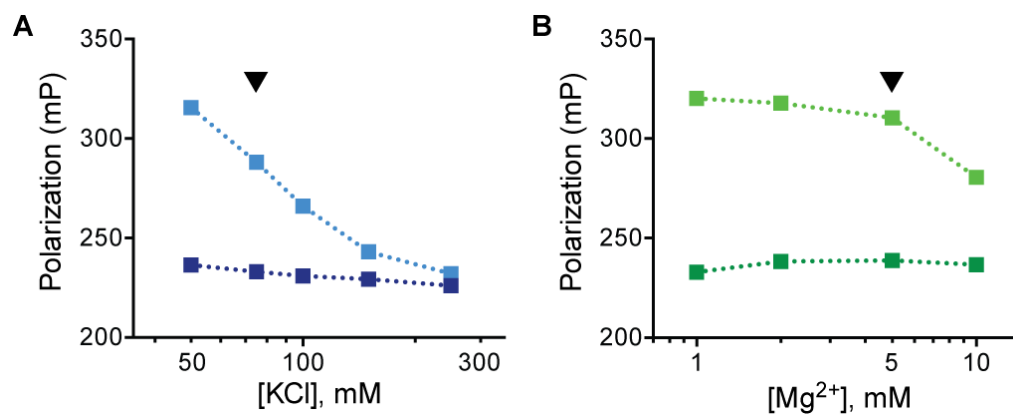


**FIGURE S2. Solution optimization and effect of ionic strength on 30S-NpmA interaction.** Fluorescence polarization comparison of free NpmA-E184C\* with 30S-bound NpmA-E184C\* with increasing concentrations of salt (50 – 100 mM KCl, 1 – 10 mM Mg<sup>2+</sup>) in buffer solution.

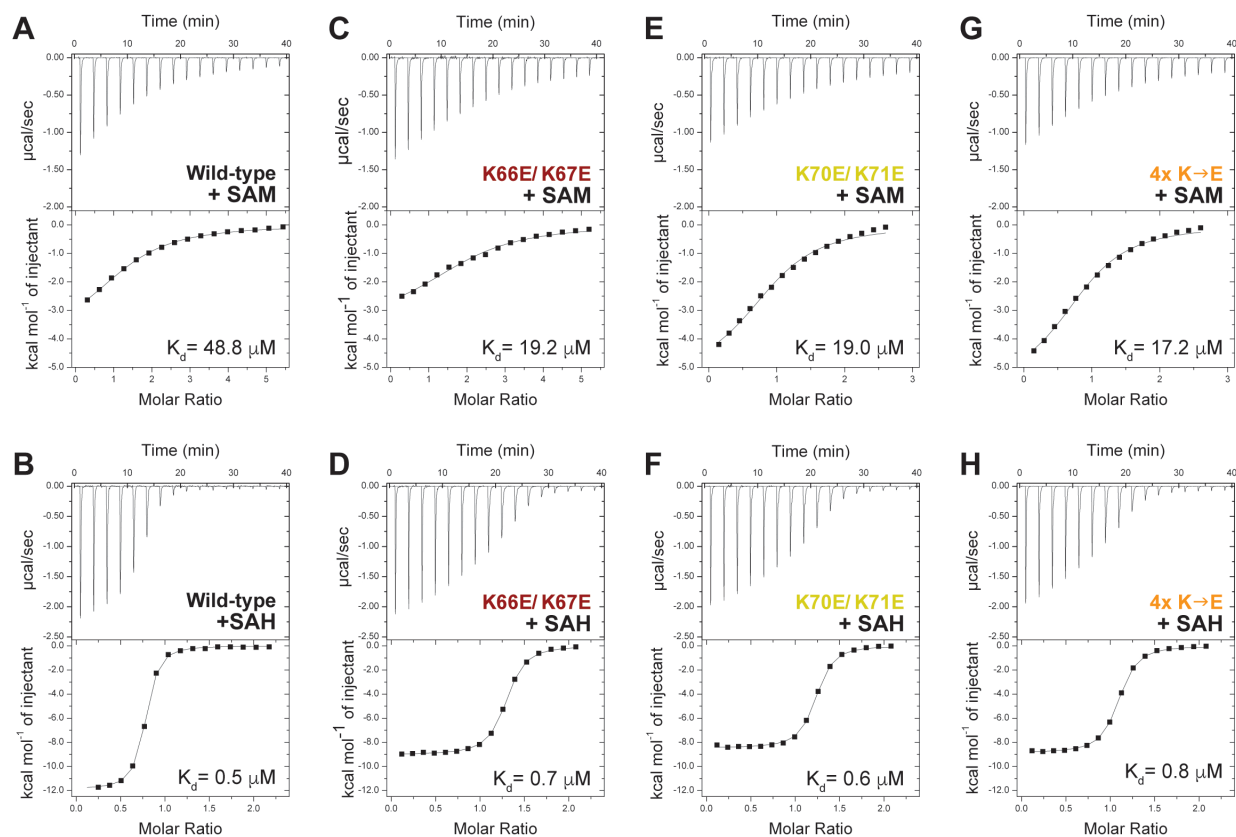


**FIGURE S3. Measurement of NpmA  $\beta$ 2/3 linker variant binding affinity for cosubstrate SAM and reaction by-product SAH.** ITC titrations for each protein-ligand pair tested: *A,B*, wild-type NpmA; *C,D*, NpmA-K66E/K67E; *E,F*, NpmA-K70E/K71E; and, *G,H*, NpmA-K66E/K67E/K70E/K71E (4x K $\rightarrow$ E) with SAM and SAH, respectively. Values for binding affinity ( $K_d$ ) are those derived from the individual titration shown.

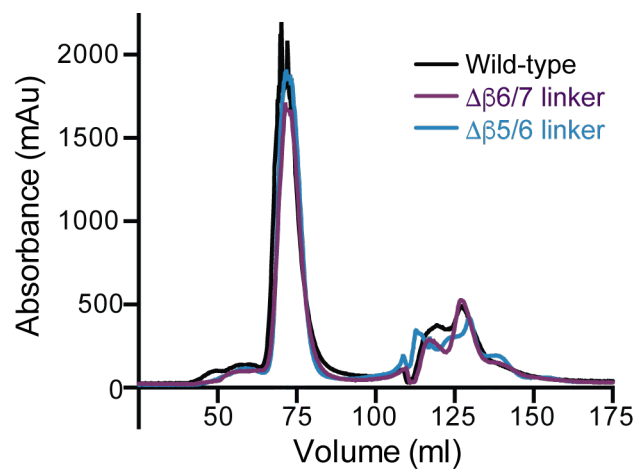


**FIGURE S4. Gel filtration chromatography purification of wild-type NpmA and linker deletion variants.** Gel filtration elution profile comparison of wild-type NpmA with two deletion variants,  $\Delta\beta 5/6$  linker and  $\Delta\beta 6/7$  linker.

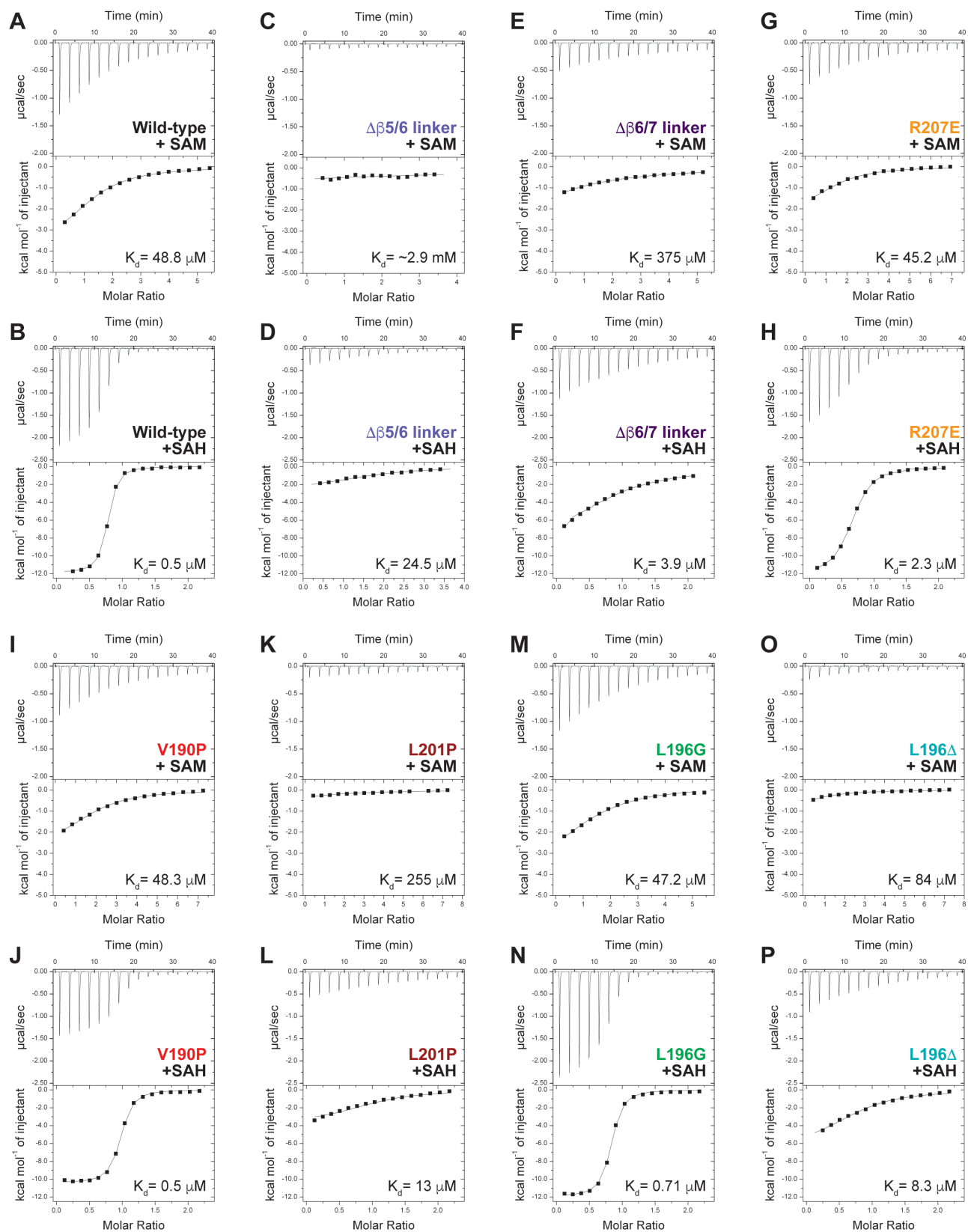


**FIGURE S5. ITC analysis of NpmA  $\beta$ 5/6 and  $\beta$  6/7 linker deletion and single residue substitution variant interaction with SAM and SAH.** ITC titrations for each protein-ligand pair tested: *A,B*, wild-type NpmA (same data as shown in **Supplementary Fig. S3**); *C,D*,  $\Delta\beta$ 5/6 linker; *E,F*,  $\Delta\beta$ 6/7 linker; *G,H*, NpmA-R207E; *H,I*, NpmA-V190P; *J,K*, NpmA-L201P; *L,M*, NpmA-L196G; and, *O,P*, NpmA-L196 $\Delta$  with SAM and SAH, respectively. Values for binding affinity ( $K_d$ ) are those derived from the individual titration shown.

**CHAPTER 4:****Conclusion**

## Conclusion

The World Health Organization (WHO) has identified antimicrobial resistance as a global health threat that necessitates immediate action. Although resistance to antimicrobials is rooted in ancient origin, development of resistance mechanisms has been accelerated by misuse and overuse of antibiotics in both food production and human medicine settings. With little attention focused on development of new antimicrobial drugs by the pharmaceutical industry, paired with our limited knowledge of how to combat existing resistance mechanisms, experts fear that we are moving into a post-antibiotic era in which there will be no known course of treatment for some microbial infections. Combating infectious disease in the future will take both increased education and awareness of antibiotic resistance, as well as a strengthened understanding of antibiotic resistance mechanisms through research and surveillance (1). Specifically, improved public health surveillance of 16S rRNA methyltransferase genes is needed to understand not only which enzymes are being propagated in what settings, but in which particular microbial species, what location and mode of transmission, and with what incidence (2). At the same time, further research devoted to characterizing the molecular mechanisms of this class of enzymes is necessary to understand the nuances of 30S recognition and methyl transfer by related aminoglycoside-resistance methyltransferases.

Antibiotic-producing soil microbes of the *Streptomyces* genus, which have been detected all over the world, are often multi-drug resistant, likely due to either evolutionary pressure from proximity of other antibiotic-producing microbes or necessity from producing multiple antibiotics themselves (3). The transmissibility of resistance

genes from these soil organisms to pathogenic bacteria through horizontal gene transfer and mobile genetic elements has been both predicted and reported with increased incidence. Antimicrobial resistance is particularly a problem in gram-negative bacteria, strains of which are developing multidrug-resistant (MDR) or extensively drug-resistant (XDR) properties (4). In particular, the emergence and transmission of 16S rRNA methyltransferase enzymes is predicted to severely impact the effectiveness of aminoglycoside antibiotics in the clinic. This class of enzymes not only confers high levels of resistance to a broad range of aminoglycoside antibiotics, but has the potential for global dissemination (4).

Previous work in our laboratory has focused on deepening our understanding of 16S rRNA methyltransferase enzymes, both in determining their molecular mechanisms of action and functionally characterizing new predicted members of the m<sup>1</sup>A1408 enzyme family. To aid in this pursuit, our lab has developed purification strategies for expression and characterization of both m<sup>1</sup>A1408 and m<sup>7</sup>G1405 enzymes (5-7). Through structural and functional analyses of these enzymes, we have identified critical residues involved in 30S substrate interaction, catalytic activity, or cosubstrate binding in the m<sup>7</sup>G1405-modifying methyltransferases Sgm (8) from the G-52 (6'-N-methyl-sisomicin) producer *Micromonospora zionensis* and the human pathogen-derived RmtD/RmtD2 and RmtG (7), and the m<sup>1</sup>A1408-modifying enzymes KamB and NpmA (9), Kmr (10), and CacKam (11). Analysis of this family of enzymes has identified that although these proteins share common structural features, they likely employ distinct molecular modes of action between the two subfamilies (i.e. m<sup>7</sup>G1405 vs. m<sup>1</sup>A1408 enzymes). Furthermore, initial characterization of new members of the m<sup>1</sup>A1408 methyltransferase

family has also revealed potential functional and mechanistic variation within this group of enzymes (6, 10, 11), necessitating a deeper understanding of both their interactions with the ribosome and control of base flipping through both high resolution structural and detailed mechanistic studies.

NpmA is of particular interest as the first m<sup>1</sup>A1408 16S rRNA methyltransferase enzyme to be isolated from a pathogen, and even more so because of the unprecedented level and range of resistance it confers to aminoglycoside antibiotics. Previous work in the lab both elucidated the crystal structure of NpmA bound to SAM and predicted specific residues and motifs with which the enzyme interacts with its substrate, the 30S ribosome. However, the molecular details of specific substrate recognition, base flipping, and nucleotide modification remained elusive. Our subsequent studies, presented in this thesis, have thus aimed to obtain a detailed understanding of the precise molecular mechanism of NpmA-30S interaction to ultimately provide a platform for inhibitor development for this resistance determinant.

In Chapter 2 I described our report of the crystal structure of the 30S subunit complexed with NpmA and the SAM analog sinefungin. In capturing NpmA in this “precatalytic state” (i.e. poised before methyl transfer occurs), we were able to examine the specific contacts NpmA makes with its 30S substrate. Additionally, in comparison with our previously published NpmA-SAM complex structure, we observed that upon binding the 30S subunit, NpmA undergoes multiple structural reorganizations. Analyses of complementary functional and biochemical data revealed specific residues critical for NpmA activity. These studies prompted development of a new model for NpmA-30S interaction in which initial docking of NpmA onto the 30S via the conformationally rigid

$\beta$ 2/3 linker induces precisely controlled, sequential conformational changes in the  $\beta$ 5/6 and  $\beta$ 6/7 linkers to stabilize flipping of the target base A1408 from h44 and precisely position it for methylation. Our results provided the first molecular basis of tertiary structure-dependent 30S recognition of an aminoglycoside-resistance methyltransferase enzyme, which might serve as a framework for understanding the action of similar enzymes.

This insight has prompted us to further examine the differences in substrate recognition and base flipping beyond that of A1408- and G1405-modifying 16S rRNA methyltransferase enzymes. Because G1405-targeting enzymes recognize a base in close proximity to A1408 and also require the full 30S subunit as a substrate, it is likely that these enzymes also exploit the adjacent conserved 16S rRNA tertiary structure in a similar manner as their A1408-targeting counterparts. However, structural and biochemical studies of G1405-modifying enzymes have identified the extended N-terminal domain of this class of enzymes as required for enzymatic activity and likely important for recognition of the 30S subunit (9, 12). The necessity for this extended N-terminal domain might reflect the local environment of G1405, in which the target base is buried within h44 and might require a significantly different mechanism for target recognition and base flipping. Furthermore, a variety of enzymes catalyze distinct modifications within this region of 16S rRNA, including  $m^4C1402$  by RsmH (13),  $m^5C1407$  by RsmF (14),  $m^3U1498$  by RsmE (15, 16),  $m^2G1516$  by RsmJ (17), and dual  $m^6_2A1518/m^6_2A1519$  modification by RsmA (15), all of which require the fully assembled 30S subunit as a substrate (see Chapter 2, Fig. S8). Our working model of NpmA-30S interaction could thus serve as a paradigm for how 30S subunit-modifying

methyltransferases interact with their substrate, as these enzymes may employ similar strategies for substrate recognition.

Our findings from Chapter 2 served as a springboard for the further mechanistic investigation of the NpmA-30S interaction described in Chapter 3. To dissect the molecular mechanism of 30S-NpmA recognition, I first developed a fluorescence polarization-based assay to probe and quantify contribution of specific amino acid residues to the NpmA-30S interaction. Using this technique, the high NpmA-30S binding affinity was approximated and critical residues for interaction with the 30S subunit were identified. We determined that four positively charged lysines of the  $\beta$ 2/3 linker are collectively critical for NpmA binding to three helices of 16S rRNA which are disparate in the primary sequence but brought into close proximity in the assembled 30S subunit structure. We also analyzed the 30S binding ability, SAM-binding affinity, methylation ability, and ability to confer resistance for a series of NpmA variants created based on previous structural and functional data. From these data, we identified and reported the distinct contributions of residues in the NpmA  $\beta$ 5/6 and  $\beta$ 6/7 linkers to precise control of enzymatic activity and methyl transfer. We revealed that the  $\beta$ 5/6 linker, although critical for optimal enzymatic activity, is not directly required for 30S binding and that specific conformational changes in the  $\beta$ 6/7 linker are critical for NpmA function. We proposed a detailed mechanism of recognition and catalysis by NpmA in which tertiary structure dictates proper stabilization of the flipped conformation of the target base. Specifically, the conformationally rigid  $\beta$ 2/3 linker of NpmA first docks onto the structurally complementary structure of the 30S subunit, triggering sequential conformational shifts within the  $\beta$ 5/6 and  $\beta$ 6/7 linkers. The  $\beta$ 5/6 linker reorganizes to avoid steric clash with

the 30S subunit, repositioning residue E146 to subsequently support R207 (of the  $\beta 6/7$  linker) to assist in positioning of target base A1408. In the  $\beta 6/7$  linker, residue R200 contributes to binding and positioning on the 30S substrate while R207 is critical for both base-flipping and catalysis. Surprisingly, conservation of tertiary structure, rather than specific amino acid sequence, dictates methylation ability of NpmA.

Future work in the lab is focused on deepening our understanding of 16S rRNA methyltransferase enzymes through structural and functional analyses of novel or largely uncharacterized enzymes. Of particular interest is the  $\beta 6/7$  linker of related 16S rRNA methyltransferase enzymes. Previous work in our lab has shown that the  $m^1A1408$  methyltransferase Kmr has a remarkably low affinity for SAM and disordered  $\beta 6/7$  linker in the crystal structure (10) but nonetheless has an enzymatic activity comparable to NpmA and other  $m^1A1408$  methyltransferases. Additionally, the enzyme activity of Kmr is apparently particularly robust, as substitution of residues that are functionally critical in related enzymes, particularly for A1408 base flipping, failed to impact enzymatic activity (10). These observations suggest that Kmr relies on the 30S substrate to drive critical aspects of its interaction with SAM cosubstrate and adoption of a catalytically competent state. Thus, further analysis of Kmr bound to 30S is required to determine how these unique features contribute to substrate specificity and enzymatic activity. Our lab has also revealed that the  $\beta 6/7$  linker of  $m^1A1408$  methyltransferase *CacKam* adopts a unique extended conformation, which might contribute to a novel molecular mechanism of controlling enzymatic activity (11). Unlike NpmA, an extensive reorganization of the *CacKam*  $\beta 6/7$  linker is required to expose the  $\beta 2/3$  linker surface and to reposition the  $\beta 6/7$  linker to position residues critical for A1408 base flipping. These analyses thus

suggest that *CacKam* might employ a distinct molecular mechanism for interaction with the 30S and subsequent methylation (11).

Currently, G1405-modifying enzymes are the most prevalent threat to clinical use of aminoglycoside antibiotics. To date, nine m<sup>7</sup>G1405 modifying enzymes have been identified, including ArmA, RmtA, RmtB (including RmtB1 and RmtB2 alleles), RmtC, RmtD (including RmtD1 and RmtD2 alleles), RmtE, RmtF, RmtG, and RmtH (4). Alarming, both global dissemination and coexistence with other resistance mechanisms have been reported for these enzymes. ArmA and RmtB in particular have been detected worldwide with high prevalence, often in bacteria coproducing New Delhi Metallo- $\beta$ -lactamases. While RmtA, RmtD, RmtG, and RmtH have been reported with low prevalence, they appear globally disseminated having been isolated in Japan, Korea, Iraq, Saudi Arabia, the United States and several regions in South America. This extensive geographical span underscores the necessity for a more robust understanding of both how these enzymes are transferred and their mechanism of action once acquired by a human pathogenic bacterial species (4). Although the resistance spectrum for the m<sup>7</sup>G1405 modification is limited to 4,6-disubstituted 2-DOS aminoglycosides, this includes many of the clinically important drugs such as gentamicin, amikacin, tobramycin, and latest generation aminoglycoside plazomicin (4, 18). To mitigate the threat of G1405-modifying enzymes to clinically useful drugs, studies equivalent to those reported in this thesis characterizing the molecular mechanisms of substrate interaction for these enzymes are urgently needed. Particularly, a crystal structure of a G1405-modifying enzyme bound to the 30S subunit could reveal a common 16S target to which an inhibitor could be developed to block binding of both families of enzymes. Additionally, adaptation of

the NpmA-specific fluorescence polarization binding assay outlined here or development of a similar binding-based assay for G1405-modifying enzymes will be important in this process.

Current studies are also in progress for m<sup>7</sup>G1405 methyltransferase Sgm to determine specific amino acid residues that interact with the 30S substrate. We seek to develop a fluorescence-based assay, similar to that reported here, to probe the Sgm-30S interaction. Additionally, the fluorescence polarization assay described in Chapter 3 of this dissertation has been adapted for *M. tuberculosis* capreoycin-resistance methyltransferase TlyA with promising preliminary results. Using this assay, we aim to probe the interaction between TlyA and the ribosome. Finally, studies are in progress to further our characterization of pathogen-derived NpmA. Our lab has shown that NpmA exhibits dual m<sup>1</sup>A1408/m<sup>1</sup>G1408 specificity, an unexpected and unique trait among the A1408-modifying enzymes. However, the basis for this activity or why it may exist only in NpmA are currently unknown.

In summary, the work presented here demonstrates a previously unknown molecular mechanism and novel insight into substrate recognition by a pathogen-derived m<sup>1</sup>A1408 16S rRNA methyltransferase enzyme. These data have significant implications as we move forward in combatting aminoglycoside resistance by 16S rRNA methyltransferases, as the molecular mechanism we have elucidated will serve as a framework for analysis of 30S interaction with related methyltransferase enzymes. Our hope is that this insight will aid in development of a specific inhibitor for 16S rRNA methyltransferase enzymes. To this end, our lab has begun developing a truncated NpmA

probe for use in high-throughput screening assays to identify potential binding inhibitors for NpmA.

Combating the threat of 16S rRNA methyltransferases will require a multipronged approach, including increased detection of 16S rRNA methyltransferase genes as well as a strengthened understanding of the molecular basis of antibiotic resistance mechanisms. Ultimately, the better we understand how these resistance-conferring enzymes work, the better equipped we will be to combat their threat to clinically useful antibiotics, especially by developing specific inhibitors for these enzymes. Additionally, it is critical to consider the dwindling repertoire of antimicrobial drugs in our arsenal and the lack of funding and effort for this avenue of research. A more concerted effort to screen existing compounds for antimicrobial activity might assist in alleviating the pressure of developing new antimicrobials. Finally, devoting more energy to education and outreach about antimicrobial resistance to both the general public as well as over-prescribing doctors is crucial to combat increasing levels of resistance.

## References

1. World Health Organization, *Global Action Plan on Antimicrobial Resistance 2015*, in [http://apps.who.int/iris/bitstream/10665/193736/1/9789241509763\\_eng.pdf?ua=1](http://apps.who.int/iris/bitstream/10665/193736/1/9789241509763_eng.pdf?ua=1)
2. Wachino JI, Arakawa, Y. (2012) Exogenously acquired 16S rRNA methyltransferases found in aminoglycoside-resistant pathogenic Gram-negative bacteria: an update. *Drug Resist Updat* 15(3):133-148.
3. Perry JA, Wright, G.D. (2013) The antibiotic resistance "mobilome": searching for the link between environment and clinic. *Frontiers in Microbiology* 4(138):1-7.
4. Doi Y, Wachino, J.I., Arakawa, Y. (2016) Aminoglycoside resistance: the emergence of acquired 16S ribosomal RNA methyltransferases. *Infectious Disease Clinics of North America* 30(2):523-537.
5. Zelinskaya N, Rankin, C.R., Macmaster, R., Savic, M., and Conn, G.L. (2011) Expression, purification, and crystallization of adenosine 1408 aminoglycoside-resistance rRNA methyltransferases for structural studies. *Protein Expression and Purification* 75:89-94.
6. Witek MA, Conn, G.L. (2014) Expansion of the aminoglycoside-resistance 16S rRNA (m(1)A1408 methyltransferase family: expression and functional characterization of four hypothetical enzymes of diverse bacterial origin. *Biochimica et Biophysica Acta* 1844(9):1648-1655.
7. Corrêa LL, Witek, M.A., Zelinskaya, N., Picão, R.C., Conn, G.L. (2015) Heterologous expression and functional characterization of the exogenously

- acquired aminoglycoside resistance methyltransferases RmtD, RmtD2, and RmtG. *Antimicrobial Agents and Chemotherapy* 60(1):699-702.
8. Savic M, Lovric, J. Tomic, T.I., Vasiljevic, B., and Conn, G.L. (2009) Determination of the target nucleosides for members of two families of 16S rRNA methyltransferases that confer resistance to partially overlapping groups of aminoglycoside antibiotics. *Nucleic Acids Research* 37.
  9. Macmaster R, Zelinskaya, N., Savic, M., Rankin, C.R., and Conn, G.L. (2010) Structural insights into the function of aminoglycoside-resistance A1408 16S rRNA methyltransferases from antibiotic-producing and human pathogenic bacteria. *Nucleic Acids Research* 38:7791-7799.
  10. Savic M, Sunita, S. Zelinskaya, N., Desai, P.M., Macmaster, R., Vinal, K., Conn, G.L. (2015) 30S Subunit-Dependent Activation of the *Sorangium cellulosum* So ce56 Aminoglycoside Resistance-Confering 16S rRNA Methyltransferase Kmr. *Antimicrobial Agents and Chemotherapy* 59(5):2807-2816.
  11. Witek MA, Conn, G.L. (2016) Functional Dichotomy in the 16S rRNA (m1A1408) methyltransferase family and control of catalytic activity via a novel tryptophan mediated loop reorganization. *Nucleic Acids Research* 44(1):342-353.
  12. Schmitt E, Galimand, M., Panvert, M., Courvalin, P., Mechulam, Y. (2009) Structural Bases for 16S rRNA Methylation Catalyzed by ArmA and RmtB Methyltransferases. *Journal of Molecular Biology* 388:570-582.
  13. Wei Y, Zhang, H., Gao, ZQ, Wang, W.J., Shtykova, E.V., Xu, J.H., Liu, Q.S., Dong, Y.H. (2012) Crystal and solution structures of methyltransferase RsmH

- provide basis for methylation of C1402 in 16S rRNA. *Journal of Structural Biology* 179(1):29-40.
14. Demirci H, Larsen, L.H., Hansen, T., Rasmussen, A., Cadambi, A., Gregory, S.T., Kirpekar, F., Jogl, G. (2010) Multi-site-specific 16S rRNA methyltransferase RsmF from *Thermus thermophilus*. *RNA* 16(8):1584-1596.
  15. Kyuma T, Kizaki, H., Ryuno, H., Sekimizu, K., Kaito, C. (2015) 16S rRNA methyltransferase KsgA contributes to oxidative stress resistance and virulence in *Staphylococcus aureus*. *Biochimie* 119:166-174.
  16. Basturea GN, Deutscher, M.P. (2007) Substrate specificity and properties of the *Escherichia coli* 16S rRNA methyltransferase, RsmE. *RNA* 13:1969-1976.
  17. Basturea GN, Dague, D.R., Deutscher, M.P., Rudd, K.E. (2012) YhiQ is RsmJ, the methyltransferase responsible for methylation of G1516 in 16S rRNA of *E. coli*. *Journal of Molecular Biology* 415(1):16-21.
  18. Karaiskos I, Souli, M., Giamarellou, H. (2015) Plazomicin: an investigational therapy for the treatment of urinary tract infections. *Expert Opin Investig Drugs* 24(11):1501-1511.